

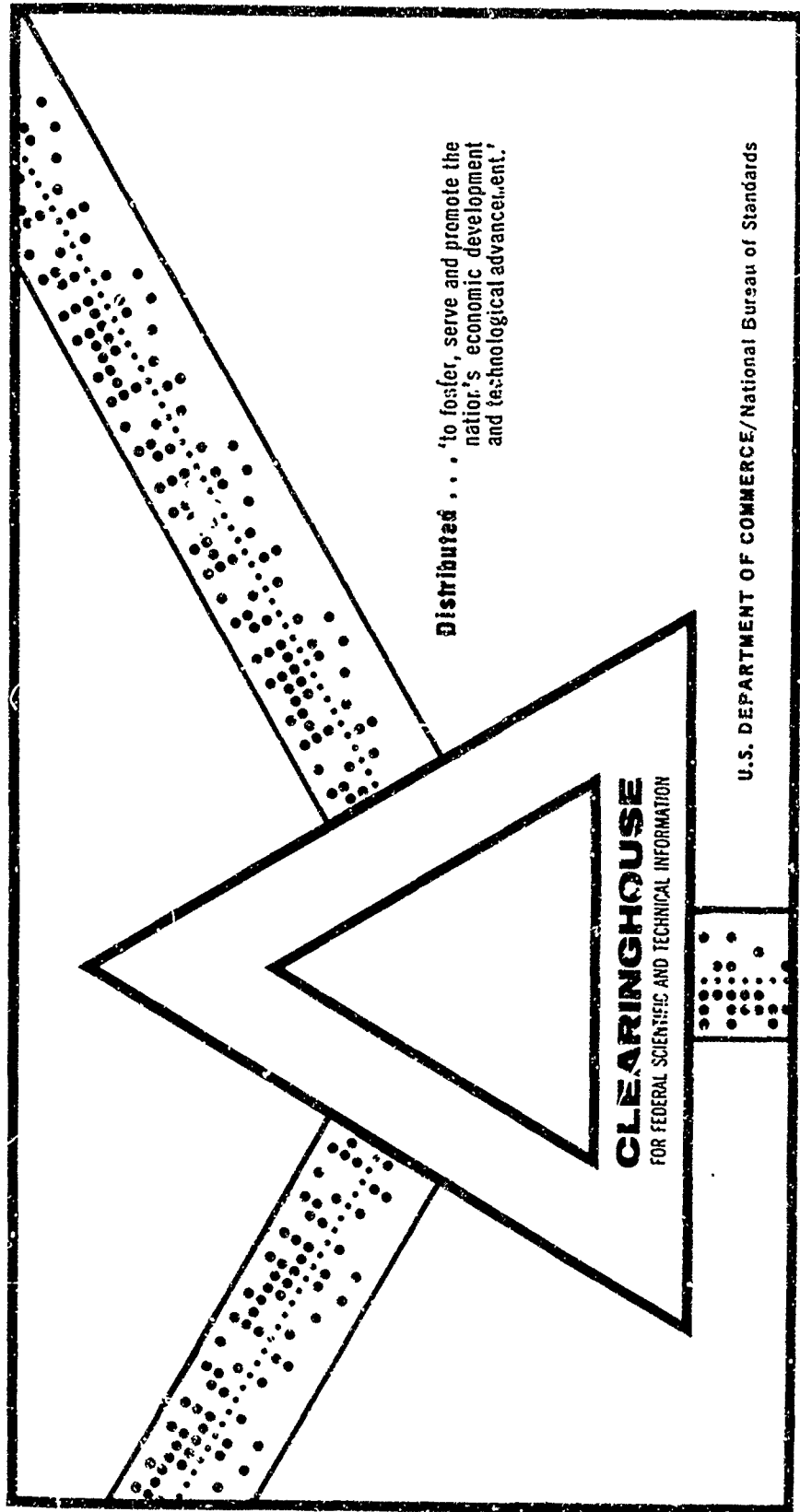
AD 701 006

VIBRATION TESTING OF RESILIENT PACKAGE CUSHIONING MATERIAL:
POLYETHYLENE FOAM

George Zell

Picatinny Arsenal
Dover, New Jersey

December 1969



This document has been approved for public release and sale.

This Document Contains
Missing Page/s That Are
Unavailable In The
Original Document

OR are
Blank pgs.
that have
Been Removed

**BEST
AVAILABLE COPY**

AD701006

64

COPY NO. _____

TECHNICAL REPORT 3610

VIBRATION TESTING OF RESILIENT PACKAGE
CUSHIONING MATERIAL: POLYETHYLENE FOAM

GEORGE ZELL

DECEMBER 1969



THIS DOCUMENT HAS BEEN APPROVED FOR PUBLIC
RELEASE AND SALE; ITS DISTRIBUTION IS UNLIMITED.

REPRODUCTION
CLEARINGHOUSE
FOR FOREIGN DISSEMINATION
Information on GPO Form 2017

PICATINNY ARSENAL
DOVER, NEW JERSEY

DDC
FEB 10 1970
C

98

ACCESSION NO.	
SCOTT	WHITE SECTION <input checked="" type="checkbox"/>
ROB	BUFF SECTION <input type="checkbox"/>
UNANSWERED	<input type="checkbox"/>
JUSTIFICATION	
BY	
DISTRIBUTION/AVAILABILITY CODES	
DIST.	AVAIL. AND/OR SPECIAL
/	

The findings in this report are not to be construed as an official Department of the Army Position.

DISPOSITION

Destroy this report when no longer needed. Do not return to the originator.

Technical Report 3610

VIBRATION TESTING OF RESILIENT
PACKAGE CUSHIONING MATERIAL:
POLYETHYLENE FOAM

by

George Zell

December 1969

This document has been approved for public
release and sale; its distribution is unlimited.

Munitions Packaging Laboratory
Feltman Research Laboratories
Picatinny Arsenal
Dover, New Jersey

ABSTRACT

A 2.3 PCF commercially produced cellular polyethylene cushioning was vibrated under simulated "in-package" conditions. Tests were performed on several "as produced" and on a laminated thickness. Vibration was imposed on samples under static loads from 0.20 to 2.0 psi. Transmissibility was recorded in the frequency range 2 to 250 Hz. It was observed that vibration behavior was strongly influenced by material preload state. Effects are discussed and illustrated by dynamic force vs deformation curves measured "in package." One preload state is shown to induce configurational nonlinearity while another is found capable of suppressing a specific type of nonlinear reaction peculiar to compression-loaded cushioning. Pertinence of observations to utilization of cushioning in protective suspensions is considered.

A technique for normalizing nonlinear cushion response data is developed. Results of comprehensive tests on polyethylene foam are reduced to this format. Data indicates the dynamic stiffness of the foam at transportation-induced vibration frequencies is increased significantly over values derived from low rate (1.0 in./min) compression tests.

Alteration of foam's cell structure with attendant change in mechanical constants was observed at specific threshold levels of resonant excitation. At all but lowest static loads (higher resonant frequencies), these vibration levels fell within envelopes representative of transport-induced vibration.

ACKNOWLEDGMENT

The writer appreciates the conscientious contributions of Messrs. F. DeGrande, B. Bencivenga, and R. Velez in the development of the recording instrumentation, preparation and test of samples, and data reduction, respectively.

TABLE OF CONTENTS

	Page
Introduction	1
Test Equipment	4
Test Results	5
Discussion of Results	9
Summary	36
Conclusion	38
Appendix A	39
Appendix B	43
Appendix C	47
Distribution List	87
 Tables	
1	Summary of ASTM Test Results (Polyethylene Foam, 2" Thick, 1.0 psi Static Stress, 2 G Dynamic Input) 50
2	Summary of Resonant Responses and Frequencies ASTM Tests on 2" Thick Polyethylene Foam, 2 G Dynamic Input, 1.0 psi Static Stress 51
 Figures	
1	Dual compression cushion vibration test fixture with preload jack. 52
2	Relative mass displacement transducer and characteristic dynamic force vs relative displacement curves for dual-compression-cushioned package. 53

Figures	Page
3 Compression-compression test package, three configurations for vibration tests.	54
4 Force on cushioned mass vs displace- ment--"normal preload" configuration. Graphical illustration of asymmetry and nonlinearity.	55
5 Force on cushioned mass vs displace- ment--package with "superimposed compression" = $2 \times D$. Graphical illustration of "linearizing" influence.	56
6 Stress vs strain for 2.2 pounds/ft polyethylene foam. Strain rate = 0.3 in./in./min.	57
7 Stress vs strain, polyethylene foam, sequential cycling. Strain rate = 0.3 in./in./min.	58
8 Peak vector acceleration transmitted vs frequency, polyethylene foam, "Virgin" samples, 8" x 8" x 2" thick. 1.0 psi static stress, 2.0 G dynamic input.	59
9 Peak vector acceleration transmitted vs frequency, polyethylene foam, "Virgin" samples, 4" x 4" x 2" thick. 1.0 psi static stress, 2.0 G dynamic input.	60
10 Peak vector acceleration transmitted vs frequency, polyethylene foam, "preworked" samples, 8" x 8" x 2" thick. 1.0 psi static stress, 2.0 G dynamic input.	61

Figures		Page
11	Peak vector acceleration transmitted vs frequency, polyethylene foam, "preworked" samples, 4" x 4" x 2" thick. 1.0 psi static stress, 2.0 G dynamic input.	62
12	Transmitted peak accelerations vs frequency for steady-state vibrations on virgin cushions. Upward increments first.	63
13	Transmitted peak accelerations vs frequency for steady-state vibrations on virgin cushions. Downward increments first.	64
14	Vibratory input vs static stress for onset of dynamic set and "linearization" of polyethylene foam.	65
15	Vibration transmitted at resonance vs resonant frequency. Polyethylene foam, 2 lbs/ft ³ (nom.)-- 1 5/16 in. thick.	66
16	Vibration transmitted at resonance vs resonant frequency. Polyethylene foam, 2.0 lbs/ft ³ (nom.)-- 1 7/16 in. thick.	67
17	Vibration transmitted at resonance vs resonant frequency. Polyethylene foam, 2 lbs/ft ³ (nom.)-- 3 3/8 in. thick.	68
18	Vibration transmitted at resonance vs resonant frequency. Polyethylene foam, 2 lbs/ft ³ (nom.)-- 4 in. thick (laminated).	69
19	Effective modulus vs relative excitation, polyethylene foam, 1 5/16" thick.	70

		Page
Figures		
20	Effective modulus vs relative excitation, polyethylene foam, 1 7/16" thick.	71
21	Effective modulus vs relative excitation, polyethylene foam, 3 3/8" thick.	72
22	Effective modulus vs relative excitation, polyethylene foam, 4" thick.	73
23	Peak displacement vs frequency for acceleration levels used in transmissibility tests.	74
24	Resonant amplification vs relative excitation, polyethylene foam, 1 5/16" thick.	75
25	Resonant amplification vs relative excitation, polyethylene foam, 1 7/16" thick.	76
26	Resonant amplification vs relative excitation, polyethylene foam, 3 3/8" thick.	77
27	Resonant amplification vs relative excitation, polyethylene foam, 4" thick (laminated)	78
28	Effective modulus vs relative excitation, polyethylene foam data from four thicknesses.	79
29	Polyethylene foam, resonant frequency vs acceleration-thickness product.	80
30	Resonant amplification vs relative excitation, data from four thicknesses.	81

Figures		Page
31	Transmissibility vs frequency ratio for single-degree of freedom system with viscous damping.	82
32	Apparent natural frequency vs static stress-thickness product. Four thicknesses.	83
33	Instrumentation for vibration programming and recording. (Photo)	84
34	Instrumentation for vibration programming and recording. (Schematic)	85
35	Approximation of idealized maximum sweep rate (for $Q = 20$ systems) with two logarithmic sweeps.	86

INTRODUCTION

Cushioning media of various types are in wide use to protect packaged items against the hazards of shock and vibration. It is becoming increasingly evident, however, that under certain conditions cushioning protection may be questionable - that it may not provide the level of "predictable protection" so essential to the safeguarding of expensive and fragile military items during world-wide transportation and handling.

Those materials capable of returning to their original state after the deformation produced by impact energy are generally categorized as "resilient cushioning materials." A considerable number of bonded fibrous materials as well as cellular plastic materials meet this general criterion. Because they are easy to fabricate, and have the ability to absorb high levels of impact energy (relative to density), the "foam" type of expanded cellular plastics has become increasingly popular with the packaging technologist.

Unfortunately, however, the term "cushioning" is generally associated only with shock protection. Experimental investigations for packaging applications, therefore, have been focused primarily on this aspect of resilient cushioning materials. However, a general awareness has been developing relative to the fact that packaging design for critical and predictable levels of protection must also consider the vibratory properties of the cushion.

When a packaged item is supported in a cushioning material, an oscillatory system is created. In such a system, the cushion suspension may be expected to resonate at specific vibration frequencies. And consequently, when this happens vibration within the package will be amplified; now, instead of providing a protective influence, the cushion suspension is actually creating a potentially hazardous environment for the packaged item. To avoid this internally created vibratory hazard, it must be possible to predict the exciting frequencies at which the cushion suspension system will resonate. Knowing this, it would be possible to predetermine whether or not the packaged item would be exposed to these frequencies (and possible damaging resonance) during the anticipated modes of transportation.

Earlier efforts to evaluate the resonant characteristics of an expanded thermoplastic closed-cell foam in a simulated package configuration were reported in Picatinny Arsenal Technical Report 3160, Vibration Testing of Resilient Package Cushioning Materials. This investigation revealed that the foam, when vibrated "steady state" at frequencies near resonance, suffers a severe loss in mechanical properties. While the tests were nominally conducted at room temperature, the observed deterioration of the foam was aggravated by the vibration-induced temperature rise in the interior of the test samples. Due to the low thermal conductivity of the closed cell structure, heat generated in the interior of the foam samples could not be readily dissipated. The thermally plasticized cell walls were progressively ruptured by the repetitive compression of the enclosed gases. As a result of this phenomenon, therefore, two observations were inescapable: should the package employing this foam be exposed to long term resonant excitation, either in testing or in shipping, the subsequent protection provided for the packaged item could be suspect; and, in order to avoid this degradation during testing, and therefore be able to collect meaningful vibration data, it would be necessary to develop some test technique other than "steady state" vibration excitation.

Therefore, as a result of the observations from the work reported in PATR 3160, it was proposed that in subsequent investigations, vibrations be applied to the simulated package in a continuous, programmed "sweep" of the frequency spectrum. It was felt that this technique of application would minimize the excessive "working" of the foam under test and consequently reduce the generation of heat. Further, it was proposed that by a proper choice of rates of frequency change, it should be possible to simulate a steady-state condition for both vibration response and material properties. It was also anticipated that sweep testing would minimize ambiguities associated with nonlinear vibrational instability.

The work discussed in this report represents an implementation of these proposals.

Specifically, answers were sought to the following questions:

1. Would the application of the sweep testing techniques and equipment produce consistent delineation of "in-package" vibration response of an expanded polyethylene foam?
2. Could the transmissibility curves of the "package," generated via sweep tests, be correlated with steady state transmissibility curves for the same configuration?
3. Would comprehensive application of the sweep technique to several thicknesses of the foam, under a broad range of static stresses and excitation levels, permit a general prediction of resonant behavior "in-package"?
4. Would similar generalization be possible as to the vibration attenuation characteristics above resonance?
5. Would vibration sweeps through resonance alter the material's properties at any excitation level within the test envelope (MIL-STD-810, Common Carrier Vibration Test)?
6. If alteration does occur, is it subject to stabilization, or is the deterioration progressive? If stabilization is possible, what is the optimum method for effecting it?

The current work has produced substantial answers in these areas of inquiry. Graphical presentations suitable for engineering design purposes have been developed. Insight into the material's vibratory behavior relative to design application has been established. In addition, observations pertinent to further experimental work are made. Accordingly it is felt that the work described constitutes a substantial contribution to the state-of-the-art in this area of material application.

TEST EQUIPMENT

A commercial vibration sweep frequency generator was obtained and the feasibility of programming the desired sweep rates into the electro-hydraulic vibrator was investigated. It was found necessary to make extensive modifications to the vibration system in order to produce stable, reproducible sweeps, utilizing acceleration feedback.

A direct response recording system was developed to allow concurrent plotting of transmitted vibratory accelerations against frequency of excitation (logarithmic coordinates on both axes). To obtain the desired performance, the completed system included both modified commercial instruments and laboratory-fabricated components. Details of the vibration programming and recording system are described in the "Discussion of Equipment" section, Appendix B. The following physical improvements have been made in the cushion test fixture (simulated "package") described in PATR 3160:

1. The 10 mv/G accelerometers were replaced with 100 mv/G transducers to improve the signal-to-noise ratio. The change permits the recording of acceleration levels down to 0.1 G.
2. The response accelerometer was relocated from the periphery to the interior of the cushioned mass. This relocation minimizes the potential influence of high frequency rocking modes on the indicated translational response.
3. A pre-load "jack" (Fig 2) was incorporated into the test fixture. This jack allowed investigation of the effects of overall compressive preloads on vibration modes as well as investigation of related physical effects. The sensitivity of the vibrational properties of the compression-compression cushion configuration to superficially "slight" variations in fixture adjustment is examined in "Discussion of Results." A secondary benefit derived from the addition of the pre-load jack was the elimination of the "creeping" of the top plate

clamps under intense resonant loading. (The present fixture configuration is shown in Figure 1.)

4. Capability for measurement of the dynamic displacement of the cushioned mass relative to the exterior fixture was developed late in the program. The development allows recording of dynamic force vs displacement relationships governing the cushioned mass motion (the "force" function is derived from the unfiltered mass acceleration signal). (The dynamic displacement facility is depicted in Figure 2. Characteristic dynamic force displacement relationships appear in the same figure.)

Initial transmissibility tests on the polyethylene foam were sponsored by the ASTM D-10 subcommittee. These tests were intended to correlate the results of sweeping frequency transmissibility tests to "steady-state" tests, and the pertinence of several other application variables (e.g., "prework" and sample dimensions). The susceptibility of the polyethylene foam to the "linearization" process at the arbitrarily chosen levels of bearing stress and dynamic input (1.0 psi and 2 G respectively) was revealed. The bulk of the testing covered in the remainder of this report explored the response characteristics of the foam at combinations of bearing stress and dynamic input up to those combinations that would initiate the transition process--i.e., the vibration properties of the virgin foam.

TEST RESULTS

ASTM Tests

Typical response curves of the 2-inch polyethylene foam under 1.0 psi loading are shown in Figures 8 through 11. The curves are mass response acceleration vs frequency for a constant 2G forcing vibration. Figures 8 and 9 are the curves for virgin samples of 64 and 16 sq in. bearing area, respectively. Figure 10 is a response curve for the preworked 64 sq in. sample (10 cycles, 10% strain). As noted, the vibration test sequence in these curves was (1) sweep No. 1, 7-200 Hz - 7 Hz; (2) sweep No. 2, 7-200 Hz - 7 Hz; (3) steady

state tests. Figures 12 and 13 are "steady state only" curves taken on 8 x 8 x 2 inch virgin cushions for 1.0 psi static load and 2-G dynamic input. In Figure 13 the steady state points were taken first in frequency decrements through the resonant frequency and then in frequency increments from below resonance to 200 Hz. In Figure 12 the sequence is reversed for a second pair of virgin cushions.

A statistical summary of the ASTM tests appears in Tables 1 and 2.

Comprehensive Tests

The maxima of the mass response curves for each thickness tested are plotted as a function of static stress and dynamic excitation in Figures 14 through 17, "vibration transmitted at resonance vs resonant frequency." To determine the resonant frequency for a particular thickness, static stress, and forcing acceleration, the plot for the pertinent thickness is selected and the intersection of the static stress and forcing acceleration established. Vertical projection of the intersection to the "resonant frequency" axis defines the resulting resonant frequency. The magnitude of the vibratory acceleration transmitted to the mass is determined by a horizontal projection from the static stress-forcing acceleration intersection to the "resonant vibration transmitted" axis.

The plots of effective modulus vs relative excitation that appear in Figures 14 through 22 were derived from the resonant "grids" of Figures 15 - 18. Effective Modulus (E_{eff}) is defined here as the elastic modulus for a linear undamped cushion system which would have the same resonant frequency as that recorded for the actual system under a particular combination of influencing parameters. The natural frequency for the linear system is given by:

$$f_n = 1/2\pi (K/M)^{1/2}$$

f_n = natural frequency of free vibration

K = spring "stiffness" in psi

M = mass in (LB sec²/in.) = wt. in pounds
: grav. acceleration, g in inches/sec²

Substituting the mass and stiffness equivalents for the distributed cushion mass system:

$$f_n = \frac{1}{2}\pi (EA_g/WT)^{\frac{1}{2}} = \frac{1}{2}\pi (Eg/S_s T)^{\frac{1}{2}}$$

E = elastic modulus = normalized stiffness in psi

A = cushion bearing area (sq in.)

T = cushion thickness (inches)

Hence the effective modulus in terms of the application parameters becomes:

$$E_{eff} = [(2\pi f_r)^2 S_s T / g]$$

f_r = experimentally determined resonant frequency

S_s = static stress in psi = cushioned wt : bearing area

The abscissa for these plots, "relative excitation," is a dimensionless parameter established by dividing the peak sinusoidal forcing displacement at each resonant point by the (single) cushion thickness:

$$\begin{aligned} \text{relative excitation, } \phi &= d_{pk}/T \\ &= Gg/(2\pi f_r)^2 : T = Gg/(2\pi f_r)^2 T \end{aligned}$$

"G" = peak vibratory acceleration in "G" units = vibratory acceleration in in./sec² : by gravitational acceleration, g in in./sec². Relative excitation might also be termed "forcing strain." The actual cushion strain would be the "forcing strain" times a resonant amplification factor.

The E_{eff} vs ϕ plots are an approach to normalization of the resonant response data. An objective here is the possibility of separation of the effects of nonlinearity (variation of modulus with displacement) from rate sensitivity of the material (variation of the apparent elastic modulus with frequency of excitation). The numbers appended to the data points represent the resonant frequencies at which the parameters were derived.

Figure 23 is a plot of peak forcing displacement vs frequency of excitation for the constant vibratory accelerations employed in testing. This plot is provided as an aid in determination of ϕ for an environmental vibration defined in acceleration units.

The plots of resonant amplification vs ϕ in Figures 24 through 27 have a similar objective to the E_{eff} vs ϕ plots, i.e., normalization of the resonant data and separation of influence parameters.

The mean relationship for E_{eff} vs ϕ , indicated in the composite plot of Figure 28, has been used to derive a generalized approximating function for resonant frequency: $f_r = 26.7/S_s (GT)^{1/2}$ (see Discussion of Results).

The relationship provides a good approximation of the f_r 's established in testing for ϕ 's greater than .0005. A family of curves portraying the empirical function appears in Figure 29. The resonant frequency, f_r , is plotted as a function of the forcing acceleration - thickness product for twelve values of static stress. (For values of ϕ less than .0005 an empirical equation for f_r , $f_r = 57.7/(S_s T)^{1/2}$ provides closer fit to the experimental data.)

In Figure 26 (the composite plot of resonant amplification vs ϕ for all thicknesses tested) the shaded area represents the envelope for resonant amplification at all static stresses - with the exception of 0.2 psi. The dotted curve representing the mean of the envelope provides a reasonable estimate for resonant amplification for a known value of ϕ . The G's transmitted at resonance may then be approximated by multiplication of the forcing acceleration by the estimated amplification factor.

Thus Figure 26, in conjunction with Figure 28, constitutes a summary of the resonant response states that may be induced in the polyethylene foam in the "dual compression" mode as a function of application and imposed vibration parameters.

Figure 14 is a summary plot of the "threshold" input accelerations for specific static stresses beyond which the "linearization + set" process was induced in a single sweep through resonance. (The numbers appended to the data points represent the associated resonant frequencies.) The inference of the plot may be summarized: $[G_{ex} (S_s)^{1/2} > 1]$ = fatigue susceptibility. Since the data points are pertinent to resonant excitation, the validity of the statement is subject to the indicated "threshold G" for the application stress being present in the environment at the resonant frequency of the configuration. The pertinence of this condition may be evaluated by reference to Figure 29.

DISCUSSION OF RESULTS

General

As a preface to consideration of the importance of the test data, a critical examination of certain basic characteristics of the "compression-compression" cushion configuration is instructive. As noted in PATR 3160, this configuration probably reflects the most common application mode of cushioning in protective packaging. In this application the item to be protected is enveloped in the cushioning medium but is not bonded to it. Under the influence of vibration in the vertical direction, the cushioning material is stressed in compression only, the cushioned item loading the lower and upper cushion pads alternately (possible shearing action in the side cushions through friction coupling to the item being neglected). Further examination of the general "dual compression" configuration indicates that three basic variations in initial geometry are possible. These variations, while subjectively superficial, strongly influence the vibration transmission properties of the total package.

The three generic initial loading modes are shown schematically in Figure 3. Type I loading, the "normal preload," results from straightforward assembly of the test "package." The static load weight is placed upon the lower cushion and allowed to compress it until the developed force in the cushion equals the load weight, and static equilibrium is established. The resultant deflection of the cushion (δ_{static}) is determined by

the static stress-strain characteristic of the cushion. This is shown in graphic form in Figure 4. The top cover, with upper cushion attached, is then positioned so as to bring the top cushion into unstressed contact with the mass in its static equilibrium position. The top cover is fastened in this position to the guide fixture (exterior "container") to complete the test package. (This arrangement is analogous to reducing the overall depth of a container to compensate for static deflection and maintain a "tight pack.") The vibration test results of this configuration may be considered to relate to the drop test configuration of ASTM D-1596-59T, wherein the top cushion does not appear and there is no preload on the bottom cushion other than the static stress. Since the cushioning of a package with only a bottom cushion is scarcely defensible, the upper cushion may be inferred to be present in a "phantom" role in that test.

The type I configuration was used in the bulk of the testing reported herein. An important feature of this initial alignment can be seen in Figures 3 and 4. In downward excursions of the weight from equilibrium, compressive restoring forces are generated only in the bottom cushion. In upward displacements, however, both cushions are acting on the weight over the displacement interval, δ static. Since the cushions are operating in series opposition in this interval (the downward force of the top cushion is increasing while the upward force in the bottom cushion is decreasing), the overall "spring rate" or "stiffness," $K = \Delta F / \Delta D$, is equal to the sum of the K's of the individual cushions. For identical cushions, top and bottom, the combined spring rate in upward excursion will be twice that for the single cushion (assuming linearity of both cushions in the interval without hysteresis). The "normal" preload configuration is thus seen to be intrinsically asymmetrical and nonlinear in stiffness about the static equilibrium position of the mass - even with identical, essentially linear cushions, top and bottom. Certain aspects of nonlinear vibration phenomena will therefore always be more or less prominent in the vibration transmission properties of this package configuration.

The asymmetry of a stiffness would be expected to cause the observed resonant frequency, for a particular thickness and static load, to vary with the level of vibratory excitation of the exterior container. The data indicates that the behavior is that of a "softening system"-the resonant frequency decreases with increasing excitation. The amplification at resonance also reduces with increasing excitation, which may be attributed in considerable degree to nonlinearity of stiffness. The nonlinearity of the "normal preload" configuration would thus seem to operate to the benefit of the cushion item.

A disadvantage not immediately obvious is the inequality of dynamic excursions of the cushioned mass induced by the asymmetrical stiffness condition. The cushion-mass system in the normal preload configuration tends to adjust to symmetrical fixture (exterior container) oscillations with unequal displacements of the cushioned mass. The motion in the upward direction is inhibited by the "two-cushion stiffness" operating in that direction as compared to the single cushion stiffness active in downward excursions. As a result, the lower cushion is subjected to an exaggerated dynamic strain as well as the static load bias (this effect was verified with the introduction of the dynamic displacement measurement facility into the test vehicle). The lower vibration level transmitted at resonance to the cushioned item is therefore achieved at the expense of increased fatigue susceptibility of the lower cushion as opposed to the upper one. Since shock protection in larger packages is primarily associated with the bottom cushion (a greater control of handling orientation is likely in larger packages), this characteristic of the "normal preload" format is probably a significant drawback.

It would appear that, where the greater fabrication cost was warranted, the advantage of asymmetry could be exploited by using a thicker cushion at the top of the container rather than at the bottom. The greater excursions would thus be sustained in the "softer" upper cushion. However, since the upper cushion is thicker, the greater excursion would not necessarily represent a larger dynamic strain than that induced in the thinner lower cushion. The vibrational advantages of asymmetrical nonlinearity could therefore be achieved with a

better balance of a fatigue susceptibility in the upper and lower cushions. Subjective opposition to providing "more cushioning" over the item than under it could be met by using a lower density cushion of the same thickness on top.

The intrinsic nonlinearity in stiffness of the "normal preload" configuration can sometimes be suppressed by superimposing an additional compression on the configuration. This "overall precompression" is shown schematically in Figure 3 (Type 2) and graphically in Figure 5. The top plate is depressed and fixed beyond the "normal preload" position so that an additional deflection, ΔD , is impressed on the bottom cushion. For static equilibrium to be established, the resulting increment in upward restoring force, ΔF , must be equal to the downward force induced in the top cushion. For equal static spring rates over the range of induced compressive displacements, the additional displacements in the top and bottom cushions will be equal, and the total superimposed compression (reduction in package height) will be equal to $2 \times \Delta D$. For linear cushions, Figure 5 indicates that a symmetrical, linear, force vs displacement relationship is established about the static equilibrium position of the weight. The effective stiffness, $\Delta F/\Delta D$, is seen to be twice that for a single cushion. This doubling of spring rate occurs for excursions from equilibrium of magnitudes up to ΔD and $\Delta D + \delta_{\text{static}}$ in the downward and upward directions, respectively.

It may be observed in Figure 5 that the superimposed compression, while equalizing the F vs D function about the static equilibrium position, will result in a more abrupt departure from linearity in the presence of the "buckling" type of nonlinearity - the type frequently encountered in cellular cushioning. This type of nonlinearity is evident in the 1.0 in./min in the stress-strain curve for the polyethylene foam and may be expected to extend to its more rapid dynamic reactions as well. The effects described above were apparent in exploratory vibration tests on polyethylene foam with superimposed preload. (The resonant frequency and amplification for a particular static stress-thickness combination were relatively independent of forcing vibration amplitude over a relatively wide range. The shift of resonant frequency, when encountered, was extremely abrupt.)

A readily comprehended advantage of the precompressed system is that it permits "total" (top + bottom) vibratory set, or creep, to take place up to $2\Delta D$ in magnitude without loss of static contact of the mass with the upper cushion. From the application standpoint, the orientation of the cushioned item would be maintained in spite of static creep in the lower cushion or dynamically induced thickness loss in one or both cushions. The earlier discussion of the "normal preload" configuration described the effect of the associated "asymmetry of stiffness" on the relative vibratory strains induced in upper and lower cushions. The equalization of directional stiffness effected by precompression might be expected to have an equalizing effect on the dynamic excursions of the cushioned mass under externally applied vibration. The dynamic displacement measurement system has verified this equalizing influence. Additional potential advantages of the "overall precompression" format from the testing standpoint are pointed out in subsequent paragraphs.

Before entering that area it is desirable to define the third state of geometry alluded to in the introductory paragraph. This third configuration will be referred to as the "uncompensated" format. It can be conceived as resulting from a "snug" assembly of the mass and two cushions in the horizontal plane without preload. On rotation of the cushion-mass system into the vertical plane, the weight compresses the lower cushion an amount, δ static. If the upper cushion is restrained in place at the top of the "container," a gap equal to δ static develops between the upper surface of the cushioned mass and the lower surface of the top cushion. This condition is shown schematically in Figure 3.

Under the influence of external vibration, the mass oscillates solely in contact with the bottom cushion until the upward mass excursions exceed δ static. At that point the mass makes contact with the upper cushion, and its properties come into play. Only a single cushion acts on the mass at any one instant, since the mass loses contact with the lower cushion at the point that contact with the upper cushion occurs. The configuration may therefore have possible subjective appeal in that the overall vibration transmissibility may be ascribed to the properties of a "single"

cushion. However, a smooth transition from "bottom-only" to alternate cushion loading will be effected in the "gapped" package only if the gap is exactly equal to δ static. For lesser gaps, simultaneous loading occurs over a portion of the range of upward mass travel.

For gaps greater than δ static, three modes of oscillation are possible: (1) the mass oscillating in contact with bottom cushion only, (2) the mass "bouncing" on the lower cushion, leaving the lower cushion but not contacting the upper cushion, and (3) the mass bouncing "between" upper and lower cushions. In a vibration sweep through resonance, all three modes of vibration are likely to be induced in various portions of the frequency range. A discontinuous vibration transmissibility value occurs at a frequency where the mass achieves or loses contact with the upper cushion. The location of the discontinuity will vary with the direction of the vibration sweep.

Because of the ambiguity of vibration behavior, and questionable pertinence to actual design application, the "uncompensated" or "gapped" package was not extensively utilized in the general testing of the polyethylene foam. However, exploratory tests were performed with this format when the dynamic displacement measurement system was incorporated into the test vehicle. The objective was the verification of a reasonable postulate: "The vibratory hysteresis loop of the individual cushions in the dual compression format must 'close' at zero strain, i.e., on the compressive unloading motion there must be no residual compressive 'set' when the developed stress reaches zero." This criterion is imposed by the absence of tensile restoring mechanisms to "cancel" compressive sets. Violation of the criterion implies a progressive compaction of the cushion under sustained vibration. Another alternative is foreseen: "Cumulative dynamic set must reach a stable, 'acceptable' value." This can take place only if the magnitude of the "set per cycle" diminishes rapidly with continuing vibration.

The two criteria summarized above are pertinent to the observed reactions of the polyethylene foam. For static dynamic load combinations below threshold values the first criterion was apparently satisfied. For combinations beyond the threshold, the transition process referred to elsewhere in the report was initiated. A rapid progression to a stable "linearized" form ensued, which again apparently satisfied the first requirement. The requirement for "closure" of the individual hysteresis loops implies that the composite force vs displacement function of the cushion-mass system must assume in the absence of simultaneous cushion activity a "figure eight" type characteristic. This pattern is exhibited by a dynamic F vs D curve generated by the "gapped" polyethylene foam package (Figure 2b). The "figure eight" pattern considered as a Lissajous figure indicates the introduction of second harmonic ("double frequency") components into the motion response of the cushioned mass with sinusoidal ("single frequency") excitation of the package as a whole. For linearity to exist in both elastic and damping qualities the composite curve must be a straight line (zero damping) or elliptical (finite damping). It thus appears that the package arrangement allowing alternate compressive cushion loading is also intrinsically nonlinear.

In Figure 2c an actual dynamic F vs D curve for a "normal" preload package is depicted. The asymmetry in stiffness, predicted earlier, is apparent. An additional feature is noted. The introduction of simultaneous cushion loading in upward mass excursions produces a single closed hysteresis loop, in contrast with the two "lobes" of the "gapped" package.

The "normal preload" format was produced by reducing vertical package height to "compensate" for static deflection in the "gapped" or "uncompensated" package. "Superimposed" or "overall" preload is produced by further height reduction to place both upper and lower level cushions in a state of static precompression. A dynamic F vs D curve recorded for the configuration appears in Figure 2d. The dynamic "loop" is found to be strongly elliptical in character. The application of overall static precompression appears capable not only of equalizing the gross unbalance of stiffness of

the "normal preload" package, but "linearizing" the necessarily nonlinear "loss" behavior of the individual compression cushions. The relative "purity" of the generated ellipse indicates that the induced motion in the cushion-mass system was nearly sinusoidal for sinusoidal excitation of the exterior fixture or "container." In suppressing the second harmonic components of mass motion, the "overall" preload package may be considered to act analogously to "push-pull" amplification in electronic circuits. The effect is probably due to the fact that, at any one instant, one of the cushions is on an "unloading" path while the other is "loading."

In summary, it is apparent that the "dual compression" cushioning configuration constitutes a complex vibratory system. Several basic application factors tend to introduce nonlinear behavior into the vibration response of the composite cushion-mass system. Consistent vibratory response can be obtained only by some preloading of the cushioning material.

Without preloading, the cushions are loaded in a quasi-impact fashion, with extremely complex and variable motions possible. "Overall preload" of the cushion-mass system can establish a state of pseudo-linearity in the observed vibration parameters of the system. The linearity can obviously be established for only a limited range of oscillations, since the cushions must eventually become nonlinear in compressive stiffness, or the preload range exceeded. Preload must also be evaluated against creep considerations. However, the "overall preload" format warrants further experimental investigation in that its susceptibility to linear analysis could establish a linear "baseline" from which nonlinear departures may be more readily evaluated.

The "normal preload" configuration, for which the bulk of the data on the polyethylene foam has been accumulated, is intrinsically nonlinear. For a continuously nonlinear cushioning material, each static loading should theoretically constitute a functionally unique vibratory system since the static loading contributes a gravitational as well as an inertial factor, i.e., the static loading determines the state of lower cushion prestress, as well as the inertial loading per square inch of cushioning bearing area.

The variation of operational stiffness in the lower cushion with static stress is not, in general, related to the variation of inertial loading with that parameter. Therefore complete normalization of data for the effect of static stress is unlikely for this configuration. On the other hand, if the cushioning material is homogeneous in the direction of loading or if it is tested in multiples of a single nonhomogeneous thickness, the observed vibration responses should be normalizable for thickness. As will be seen, normalization for the thickness and the inertial component only of static stress allowed fairly good generalization of material properties in the normal preload format.

ASTM

The six vibration response curves (Figure 8 through 11) included from the ASTM testing are typical of those recorded in that test sequence. The arbitrary values of static stress (1.0 psi) and dynamic input (2G) were chosen without prior knowledge of the material's properties. They resulted in the generation of several significant phenomena relative to application and test of the foam in the dual compression format. In the first upward frequency sweep on virgin samples (Figures 8 and 9), a response "jump" is apparent at 16 and 19 Hz for the 16 sq in. and 64 sq in. (bearing area) samples, respectively. (The jump in response could be observed visually, as well.) This jump may be attributed to the pronounced "buckling" effect evident in the static stress-strain curve for the polyethylene foam (Figure 6) at approximately 12% strain. Conversion of the peak mass acceleration at the "jump frequency" to peak equivalent sinusoidal displacement via the expression $d = 10G/f^2$ results in an approximate¹ indicated strain in the 2-inch-thick cushion of 12%. This strain is seen to correspond to a strain that lies on the "knee" of the stress-strain curve.

Beyond the jump frequency, the response continues to decrease at an average rate of approximately 12 db/octave. On the frequency sweep downward, the transmission

¹The formula yields absolute rather than relative mass displacement.

curve initially follows that of the upward sweep quite closely, indicating that, during the first upward sweep, negligible alteration of the cushions properties has occurred. After passing the upward jump frequency, however, the response is observed to continue to increase to a peak at 10 Hz for the 8-inch-square sample, and to a peak of 12 Hz for the 4-inch-square sample. The responses of 13 G for the former and 10 G for the latter represent amplifications of 6.5 and 5 to 1, respectively. Reference to the statistical summary in Tables 1 and 2 indicates the variations are largely due to deviations in the particular sample curves presented. Averages for 16 and 64 square inch bearing areas are seen to be much closer numerically.

The achievement of a significantly higher resonant peak in a downward frequency sweep is compatible with the behavior of "softening" or "buckling" cushion systems as discussed in PATR 3160.

The second upward sweep in Figures 8 and 9 produces a drastically altered response curve. The response jump between 16 and 19 Hz is totally absent in both specimen pairs. Instead, the response "peaks" at virtually the same frequency and amplitudes as established in the first downward sweep. Beyond this peak, the response drops abruptly to an attenuation rate approximately paralleling the initial curve, but which is displaced downward in frequency by approximately an octave.

This transition may be explained as follows: On the first upward sweep, the lower response states of the nonlinear system are excited. The response jump to the upper curve "by-passes" the maximum response state. On the first downward sweep, however, this maximum response state is excited with a maximum mass response of over 10 G. The equivalent sinusoidal displacement would entail a vibratory cushion strain of approximately 50%, well beyond the buckling point at about 12% strain. A plot of repeated low-rate stress

cycles in Figure 7 indicates that the buckling mechanism is relatively inelastic and that repeated strains beyond the buckling value result in progressive yielding, with corresponding reduction of the high initial compressive modulus (50 to 70 psi). This process is the "linearization" referred to in the summary. The cell membranes may be assumed to remain in a "pre-flexed" attitude after buckling, rather than returning to the geometry associated with the higher "pre-buckling" modulus. The repeated compression through buckling also results in progressive thickness loss (see Fig 7), but with diminishing incremental "sets" for each successive compression. The hysteresis loop is reduced accordingly. The progressive reduction in hysteresis losses would result in a corresponding increase in amplification under resonant vibration. Since it was noted that the "knee" or buckling strain was just attained at the first sweep "jump frequency," it is evident that sweeping downward below that frequency would result in very rapid "linearization." (The excitation amplitude for the constant 2 G vector acceleration increases as the inverse square of frequency, and the amplification would tend to increase as the inverse first power of the hysteresis loss.)

The time to traverse the frequency band 20 to 10 Hz, as shown in Figure 32, is approximately 32 seconds. The number of cycles of oscillation in that band, obtained by integration of the frequency relation, is approximately 460. The fact that "linearization" and "stabilization" have been essentially effected by the first downward sweep is verified by the close correlation of the second downward sweep curve with the second upward sweep curve, as well as by the subsequent good agreement of steady-state-excited responses with second sweep values.

In fact, there actually appears to be a slight indication of "stiffening responses," as evidenced by the upward displacement (in frequency and magnitude) of the second "up" sweep as compared to the "down" sweep. The "set" in the bottom cushion of each cushion pair, after the complete sequence, is equal numerically to approximately 12% of cushion thickness, indicating that the lower cushion is almost totally "buckled." The lesser value of vibration-induced "set" in the top cushion (6%) is indicative of the greater dynamic loading of the bottom cushion because of the static load

"bias." (While the bias is nominally "static," it results in an increase in peak dynamic strain in the lower cushion.) The asymmetry of stiffness in the normal preload format further exaggerates the dynamic strain in the lower cushion. The "sets" recorded in the top and bottom cushions are observed to total 3/8 inches. The set in the bottom cushion was measured after removal of the static load. If the set was induced without change in the static stiffness of the bottom cushion, the gap developed between the weight and the upper cushion would have been equal to that "total unloaded set." Since the lower cushion underwent "softening" as well, the actual gap was probably considerably larger.

The octave shift of the response curve above resonance, observed in the second sweep, and subsequent steady-state measurements, is attributable to the two related physical changes induced by the resonant vibration in the first downward sweep: (1) Reduction in modulus of the bottom cushion. (2) Development of the gap in the package.

Figure 7 indicates that a reduction of initial modulus by a factor of approximately 1/2 may be expected as a result of the permanent buckling of the foam. However, the octave response shift, if totally attributable to modulus reduction, would require a reduction factor of 1/4, since the resonant frequency is generally proportional to the square root of the modulus. The response acceleration at resonance, when converted to equivalent sinusoidal displacement, indicates that in the "gapped," "linearized" package, the mass loses contact with the upper cushion at a frequency slightly beyond resonance. The "downshifted" response curve therefore describes the response of the mass bouncing on, or vibrating in contact with, the linearized bottom cushion only.

From the standpoint of vibration isolation above resonance, the linearized, gapped, polyethylene foam package would seem numerically superior to the virgin foam in the original "normal preload" configuration. The relative desirability of this condition in an actual application must, of course, be evaluated in the light of its unfavorable aspect - the reduction in positive positioning within the container.

The prework cycle utilized on 50% of the 4 x 4 x 2 inch samples prior to vibration (10 compressions to 10% strain) is shown in Figure 11 to have produced, as compared to the unworked samples, relatively little variation in vibration response.

Increasing the severity of the prework (10 compressions, 20% strain) for the preworked 8 x 8 x 2 inch cushions did induce a noticeable effect on the response curve generated in the first frequency sweep. Comparison of a typical plot (Fig 10) with those for the cushions without prework indicates a downward frequency shift in the first sweep of approximately 1/6 octave for the response jump and the overall response curve. The first downward sweep through resonance again achieves almost total transition. This transition is evidenced by the absence of the upward response jump in the second sweep, as well as by a further shift of the high frequency portion of the curve to the position attained after the 3-test sequence in virgin cushions. A single sweep through resonance at the 2-G excitation level is obviously more effective in bringing about the stable linearized condition than the 20% compressive prework cycle.

As shown in Figure 7, an increase in low rate cyclic strain to 50% will produce relatively complete linearization, but not stabilization, of thickness loss.

The steady-state response points (taken after the second sweep on all cushion pairs) correlate best in the region of the response peak with the curve obtained for the second upward frequency sweep. As noted earlier, the terminal resonant characteristics of the cushion-mass system in the latter test sequence manifest a slight "stiffening" jump process. This process would allow the existence of multiple response levels at resonance. Figure 7 indicates that "stiffening" (increase of the modulus with increasing strain) starts at about 30% strain in the virgin foam, and 25% in linearized foam. With a dynamic strain of 50% estimated from the mass response acceleration, the appearance of the stiffening jump could be predicted after suppression of the drastic softening (buckling) nonlinearity.

The statistical comparison of the resonant frequencies in Tables 1 and 2 indicates relatively good correlation of resonant G's and frequencies in the second upward sweep and the corresponding values obtained in the steady-state tests which followed. The test curves included indicate that better correlation would have resulted had steady-state points been taken at frequencies intermediate to the integral frequencies used to define the resonant peak. (The value of peak response acceleration for a particular sample pair used in determination of averages for steady-state resonance was necessarily the maximum value excited for that pair. The 1.0-Hz integral frequency intervals had been previously decided upon as representing a feasible resolution for frequency that could be explicitly specified in steady-state test procedure.) The "sharpness" of the indicated resonant peak allowed it to fall, for some cushion pairs, between the integral steady-state test frequencies.

The maximum steady-state response value recorded for a particular cushion pair exceeded the corresponding second "up-sweep" value in only two instances (one example: Fig 9, sample pair 31 and 32). In both instances the differential was 0.5 G for an indicated steady-state response peak of 13.0 G. Since the transition to the "linearized," "stable" state involved a significant reduction in the hysteresis loop for the foam, the differential might well be attributable to somewhat less than total stabilization having been effected in the sweep peak. (It will be recalled that a downward sweep through resonance was imposed between the tests under comparison.)

As noted in Appendix A, the replicate test sequence discussed above was modified to the final format after initial steady-state tests on the virgin foam produced anomalous results because of "jump" phenomena and the transition process. Since a prime objective of the test series was the evaluation of the practical utility of sweep tests in defining "steady-state" vibration response, a steady-state condition of cushioning material properties was obviously mandatory for comparison.

Two of the more informative curves obtained in steady-state tests on the virgin foam are shown in Figures 12 and 13. In Figure 12, the data points were taken at frequency increments starting at 7 Hz and progressing up to 200 Hz. (The vibratory input was reduced to zero after taking a data point and allowed to build up to the 2 G value after the next frequency set point was programmed.) Subsequently the frequency progression was reversed, again suppressing the vibratory input between frequency setpoints. It will be noted that in this sample pair, the lower response path and subsequent "jump" are precisely defined, indicating that the jump recorded in the first upward sweep in the replicate tests is a definite facet of steady-state behavior of the virgin cushion system. It will be noted further that in the decreasing frequency set points, the higher level response states were encountered below 25 Hz. Stable excitation was effected down to 15 Hz. Below that frequency, the recording pen jumped erratically between upper and lower responses as indicated, with similar behavior of the cushioned mass being observed visually. (The lower limit of the pen excursions lying above the previously established locus of "low level response" would indicate that "linearization" of the cushion was in progress.)

In the second plot of "steady-state only" testing (Fig 13), the data points were taken in reverse progression (downward in frequency through resonance, and subsequently upward.) In this particular sample pair, the steady-state points on the "high level" response path were quite stable, even during the process of linearization. Subsequent upward frequency data points verify that the "linearization + thickness loss" had been effected by the preceding resonant excitation. The resultant curve is seen to be identical to the terminal "steady state" curves of the replicated test sequence. (In the upward steady state plot of Figure 13, the maximum response point at 11.2 Hz was "tuned" by slight variation of frequency about the 11-Hz setpoint, to precisely resolve the resonant frequency and resonant response values.)

Comprehensive Testing

In the ASTM test series the "true" resonance for the particular static stress and thickness combination could not be excited in a sweep at the chosen excitation level without causing a rapid change in material characteristics and an accompanying thickness loss. Subsequent tests on several thicknesses of the foam under a range of static stresses from .2 to 2.0 psi indicated that, for a particular thickness and static stress, dynamic excitation thresholds appeared to exist. For excitation levels below the threshold, repetitive sweeps could be performed with negligible variation in the response curve. Forcing accelerations above the threshold resulted in the phenomena observed in the ASTM tests, i.e., rapid thickness loss, linearization of the foam's stress-strain relationship, and a corresponding shift downward in the response curve. As would be expected, the level at which the linearization was initiated varied inversely with the static stress.

A plot of static stress vs the highest excitation level not inducing the shift in characteristics is made in Figure 14 for the thicknesses tested. Combinations of static stress and forcing accelerations below the plotted points may be assumed to be relatively insensitive to the linearization phenomena. (It may be observed that in some instances, for a particular thickness, the indicated forcing acceleration did not change for an incremental change in static stress. The actual threshold value in these cases may be assumed to be between the last acceleration input not inducing linearization and the next higher programmed acceleration.) An average curve for the points plotted would appear to be a straight line on the logarithmic coordinates with a linear slope of $(-\frac{1}{2})$. An empirical relationship of the form $G = C(S_s)^{-\frac{1}{2}}$ is inferred. Both upper and lower "edges" of the data distribution appear to follow a similar trend. A "fit" for the upper edge of the envelope is found to be $G_{ex} = 1.3(S_s)^{-0.54}$ and for the lower edge $G = (S_s)^{-\frac{1}{2}}$. Because of its simplicity, and in the interest of conservative application, the latter relationship would appear to be a useful guide. A restatement of the function might be made as: $G_{ex} (S_s)^{\frac{1}{2}} > 1 =$ fatigue susceptibility. The combination employed in the ASTM testing ($G = 2, S_s = 1$) is seen to lie well above the outer envelope.

It will be noted that the empirical relationship is independent of frequency, as stated. The data points, however, were derived for an acceleration level that sweeps through the resonant frequency and therefore includes the effect of resonant amplification. Thus, for use of the function as a criterion for "susceptibility," the limiting environmental acceleration indicated for a tentative static stress must be present in the environment at the resonant frequency of the particular cushion-mass system.

The natural frequency relationship for a linear cushion-mass system was obtained earlier by substituting the distributed elastic spring constant into the single-degree-of-freedom function to obtain: $f_r = \frac{1}{2}\pi (E'_g/S_s T)^{1/2}$. In the general nonlinear cushion system the elastic modulus, E' , is not a constant and may be a function of many variables: $E = P(\delta, f, \text{Temp}, S_s)$. However, since S_s and T are discrete application variables, they must have specific values for any actual test.

In Figures 15 through 18 the maximum response accelerations recorded, and the frequencies at which they occurred, are plotted as a function of static stress and forcing acceleration for those thicknesses tested. The stable resonant frequencies measured (for the range of static stress and thicknesses tested) ranged from 9 Hz to 120 Hz. Assuming linearity, and based upon the approximate "initial" static modulus of the foam of 50-70 psi, an overall range of resonant frequencies of approximately 8 to 56.0 Hz would be estimated. Obviously, nonlinearity and/or dynamic effects were present in the test results. As had been discussed earlier, however, the "normal preload" configuration used in the testing introduces nonlinearity, increases the effective spring rate, and hence the apparent modulus.

In order to gain an insight into the relative effects of the parameters causing the deviation, various schemes for "normalizing" the "resonant grid" data were attempted. In the equation for the natural frequency of a linear cushion system, the factor " E' " the elastic modulus, is the parameter that is characteristic of the material rather than the application. Its variation as a function of specific parameters affecting it in a dynamic application therefore constitutes a partial description of the

dynamic properties of the material. Modulus is generally defined as the ratio of an infinitesimal incremental stress to the resulting infinitesimal incremental strain.¹ Since the dynamic strains were not measured across the cushions in the bulk of the vibration testing, the modulus plotted in the normalization curves (Figures 18 through 22) could not be actual instantaneous values. The modulus considered here is the "equivalent linear elastic modulus" or more briefly, "effective modulus." The effective modulus may be defined as that value of E which, when inserted into the function for the natural frequency of a linear cushion system, will yield a frequency equal numerically to the resonant frequency measured in a nonlinear system under a particular set of application variables.

The parameter chosen for normalization was "relative excitation," ϕ . It represents the ratio of the forcing vibratory displacement into the cushion-mass system to the single cushion thickness.

The reasoning here is as follows: The elastic modulus is known to be affected by several factors. For viscoelastic materials at constant temperature, the elastic modulus may vary with frequency of excitation. The effective modulus for the test configuration is also affected by the static stress, which determines a particular initial asymmetry of stress. Due to its cell structure, the static modulus of the material is drastically nonlinear; the dynamic modulus may be expected to evidence a similar nonlinearity with strain. The dynamic strain in the cushion was not generally measured

¹In sinusoidal loading of viscoelastic materials, the strain is not generally in "phase" with the stress but lags it in time. Under those circumstances the "elastic modulus" is regarded as the ratio of the component of stress in phase with strain, to the strain. As was pointed out earlier in the discussion, the actual loading function induced in the individual cushion was nonsinusoidal for sinusoidal input to the future.

i. the testing. However, this dynamic strain is the dynamic relative displacement divided by the cushion thickness. The dynamic displacement across the cushion at resonance is the dynamic displacement input to the system, times some resonant amplification factor. However, this factor is not a constant independent of forcing amplitude, since it must eventually be limited by "bottoming," or some earlier nonlinearity. The vibratory input displacement in the tests is not a normalized parameter since the same schedule of forcing amplitudes vs frequency was applied for all thicknesses of material (Fig 29).

However, for a particular thickness of material and for a particular forcing amplitude at resonance, a certain range of strains will be traversed, and a certain "effective" elastic modulus will be operating. An increase in forcing displacement would drive the mass farther into the nonlinear cushions, and a different effective modulus would result. It is readily seen that reduction of cushion thickness for a constant forcing displacement would have a similar effect on strain-sensitive parameters as the increase in displacement for a particular thickness. For a 6-inch-thick cushion, a resonant displacement amplification of 5 to 1 for a forcing displacement of .5 inch is possible. A 5:1 displacement amplification is obviously impossible for a .5 inch displacement input applied to a 1-inch-thick cushion pair. Thus the strain sensitivity of the dynamic elastic modulus would appear to be properly expressed in terms of its variation with the ratio of forcing displacement at resonance to the cushion thickness. This parameter is referred to in this report as the "relative excitation," δ (an alternative designation would be forcing strain). The dimensions of the parameter are seen to be in./in.

In the vibration sweeps conducted at constant vibratory acceleration, the vibratory displacement input reduces as frequency is increased by the relationship $d_{pk} = 10G/f^2$. The corresponding displacement excitation spectrum for the constant "G's" excited in the testing are plotted in Figure 23.

Since the displacement inputs changed continuously in each sweep, the ϕ value changed continuously also. The values for ϕ in the plots are therefore derived from the input "G" values and the resultant resonant frequencies established for a particular thickness and static stress. It is possible that more cohesive plots of E_{eff} vs ϕ would have resulted had vibratory displacement input, rather than vibratory acceleration input, been held constant in the tests (i.e., tests conducted at constant ϕ).

The most coherent plot is seen to be derived from the 1 7/16-in.-thick material, with all points but one lying on a well defined curve. The effective modulus is seen to tend toward a constant value at low values of ϕ - which, upon reflection, is reasonable. The "effective modulus" was derived by assuming different linear elastic moduli as controlling the resonant frequency at different amplitude levels in a nonlinear cushion-mass system. Each value for E_{eff} , therefore, defines a linear stress-strain relationship through the static equilibrium point. As the amplitude of oscillation is reduced to very small values, the line established by the corresponding E_{eff} approaches a tangent to the actual stress-strain curve controlling the motion of the mass about the static equilibrium point.

This analysis may appear to conflict with the graph in Figure 4. This graph portrays a discontinuity in the stress vs strain relationship at the static equilibrium point in the "normal preload" configuration. Obviously the tangent would be undefined under those conditions. The apparent conflict stems from the simplistic portrayal of the F vs D for the cushions in Figure 4 as straight lines extending through zero deflection. In the case of the polyethylene foam, the actual stress vs strain curve (Figure 6) shows a concave transition region to the quasi-linear region before the buckling point. As a result, the combined F vs D relationship for the "normal preload" arrangement will have a relatively smooth transition at the static equilibrium point between the "single slope" and "double slope" characteristic. A relatively well defined tangent (and hence effective modulus) would thus be plausible.

A comparison of Figure 6 and 20 indicates that a maximum "static" modulus of 70 psi occurs in the quasi-linear area before buckling; while an average effective modulus of between 350 and 400 psi is indicated at low ϕ 's in the vibration test data.

Because of the asymmetrical character of the "normal preload" format, the effective modulus at low oscillation amplitudes would be expected to be greater than the single cushion value, by a factor lying somewhere between 1 and 2. The actual value derived from the testing is greater than the single cushion static value by a factor of at least 5 to 1. A minimum dynamic factor of at least 2.5 to 1 is therefore active on the elastic modulus at low values of ϕ .

A means frequently used to describe the dynamic stiffness effects in homogeneous elastomeric materials (at constant temperature) is the plot of elastic modulus vs frequency.

If the variation of dynamic elastic modulus of the foam tested was continuous over the range of frequencies covered in the tests, one would expect that, for a constant value of ϕ , a vertical distribution of E_{eff} would occur that would be pertinent to the multiple f_r 's excited at the same value of ϕ . "Parallel" contours of E_{eff} vs ϕ could then be established for different values of resonant frequency. (The multiple frequency points for a particular cushion thickness resulted from the varying static stress in the tests; this stress varies the inertial loading on each square inch of material.) While vertical scatter of E_{eff} is seen to be considerable in the E_{eff} vs ϕ plots for some of the thicknesses tested, the stratification would not conclusively appear to be related to frequency. In the 1 7/16 in. thickness plot (Fig 20) points of approximately equal frequency are seen to lie directly on the curve of E_{eff} vs ϕ for widely varying values of E_{eff} . This would seem to indicate that the wide range of effective moduli encountered in the testing was largely attributable to variation with ϕ , rather than frequency. A further inference is thus contained in the plots: The dynamic multiplying factor on the modulus noted earlier must vary quite slowly over the range of resonant frequencies spanned in the tests. This frequency range was seen in the G transmitted vs f_r plots

(Figs 15-18) to span approximately a decade, 9 to 120 Hz. The "static" stress-strain curve for the polyethylene foam was taken at a loading rate of 1.0 inch/min. on a 4-inch-thick sample. Converted to a cyclic rate for 2 cushions, a cycling "frequency" of 1.7×10^{-3} Hz results. A span of frequency of approximately 5 decades therefore separates the frequencies at which the ratios of maximum static and dynamic moduli were estimated. Thus a relatively small variation in the dynamic factor over the range of test frequencies is not incompatible with the maximum dynamic factor inferred in the E_{eff} vs ϕ plots.

In the larger thicknesses tested, considerable vertical dispersion of E_{eff} vs ϕ occurs as a function of the static stresses employed. This may well relate to the actual properties of the particular asymmetrical vibratory configuration created. However, the reason for the trend observed is not immediately apparent. For static stresses in the lower cushion in the region of stress-strain - wherein the slope is increasing to its maximum pre-buckling values - it would be expected that the effective modulus at small ϕ 's would increase with increased static load. Since the deviations tend to minimize with greater excitation, they may very well result from the somewhat indeterminate nature of the normal preload configuration in the presence of irregularity in the cushion surfaces. "Bringing the top cushion into unstressed contact with the top surface of the mass in its static equilibrium position" is a relatively indefinite procedure under those conditions. Another possible explanation is a greater departure of "unloading" as compared to "loading" curves at greater static deformations.

In Figure 28, all of the E_{eff} vs ϕ data points are plotted collectively, irrespective of thickness and static stress. The distribution of points on the logarithmic plot strongly suggested a bi-linear plot as a single "best fit" relationship for all the data. A least squares linear fit from $\phi = 0.001$ to 0.10 produced a relationship $E_{eff} = 10 (\phi)^{-.47}$ and from $\phi = 0.0001$ to 0.001, a least squares constant value $E_{eff} = 340$ (the least squares line was fit to the spatial dispersion of the data points on the logarithmic plot.)

The determination of an average functional relationship for E_{eff} vs ϕ appears useful since the resonant frequency varies as the square root of E_{eff} . A normalized relationship for approximating resonant frequency in the normal preload format appears feasible by substituting the generalized relationship for E_{eff} vs ϕ back into the functional relationship for resonant frequency,

$$f_r = \frac{1}{2}\pi \cdot (E_G S_S T)^{\frac{1}{2}}$$

by which E_{eff} was originally derived.

To simplify the derivation, the least squares relationship $E_{eff} = 10 (\phi)^{-0.47}$ was modified slightly to $E_{eff} = 8.5 (\phi)^{-\frac{1}{2}}$. This modified curve is also shown in Figure 28. The substitution of the modified E_{eff} vs ϕ , with subsequent simplification, yields a relationship for approximate resonant frequency:

$$f_r = 26.7/S_S (G_{ex} T)^{\frac{1}{2}}$$

This relationship is shown in Figure 29. f_r is plotted as a function of the GT product for twelve values of static stress S_S . The limits of the data are indicated on the overall plot.

In Figures 24 through 27, the resonant amplifications encountered in the testing are plotted against the parameter ϕ . The numbers appended to the data points again represent the pertinent resonant frequencies. Examination of the curves does not appear to indicate a concretely defined variation of amplification with static stress or frequency. However, a general minimum is apparent in all thicknesses in the range of ϕ between .001 and .012 for all but the lowest static stress, 0.2 psi. The scatter in the data for various static stresses may well be attributable to material variation since a separate cushion pair was utilized for each static stress condition. This procedure was necessitated by the "transition" of the samples before reaching the maximum programmed excitation. Reference to the summary of the ASTM replicated tests also indicates that greater percentage variation was encountered in resonant response than in resonant frequency.

A common plot of amplification vs ϕ for all thicknesses (Fig 30) summarizes the general amplification properties of the polyethylene foam in package. Upper and lower envelopes enclose all data points but that for the lowest static stress, 0.2 psi. A broad area of minimum amplification with a mean value of 4.6 is seen to be centered about a ϕ of .004. For a linear, viscously damped system with an elastic modulus independent of frequency, the resonant amplification is inversely proportional to the resonant frequency. Inspection of the gross plot does manifest some evidence of an amplification decreasing with resonant frequency. However, the plot indicates that in a practical application, such sensitivity is likely to be obscured by sample variation. Since the indications are that the vibration properties prior to "transition" are largely associated with the behavior of the superficial, nonhomogeneous cell layer, considerable dispersion of observed properties in the as-foamed state is to be expected. It is possible that the more uniform "core" material or the "stabilized" material in which the non-uniform cell layer has been "collapsed" would manifest more consistent amplification properties.

The discussion thus far has been largely centered on the resonant properties of the polyethylene foam in the test configuration. The following discussions will consider the observed vibration attenuation (isolation) behavior. The designer is interested in the characterization of this beneficial phenomenon as well as the adverse one of resonance. The response curves of the ASTM test sequence are informative in this regard as they are representative of the curves obtained in the comprehensive testing as well.

A salient aspect of the logarithmic "transmitted acceleration vs frequency" curves generated in the comprehensive testing on the "virgin" polyethylene foam was the tendency to a straight line character at frequencies above resonance. This trend was particularly pronounced at the higher states of excitation of a particular configuration. The slope of the straight line "asymptote" averaged very close to 12 decibels/octave (db/oct)--i.e., a doubling of excitation frequency effected a reduction in transmitted acceleration by a factor of 4.0.

Reference to Figure 31, a plot of "transmissibility vs normalized frequency" for an idealized cushion mass system with a constant elastic modulus and viscous (velocity proportional) damping force, shows the 12 db/oct asymptote to be a property of the system when the system has an infinite "Q"--zero damping. The observation is not intended to imply that the "local" similarity in transmission characteristic denotes a specific physical correlation. Rather, a method is suggested for reconstructing the experimental response curve in the transmissibility vs frequency "domain."

The "effective modulus" and "relative excitation" concepts permitted the location of the point of maximum transmissibility as a function of application parameters. We desire to do the same with the 12 db/oct attenuation characteristic. To develop the method we refer again to Figure 31. The complete transmissibility function of the undamped linearly elastic model is given by: Transmissibility, $T(f) = 1/1 - (f/f_n)^2$. The function indicates unity transmissibility when $f = \sqrt{2} f_n$. As the forcing frequency, f , increases further, the function reduces to: $T(f) = (f_n/f)^2$. The latter function is the equation of the 12 db/oct asymptote in Figure 31. The function produces an indicated unity transmissibility when $f = f_n$, rather than $\sqrt{2} f_n$. This is graphically equivalent to extending the 12 db/oct line of Figure 31 to intersect the horizontal line, transmissibility = 1.0. The graphical intersection occurs at $f = f_n$, in agreement with the extension of the function $T(f) = (f_n/f)^2$ below its applicable frequency limit. This trivial observation will be used for our normalizing scheme:

"The projection of the 12 db/oct asymptote of the undamped linear model to intersect the line of unity transmissibility "located" the natural frequency. Similarly, the projection of an experimental 12 db/oct asymptote to the intersection with a line of transmissibility = 1.0 locates an "apparent natural frequency," f_a . If the apparent natural frequency is "tabulated" in terms of application parameters, it may be subsequently reconstructed in a logarithmic transmissibility vs frequency plot. A point of transmissibility = 1.0 and $f = f_a$ can be located and a 12 db/oct asymptote projected through it."

The f_a 's constructed on the experimental response curves were invariably significantly higher than the respective f_r 's (resonant frequencies). This would be expected, since the cushion system was observed to be demonstrably nonlinear at resonance. The f_a 's for specific static stress-thickness combinations were, however, largely independent of the accelerational excitations applied. This implies that the systems were behaving linearly over the range of frequencies in which the 12 db/oct lines were defined. (The tendency to linear behavior above resonance would be abetted by the conduct of the frequency sweeps at constant forcing acceleration. As noted earlier, and depicted graphically in Figure 14, the associated exciting motions (displacements) in a particular sweep decreased as the square of an increase in forcing frequency.) In a downward frequency sweep at constant acceleration input, the "normally preloaded" polyethylene foam package may be considered to undergo a transition from an undamped linear system to a nonlinear system with finite damping as resonance is approached.

The statement that the f_a 's were largely independent of exciting acceleration for specific static stress-thickness combinations implies that they were completely associated with static stress and thickness factors. The linear attributes of the asymptotes, and the correlation of f_a with f_n for the idealized system, lead one to again consider the variation of the idealized natural frequency with static stress and cushion thickness. The relationship was given earlier as:

$$f_n = \frac{1}{2}\pi \times (E'g/S_sT)^{\frac{1}{2}}.$$

A plot of f_a vs S_sT is thus suggested as a test of the possibility that the superficial implication of the 12 db/oct asymptotes corresponds to a physical reality-- i.e., that, at small motions, the system manifests a constant elastic modulus and negligible hysteresis. Plots of f_a vs (static stress \times thickness) are made on logarithmic coordinates in Figure 32 for the four thicknesses tested.

A log-log plot of the idealized linear f_n vs S_sT would generate a straight line of -0.5 slope. The plots of f_a vs S_sT for 1 7/16-inch, 1 5/16-inch and the laminated 4-inch-thick cushions in Figure 32 appear to tend to such a relationship at low values of S_sT . For a particular thickness, at the higher static stresses, the f_a 's drop below the "linear" slope of -0.5 as defined by the low S_sT points. It will be recalled that separate cushion pairs were utilized for each static stress station due to the "linearization and set" phenomena. The extreme departure of the 2.0 psi station on the 1 7/16-inch material may thus well be due to an unusually "soft" cushion pair. The plot for the 3 3/8-inch material indicates a uniformly "softer" character than the other thicknesses. (The "resonant moduli" for the 3 3/8-inch thickness were also significantly lower than the other thicknesses.)

The consistency with which the slopes for the four thicknesses diverge from the -0.5 value of the "constant modulus" model would appear to definitely belie the physical reality of that model. The increase in slope of the f_a vs S_sT curve for a particular thickness might be interpreted as signifying a decrease in small motion modulus associated with increasing static stress. The indicated elastic modulus for the 1 5/16, 1 7/16, and 4 inch thicknesses at low S_sT values is 830 psi. (Since the "natural frequencies" we are plotting are "apparent" ones, the associated elastic moduli should be termed "apparent elastic moduli," abbreviated E_a .) At 2.0 psi static loading, the E_a 's are found to have reduced to 300, 490, and 510 psi for the 1 7/16, 1 5/16 and 4-inch thicknesses respectively. A "larger departure of the unloading curve from the loading function" was proposed as a mechanism which might relate a decrease in "effective" (resonant) modulus to an increase in static stress in the "normal preload" configuration. This explanation would not appear reasonable to explain the reduction in the "small motion" modulus, E_a . A more persuasive explanation is that the apparent elastic modulus is affected by frequency: An increase in static stress, for a specific thickness, shifts the entire response curve downward in frequency. The dynamic elastic modulus also apparently reduces with frequency, which reduces the f_a still further. Figure 32 may be reasonably utilized to estimate attenuation factors in conjunction with

the 12 db/oct "projection" procedure. The determination of an E_a of 830 psi as compared to a maximum "low rate" modulus of 70 psi verifies that more conservative estimates of "potential" attenuations accrue from the testing.

SUMMARY

In replicate vibration tests on the polyethylene foam, sweep frequency tests generated transmissibility curves comparable to steady-state curves after the mechanical properties of the foam were stabilized by preliminary vibration sweeps. These preliminary sweeps generated reproducible curves, from sample to sample, despite change in material characteristics during the sweeps. Steady-state tests under the particular state of static and dynamic loading did not produce consistent definition of resonant response until after stabilization had been effected. The stabilization process involved a transition of the foam's stress-strain relationship from the markedly nonlinear characteristic of the virgin foam to an essentially linear one after stabilization. The transition was associated with the collapsing of a nonuniform cell layer at the surface of the foam samples and was accompanied by a thickness loss of approximately 12%.

When the foam was sweep-tested at several levels of vibratory acceleration input, well defined threshold levels were encountered. At these levels, it was possible to induce the linearization-thickness loss process in a single sweep through resonance. The testing defined the threshold accelerations as a function of the applied static stress (weight loading). At all but the lowest static stresses, the threshold excitation value fell within the program envelope (Mil Std 810, common carrier vibration test). When excited at acceleration levels below the threshold value (for a specific static stress) the foam was relatively resistant to the transition process.

Vibration sweeps, when conducted at forcing acceleration - static stress combinations below the threshold, generated transmission curves reflecting the nonlinear properties of the virgin foam and package configuration. (Under specific static stresses, resonant frequencies

varied as much as 2:1 with variation of dynamic input within the program envelope. Resonant jump phenomena were pronounced at higher input levels. Resonant amplification varied from 2.5 to 7, largely as a function of forcing level, rather than static stress. Attenuation rates above resonance tended to consistently approach a constant 12 db/octave. (The 12 db/octave line at higher levels of input was displaced upward in frequency compared to the undamped linear system with the same resonant frequency.)

A normalizing approach was devised for analysis of the test data that resulted in a relatively simple empirical formula for predicting resonant frequencies as a function of application parameters and environmental vibration levels. A similar approach to resonant amplification encountered in the data produced a less clearly defined relationship, but one of considerable comparative value.

The overall range of resonant frequencies established for the range of parameters employed in testing was 8 to 120 Hz. This span is significantly greater than could be predicted from static data and linear system estimates, indicating a considerable increase in dynamic over static modulus.

Preliminary tests verify that appropriate precompression of the foam within the package allows the 12% set (if induced) to be absorbed within the package, thereby precluding the development of a "loose pack." It was also determined that precompression of the foam in-package can equalize the directional stiffness of the cushion system and create a condition of pseudo-linearity in elastic and loss mechanisms operating in the package.

CONCLUSION

Equipment cushioned with polyethylene foam at static stresses favorable for efficient shock mitigation (0.2 to 2.0 psi) will be subject to amplified (increased) environmental vibration at specific frequencies in the 8-120 Hz range. This frequency range is encountered in wheeled and tracked vehicles, aircraft, and helicopters.

In packages utilizing polyethylene foam, some degradation (thickness loss and softening) may be expected during standard military package vibration tests (e.g., Mil Std 810). This thickness loss (12%) may be regarded as objectionable, particularly in packages utilizing large foam thickness where the total "gap" or "set" developed will be proportionately larger.

Because of the apparent "stabilization" that follows the initial degradation of the foam, "preworking" of the foam may be considered a desirable procedure. The tests indicate that such a procedure could be most readily effected by preliminary vibration of the foam under static load. In this way, the required number of stress cycles to induce the stabilization can be accumulated very rapidly. If size and/or geometry of the package are not prohibitive, overall preloading of the foam would appear to be an acceptable alternative for coping with the thickness loss phenomena. Preloading will, in general, increase the resistance of the cushion system to fatigue by equalizing vibratory excursions in the upper and lower cushions. The equalization tends, however, to increase resonant amplifications by suppressing nonlinearity. Preloading also facilitates the generation of dynamic force-displacement relationships analogous to those derived in classical, small-amplitude, tension-compression tests.

Sweep frequency testing can define reproducible vibration transmissibility curves in fatigue-prone cushioning materials. Under conditions of cushion material "stability," sweep frequency testing can define the materials response to "steady-state" vibration.

APPENDIX A

Transmissibility Test Procedures (ASTM)

Sample Preparation. Fifty-six 2-inch-thick specimens of polyethylene foam were divided into two groups: Group I with a square bearing area of 8 in. x 8 in., and Group II with square bearing area of 4 in. x 4 in. The samples were measured and weighed to establish density. Fourteen specimens from each group were then given a prework cycle in a Riehle compression machine: 10 compressions to 20% strain for the 8 x 8 x 2 samples and 10 compressions to 10% strain for the 4 x 4 x 2 samples.

Test Configuration. Following storage for one week at 70°F and 50% RH, twin samples of each size and prework condition were assembled into the dual compression test fixture (Fig 1) in the type 1 (normal pre-load) configuration depicted schematically in Figure 3. Load weights for the 8 in. x 8 in. x 2 in. x 4 in. x 2 in. specimens were 64 pounds and 16 pounds, respectively, creating a static bearing stress in the bottom cushion of 1.0 psi for each size sample.

The sequence of assembly was as follows:

1. The guide fixture (exterior "container") was rigidly bolted to the vibration exciter.
2. The bottom cushion was adhered to the bottom of the guide fixture with double-backed pressure-sensitive tape.
3. The appropriate load weight was lowered onto the bottom cushion until it was totally supported by the cushion.
4. The top plate ("container" cover) with upper cushion taped to its under surface was lowered into the guide fixture until the lower surface of the top cushion made uniform contact with the upper surface of the load weight in its static equilibrium position.

5. The top plate was clamped to the guide fixture as positioned in (4), completing assembly of the simulated package.

Vibration Test Procedure

Steady State Tests. The sinusoidal "command" oscillator was set at a specific test frequency. The driving signal to the vibrator was increased until the accelerometer on the guide fixture indicated 2.0 G peak vibratory acceleration. The excitation was maintained until the accelerometer within the cushioned weight produced a stable deflection of the recording pen. This point was recorded by "setting" of the pen. Excitation to the vibrator was then reduced to zero and a second frequency set point established. Frequency intervals at which transmitted vibration was measured were 10 Hz below 20 Hz, and 5 Hz from 20 Hz to 200 Hz.

Sweep Frequency Tests. The vibration input was brought up to an indicated peak acceleration of 2 G at 7 Hz. The vibration frequency was then programmed to advance at the rate of 1.8 octaves/min, with the peak vibratory acceleration applied to the guide fixture (container) being maintained at 2.0 G's by feedback from the fixture accelerometer into a closed loop control circuit of the command oscillator. The peak vibratory acceleration transmitted to the mass through the cushioning material was continuously recorded as frequency was varied. At 20 Hz the rate of frequency advance was changed to 20 octaves/min, with an appropriate change in the response speed of the G transmission recorder being made. The 20 octave/min variation of frequency was continued to 200 Hz. At 200 Hz the direction of frequency scan was reversed and the range from 200 Hz to 7 Hz covered at the same scan rates used in the upward frequency sweeps, again recording peak transmitted acceleration with the "input" vibration magnitude held constant at 2.0 G.

Vibration Test Sequence. An initial attempt was made to perform the steady state vibration transmission determination before the sweep tests. When obvious degradation of the cushion resulted during measurements at frequencies near resonance, this format was abandoned, since it would obviously preclude correlation with sweep tests. The sequence subsequently followed for each cushion pair was the application of two bidirectional sweeps (from 7 to 300 Hz and return) followed by the steady state determinations.

Post Vibration Tests. Following the vibration sequence, each cushion was measured for thickness loss and subjected to a "static" stress-strain determination (1.0 in./min loading).

Comprehensive Tests on "Virgin" Characteristics. Since the ASTM tests were performed to evaluate test procedures with a limited number of pertinent parameters, a more extensive evaluation was subsequently initiated. Four "as manufactured" thicknesses (1.3, 1.4, 2.1, and 3.4 inches) and one "assembled" thickness (double 2 inches thick - 4 inches thick) were tested. A minimum of four static loads ranging from 20 to 200 pounds were employed with each thickness for cushion bearing areas of 10 in. x 10 in. = 100 sq in. Up to eight levels of vibratory input were excited, ranging from 0.25 G to 5 G's, with the upper limit of applied G's determined by the test envelope (Mil Std 810 transportation vibration test) or that value within the envelope which induced a discernible shift in vibratory operating point, discernible set, or heat buildup in excess of 10°F. Constant acceleration inputs were used because of the possibility of sweeping larger portions of the frequency spectrum without exceeding the program envelope. In addition, acceleration response curves thus generated on logarithmic coordinates are convertible to transmissibility functions by a mere shift of ordinates.

Sample Preparation. The test samples were cut into 10 in. x 10 in. bearing areas, their dimensions measured, and density calculated. The samples were stored at 70°F, 50% RH for one week prior to test.

Test Configuration. The comprehensive tests were performed with two cushion samples, approximately matched in density, assembled with specific static weights into the "normal" preload (Type I) configuration of Figure 3. A resistance temperature sensor was placed in the lower cushion of each pair at its geometric center. Insertion of the sensor was made via a slit cut into the top surface of the lower cushion at a 45° angle.

Vibration Test Procedure. With a cushion pair assembled in the test fixture supporting a specific static load, vibration was applied to the fixture along its vertical axis. The peak vibratory acceleration was maintained constant while the frequency of vibration was swept downward from 200 Hz at the rates depicted in Figure 32. The lower bounding frequency of the downward sweep was 7 Hz, or that frequency established by the intersection of the vibratory input with the program envelope (Fig 29). Upward sweeps were employed on several samples to further verify the general dynamic "softening" of the cushion configuration under increasing excitation. Superimposed "overall" preload (Type II, Figure 3) was used on several selected configurations to compare the effects with the "normal" preload configuration.

APPENDIX B

Discussion of Equipment

Vibration Exciter. The vibrator utilized in the testing was a programmable, servo-controlled, electro-hydraulic exciter with an overall frequency range of DC to 500 Hz. The vibrator employs real-time displacement and velocity feedback and hydrostatic bearings for optimized waveform. DC acceleration feedback was utilized in the testing to control the magnitude of the vibratory acceleration imposed on the simulated package.

Vibration Programming and Response Recording Equipment. The instrumentation used to program the vibrator and record the vibration transmitted through the cushioning can be seen in Figure 33. A functional schematic is shown in Figure 34.

The sinusoidal command signal is derived from the servo-sweeping oscillator. The oscillator is a beat frequency type, with a fixed frequency internal oscillator being heterodyned against a variable frequency oscillator. The output frequency is the difference frequency between that of the fixed oscillator and the variable oscillator. The calibration of the variable oscillator is such as to produce equal logarithmic frequency increments for equal increments of dial rotation. With the variable dial driven at a constant rotational rate, the traverse time is a logarithmic function of the frequency ratio ($t = 1/\alpha \ln f_2/f_1$), a procedure commonly referred to as a "logarithmic sweep." The sweeping sinusoidal signal is converted into a sweeping mechanical vibration by application of the signal through the servoamplifier into the multistage hydraulic servo-valve which controls the flow of hydraulic fluid to the differential "ram" (vibration exciter.) Because of the displacement-sensitive feedback loop around the amplifier, the ram displacement tends to be a constant function of the command signal level. Variation of the command level is thus required in order to maintain a constant vibratory acceleration (G) as frequency is varied. (For a sinusoidal motion, $D_{pk} = 10 G/F^2$, where D_{pk} = peak vibratory displacement

from equilibrium.) Automatic control of the command signal is effected by feedback of the acceleration signal from the "table" (G_t in Figure 31) into a control circuit of the sweep oscillator to regulate the oscillator amplitude so as to maintain a constant vibratory acceleration at the table. The piezoelectric accelerometer, A_t , is matched to the control circuit by a cathode follower. The double-shielded input cable has its inner shield "driven" by the cathode follower output to nullify its capacitance and maintain the high open-circuit voltage sensitivity of the accelerometer. The operating sensitivity is trimmed to exactly 100 mv/g by adjustment of the sensitivity standardizer (variable shunt capacitor.)

Transmitted Acceleration Recording System. With the servo-sweep oscillator maintaining a preset level of vibratory acceleration (G_t) and sweeping a frequency range, the vibratory G's transmitted to the cushioned mass are directly plotted on a logarithmic scale against the logarithmic frequency.

The frequency scale of the x-y plotter is driven via a potentiometer mechanically coupled to the tuning dial of the programming oscillator. The potentiometer is energized with a constant DC voltage from the oscillator. Since the tuning dial frequency calibration is logarithmic, a DC voltage proportional to the logarithm of the programmed frequency is produced at the moveable "tap" of the potentiometer.

The accelerometer at the center of the cushioned mass, A_m , is coupled to the recording system in a manner similar to that used for the table accelerometer, A_t . The G_m voltage signal from the cathode follower output is passed through a tracking band pass filter of 2 Hz nominal bandwidth. The filter is synchronized to follow or "track" the programmed frequency during a vibration sweep. All frequency components in the response signal with greater than 1 Hz deviation from the instantaneous programmed frequency are strongly attenuated (suppressed) in the filter output. The output signal thus represents the component of mass response at the same frequency as the exciting vibration. (The generation of harmonics of the forcing frequency in nonlinear vibratory systems with sinusoidal inputs is documented

in the literature. However, the rationale here is that the amplification of environmental vibration by the cushion-mass system is most damaging in the presence of resonances in the cushioned item at the same frequencies. Since the cushioned item resonance would itself constitute a mechanical filter, the amplitude of the fundamental frequency transmitted would be the significant parameter in damage, rather than the amplitude of the complex transmitted waveform.)

After passage through the tracking filter, the harmonic free G_m signal is amplified and applied to a logarithmic attenuator (nonlinear resistor-diode network) whose instantaneous output is proportional to the logarithm of the instantaneous input signal. For the sine wave G_m signal, the output is a "compressed" sine wave. The logarithmically attenuated signal is subsequently fed into an AC to DC peak converter. The output signal from the converter is thus a DC voltage proportional to the logarithm of the peak "fundamental" transmitted acceleration. This signal is applied to the DC-sensitive "y" axis of the x-y plotter.

The AC to DC converter is an AC vacuum tube voltmeter modified for the purpose. Variable time constants have been incorporated into the rectifier-filter circuits to allow selection of response speed commensurate with the sweep speeds utilized. The VTVM has the facility for peak, RMS, or average AC to DC conversion. When fed the unfiltered complex mass response waveform without preceding logarithmic attenuation, either of the three characteristics of the signal may be plotted linearly against frequency. With the logarithmic attenuator in the circuit, only the peak conversion is valid. The peak of the logarithmically attenuated signal is equal to the logarithm of the peak signal. The equality would not generally hold true for the two "mean" conversions.

Calibration of Programming and Recording System. Frequency calibration of the oscillator and frequency scale of the plotter is accomplished via monitor of the oscillator output frequency by an electronic counter with crystal reference. Acceleration calibration of the acceleration programming and recording channels is effected by insertion of calibrated sine wave voltages

into the cathode follower inputs and appropriately adjusting deflections of the G_t meter and the G_m axis of the plotter to indicate the equivalent calibration accelerations. The voltage-per-unit-G conversion sensitivity of the accelerometer is standardized to the 100 millivolts/G figure by adjusting the "dynamic shunt capacitance" across the accelerometer to the required values as measured by the capacitance meter.

Sweep Programming. The maximum sweep rate relationship permitting 95% resonant response for cushion-mass systems with $Q = 20$ was quoted in PATR 3160 as $df/dt = f^2/400$. The variation of frequency with time for constant speed drive of the tuning oscillator is seen to be of the form $f = f_0 \exp(\alpha t)$ and the corresponding sweep rate, $df/dt = \alpha \times f$. Since the desired sweep rate relationship allows a sweep rate, df/dt , proportional to the square of frequency, and the programmer varies sweep rate as the first power of frequency, it is clear that the adjustment of α to approximate $df/dt = f^2/400$ at low frequencies will result in excessively conservative (slow) rates at the higher frequencies. A closer "fit" was achieved in the testing by using two logarithmic sweeps to simulate the desired function. This approach is shown in graphic form in Figure 32. A sweep rate of 1.8 octaves/min was employed below 20 Hz and a rate of 20 octaves/min above 20 Hz. This format is seen to be still conservative, since the actual time to traverse any portion of the frequency band is slightly longer than specified by the idealized function.

APPENDIX C

NOMENCLATURE

1. Cushioning material. A material interposed between an item of equipment and its external container to mitigate the effects of environmental shock and vibration. A "resilient" material is capable of rapid recovery from extreme deformation such as experienced in shock loading.
2. Vibration. The continuous variation of a force or motion parameter about an average value, usually zero.
3. Sinusoidal vibration. The simplest form of periodic vibration. Force and motion parameters are definable as sinusoidal functions of time. A complete positive and negative variation is repeated in a time interval, the "period." A single sinusoidal vibration parameter is completely defined by specification of its peak or "vector" amplitude and its "frequency."
4. Frequency (f). The number of repetitions of complete motion or force cycles completed by a sinusoidal vibration function per unit time. The reciprocal of the period. Units: Hertz (Hz) = cycles/sec.
5. Periodic Vibration. A vibration in which the time variation repeats in a time interval, the period, but the variation is not specifically sinusoidal. A periodic vibration may generally be decomposed into an infinite series of constituent sinusoidal vibrations (Fourier series.) The series contains a fundamental sine wave vibration of frequency, $f = 1/\text{period}$, and "harmonic" frequencies, $2f$, $3f$, $4f$, ..., nf , in proportions and relative time position as determined by the nature of the variation of the composite waveform. The motion of the cushioned mass in the testing was periodic when a sinusoidal vibration was applied to the external container. Only the magnitude of the fundamental vibration was measured. The fundamental component was separated from the harmonics by a "tracking filter."

6. Steady-state vibration. A vibration in which the descriptive parameters are invariant in time.
7. Sweep frequency vibration. In the testing, a vibration in which the vector acceleration is held constant but the frequency is varied in a continuous programmed manner.
8. Steady-state response. The terminal vibrational conditions induced in an oscillatory system by a steady-state external vibration. The vibration persisting in the system after the transient free vibrations resulting from the initial imposition of the steady-state excitation have decayed.
9. Transmissibility. The ratio of the magnitude of a steady-state response parameter to the magnitude of the corresponding vibration excitation parameter. In general, dependent upon the frequency of the excitation. In the testing, the ratio of the peak fundamental cushioned-mass acceleration to the peak acceleration impressed on the external "container."
10. Resonance. A phenomenon encountered in mechanical systems (such as the cushion-mass systems in the testing) which possess both inertial and elastic properties. At certain frequencies of excitation the vibration conditions within the system build up to exaggerated levels, the steady-state excitation is "amplified," the transmissibility function is greater than unity.
11. Resonant frequency (f_r). The frequency in a resonant mechanical system at which the amplification factor is maximal—any change of excitation frequency results in a lower amplification. A constant in a linear cushion-mass system, independent of magnitude of exciting vibration. In the testing, a function of magnitude due to intrinsic nonlinearity of the material tested and imposed nonlinearity of test format. (Units: Hz).
12. Linear cushion-mass system. One in which the elastic and damping coefficients in the equations of motion are constants.

13. Elastic stiffness ("spring rate") (k'). The ratio of that component of force in a cushion system that is dependent only on deformation, to the deformation (units: pounds/inch). For vibratory loading of the cushion system, the ratio of the developed force that is in time phase with the deformation, to the deformation. A constant for a linear system.
14. Elastic modulus (E'). The normalized elastic stiffness for a cushion system. Obtained by multiplying the elastic stiffness, K' , by the ratio of cushion thickness to cushion bearing area. $E' = K' \cdot T/A$ (Units: psi)
15. Effective modulus (E_{eff}). The modulus derived by assumption of a "linear" (constant) elastic modulus as producing a natural frequency numerically equal to the observed resonant frequency of a nonlinear cushion-mass system. The modulus is assumed to be constant for a given set of application conditions, but assumes a different constant value for a different set of conditions. (Units: psi)
16. Relative excitation (" ϕ "). A significant vibration parameter in cushion-mass systems in which the elastic stiffness and amplification factor are functions of relative induced strains. Defined as ratio of vector (peak) sinusoidal excursion of the containing envelope to the cushion thickness. (Paraphrased: forcing strain; units: dimensionless or in./in.)
17. Q. The ratio of total elastic energy to total dissipated energy in a complete vibration cycle at resonance. For a linearly elastic, viscous damped system, closely equal to the "resonant amplification" for $Q's > 4$. For the nonlinear systems tested in this report, considered to be synonymous with resonant amplification.

TABLE 1

Summary of ASTM Test Results (Polyethylene Foam,
2" Thick, 1.0 psi Static Stress, 2 G Dynamic Input)

Test	Parameter	Mean (\bar{X})		Variance (S^2)		Std Dev (S)	
		Up	Down	Up	Down	Up	Down
4" x 4" x 2" (Virgin Samples)							
Sweep No. 1	F _F	21.17	11.36	20.37	1.47	4.51	1.21
	G _F	6.3	11.35	0.07	5.26	0.26	2.30
Sweep No. 2	F _F	12.58	10.40	0.51	1.18	0.71	1.08
	G _F	11.46	9.92	4.59	0.50	2.14	0.707
Steady State	F _F	11.88		0.76		0.877	
	G _F	10.90		1.72		1.30	
4" x 4" x 2" (Preworked to 10% Strain, 10 Cycles)							
Sweep No. 1	F _F	15.92	11.43	4.81	1.66	2.19	1.28
	G _F	6.90	11.64	12.75	3.36	3.56	1.83
Sweep No. 2	F _F	12.20	10.78	2.09	1.54	1.45	1.24
	G _F	13.33	11.04	5.87	1.51	2.42	1.23
Steady State	F _F	11.75		1.78		1.33	
	G _F	11.97		5.75		2.40	

TABLE 2

Summary of Resonant Responses and Frequencies
 ASTM Tests on 2 in. Thick Polyethylene Foam
 2 G Dynamic Input, 1.0 psi Static Stress

Test	Parameter	Mean (\bar{X})		Variance (S^2)		Std Dev (S)	
		Up	Down	Up	Down	UP	Down
8" x 8" x 2" (Virgin Samples)							
Sweep No. 1	Fr	18.07	10.35	5.12	0.31	2.26	0.56
	Gr	4.43	10.43	0.05	4.37	0.22	2.09
Sweep No. 2	Fr	11.79	9.29	0.21	0.07	0.46	0.26
	Gr	17.04	10.79	7.51	1.29	2.74	1.14
Steady State	Fr	12.29		0.20		0.44	
	Gr	15.64		3.64		1.91	
8" x 8" x 2" (Preworked to 20% Strain, 10 Cycles)							
Sweep No. 1	Fr	15.03	10.85	4.45	0.73	2.11	0.85
	Gr	6.09	12.64	15.48	1.46	3.93	1.21
Sweep No. 2	Fr	12.07	10.21	0.58	0.49	0.78	0.70
	Gr	14.43	11.40	3.91	1.88	1.97	1.37
Steady State	Fr	12.50		2.23		1.48	
	Gr	11.89		5.93		2.44	

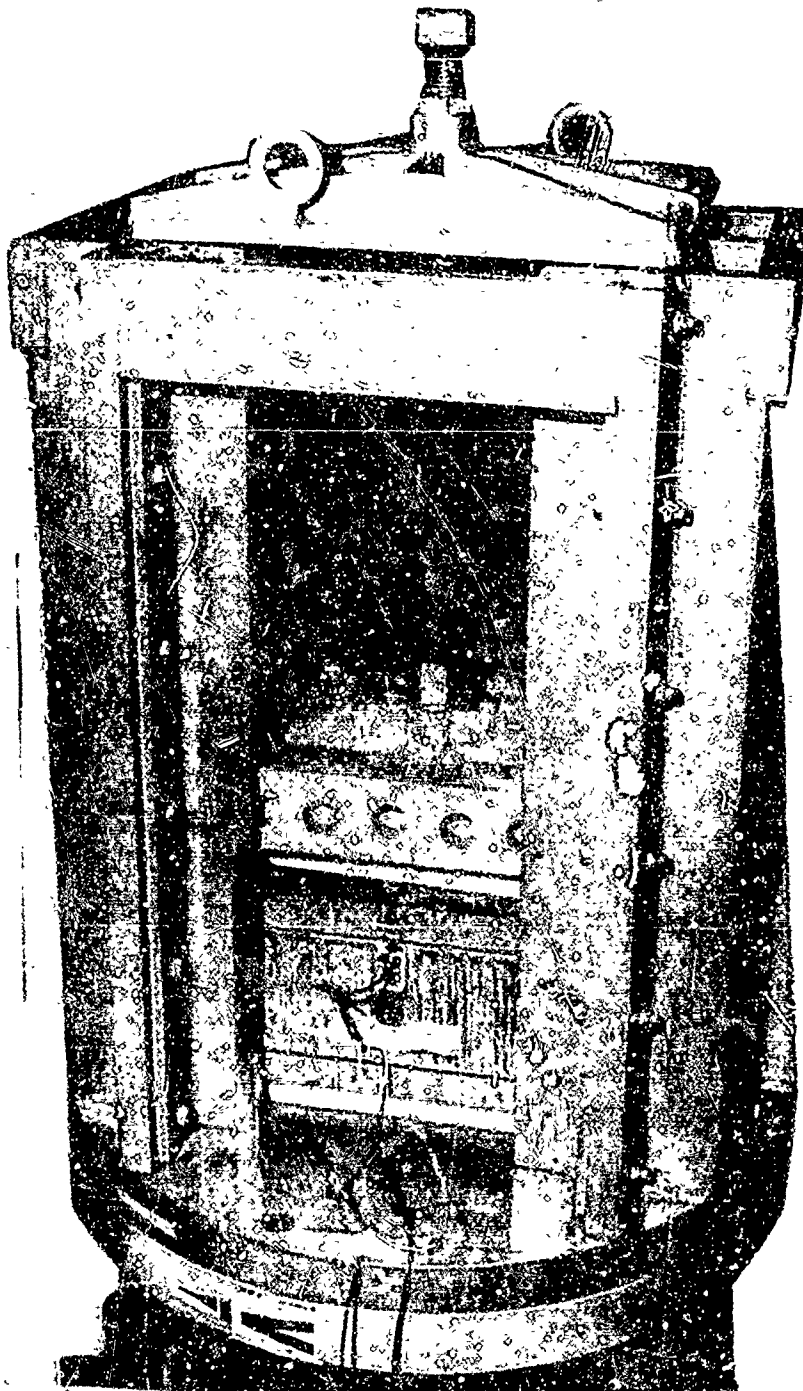


Fig 1 Dual compression cushion vibration test fixture with pre-load jack

FIG. 2 (a) (RIGHT)

RELATIVE MASS DIS-
PLACEMENT TRANS-
DUCER

FIG. 2 (b) (BELOW)

DYNAMIC FORCE VS.
REL. DISPL. FOR
"GAPPED" P.E. FOAM
PACKAGE



ELECTRICAL PICKOFF ON
CUSHIONED MASS RIDES D.C.
ENERGIZED CONDUCTIVE
PLASTIC STRIP MOUNTED ON
EXTERIOR "CONTAINER"

FIG. 2 (c) (BELOW)

DYNAMIC FORCE VS. REL.
DISP. FOR "NORMAL PRELOAD"
P.E. FOAM PACKAGE

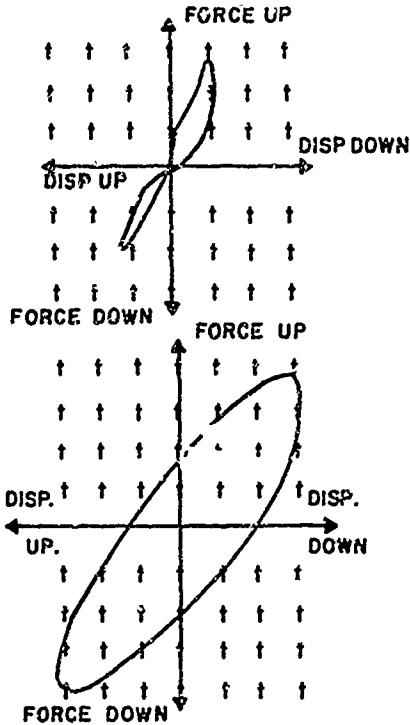


FIG. 2 (d) (ABOVE) DYNAMIC FORCE VS.
REL. DISPL. 3% STRAIN "OVERALL PRE
LOAD" ON P.E. FOAM PACKAGE.

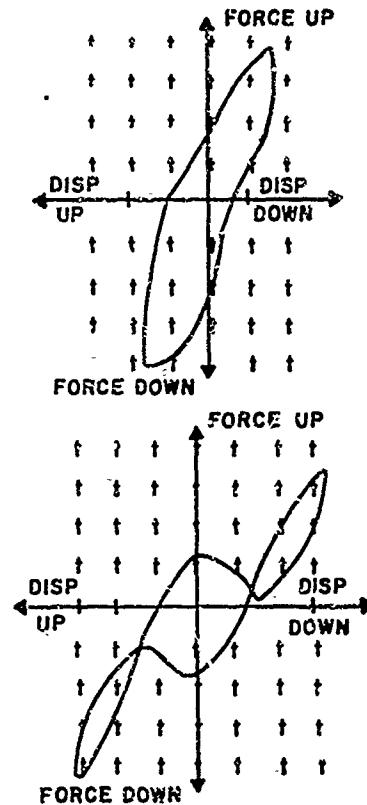
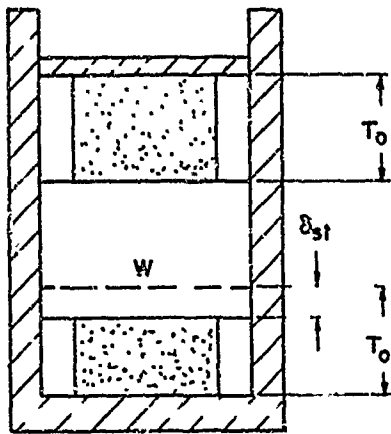
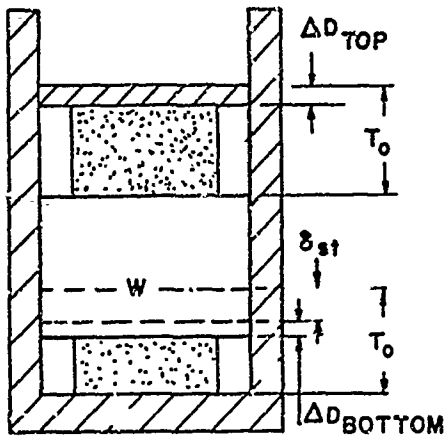


FIG. 2 (e) (ABOVE) DYNAMIC FORCE VS.
DISPL. FOR "GAPPED" P.E. FOAM
PACKAGE OF FIG. 2 (b). EXCITATION
INCREASED BY FACTOR OF 4.0.

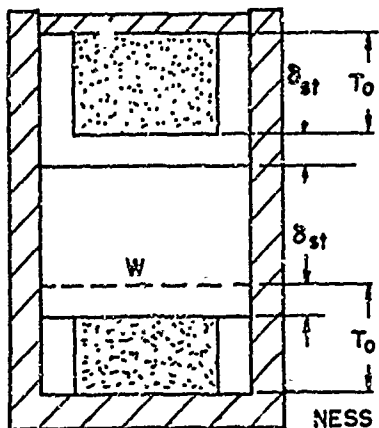
Fig 2 Relative mass displacement transducer and characteristic dynamic force vs relative displacement curves for dual-compression-cushioned package



TYPE 1
NORMAL PRELOAD
 HEIGHT COMPENSATED
 FOR STATIC DEFLECTION OF
 LOWER CUSHION.
 NON-LINEAR ABOUT STATIC
 POSITION.



TYPE 2
NORMAL ±
"OVERALL" PRELOAD
 $\Delta D_{TOP} = \Delta D_{BOTTOM}$ FOR
 LINEAR CUSHIONS.
 LINEAR ABOUT STATIC POSI-
 TION WITH LINEAR CUSHIONS.



TYPE 3
UNCOMPENSATED
 GAP BETWEEN WEIGHT &
 UPPER CUSHION = δ_{st} . 2
 CUSHIONS ACT FOR LARGE
 OSCILLATIONS ($> \delta_{st}$). 1
 CUSHION ACTS FOR SMALL
 OSCILLATIONS (WT. "BOUNCES"
 ON LOWER CUSHION).

W = STATIC WT., T_0 = CUSHION THICK-
 NESS (UNSTRESSED), δ_{st} = STATIC DISPL., ΔD =
 "OVERALL PRECOMP." CUSHION.

Fig 3 Compression-compression test package--
 three configurations for vibration tests

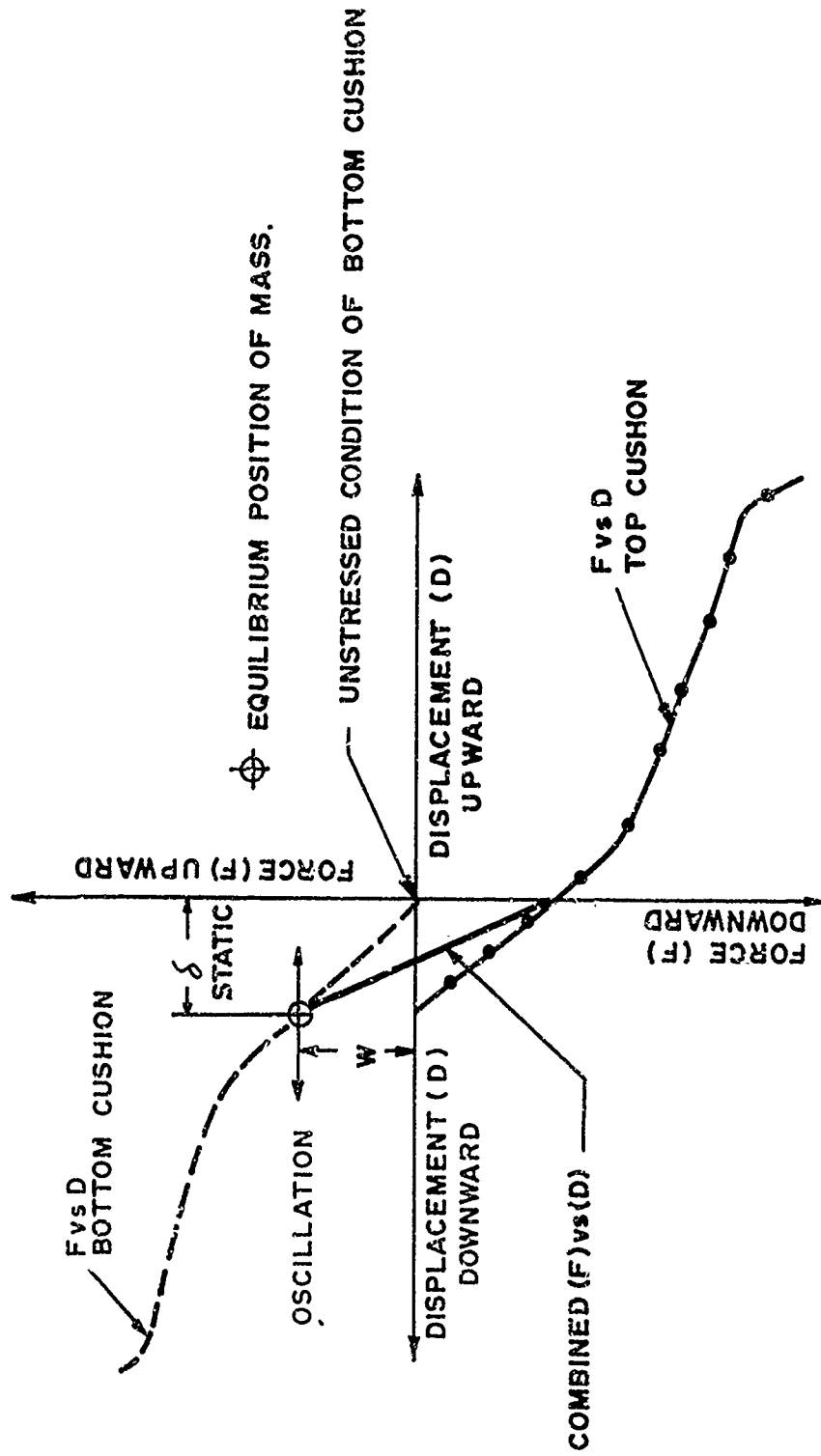


Fig 4 Force on cushioned mass vs displacement--"Normal Preload" configuration. Graphical illustration of asymmetry and non-linearity. (package WT. = HT of cushioned mass + (2 x cushion thickness) - δ static). Configuration is intrinsically non-linear

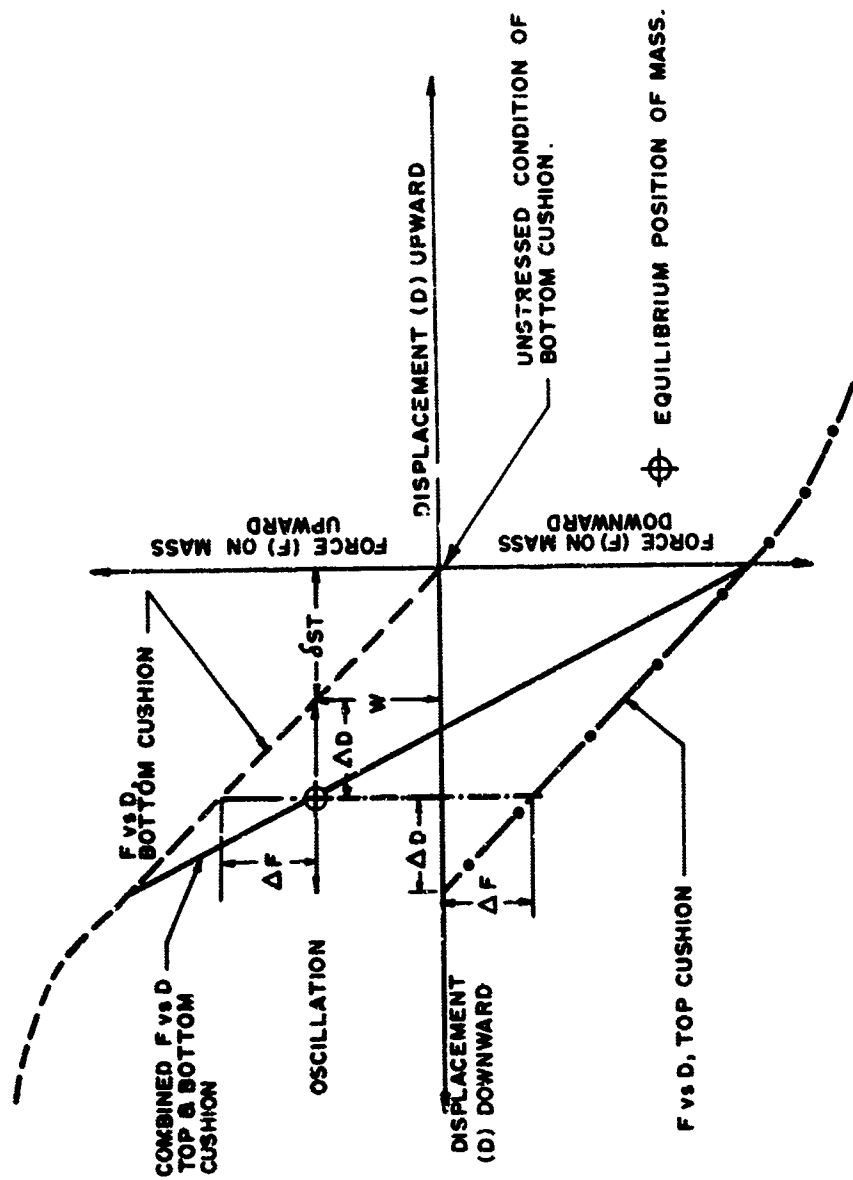


Fig 5 Force on cushioned mass vs displacement--Package with "super-imposed compression" = $2 \times \Delta D$. Graphical illustration of "linearizing" influence. For linear cushions, configuration is linear for oscillation amplitudes less than ΔD

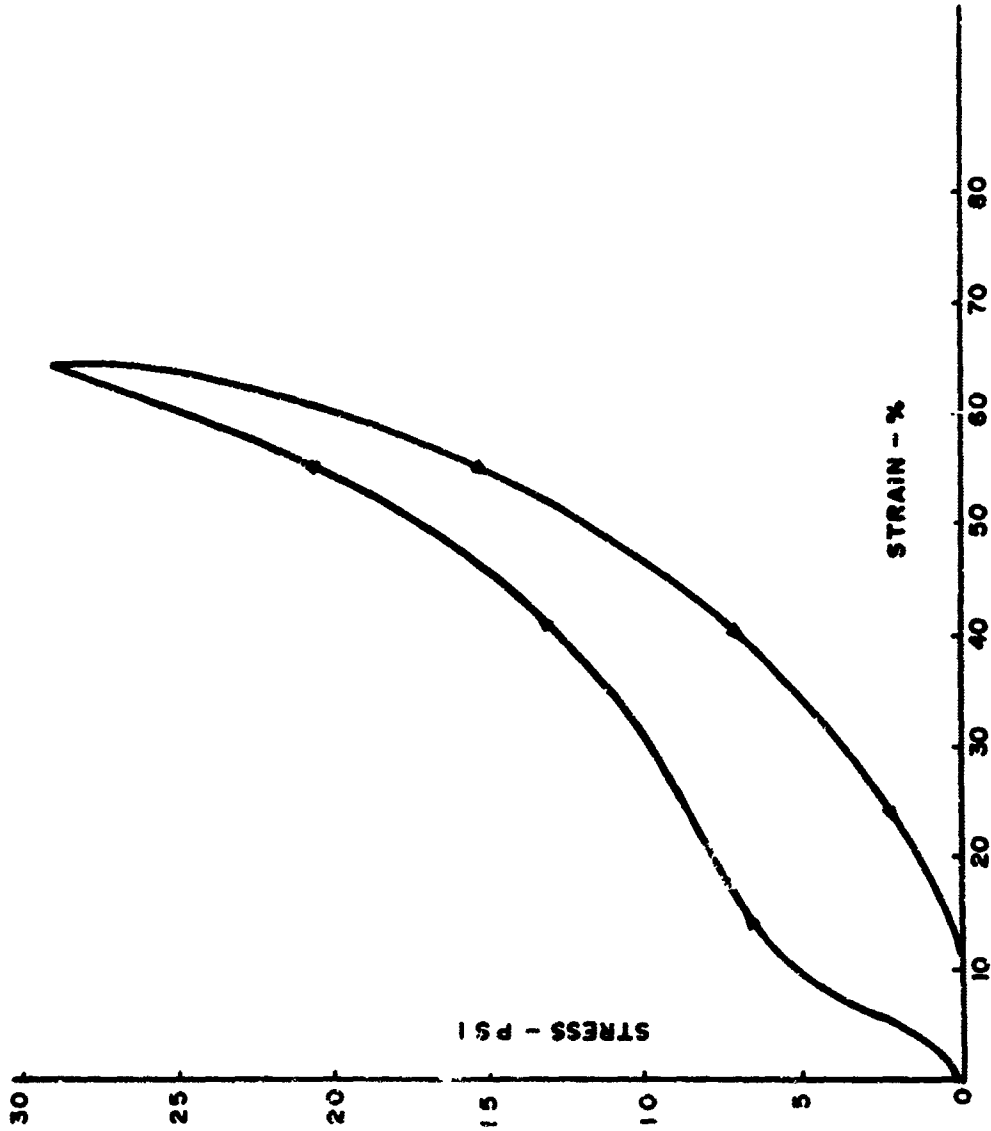


Fig 6 Stress vs strain for 2.2 pounds/ft polyethylene foam.
Strain rate = 0.3 in./in./min

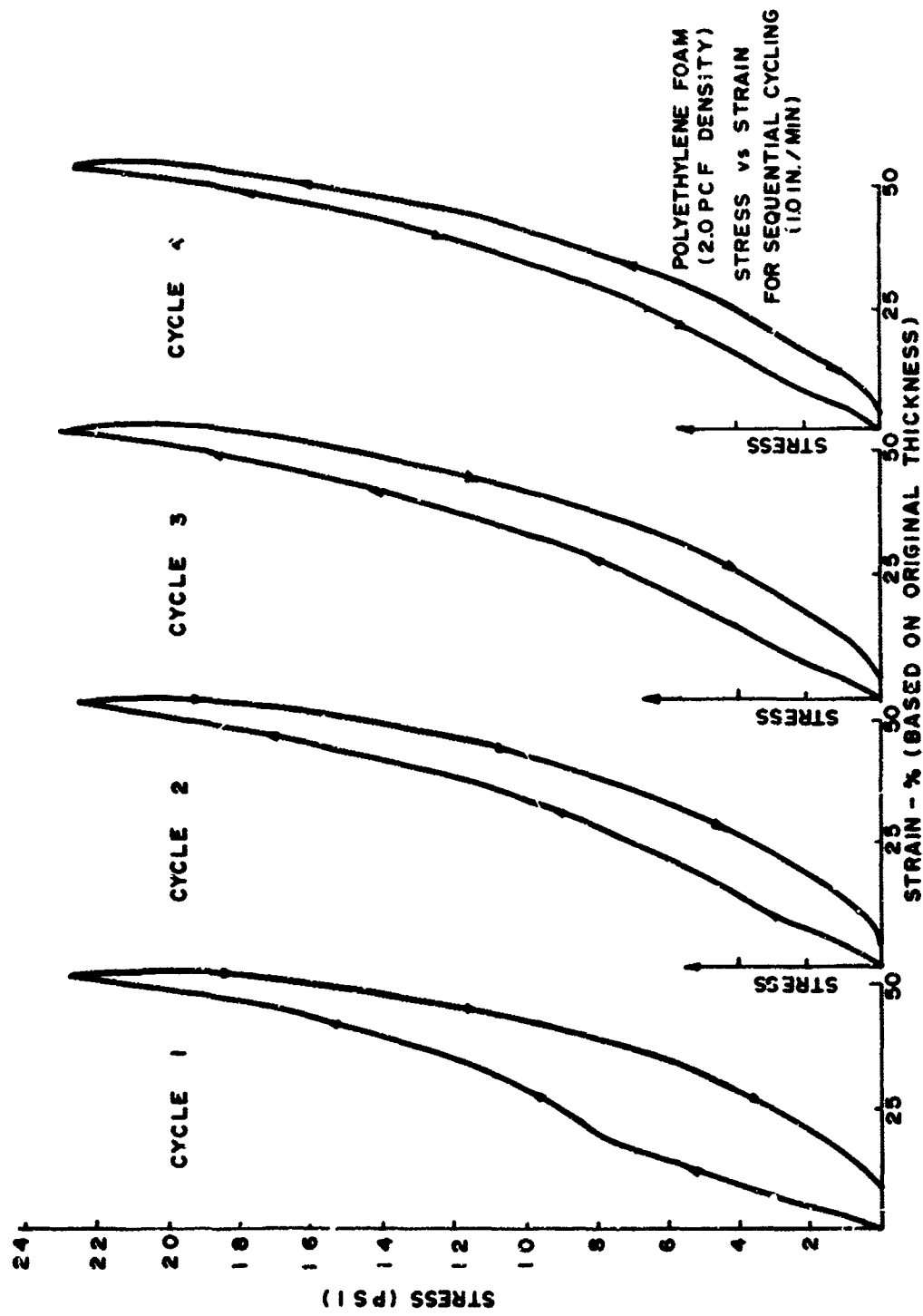


Fig 7 Stress vs strain, polyethylene foam, sequential cycling.
Strain rate = 0.3 in./in./min

ASTM RD ROBIN VIB. TEST
 POLYETHYLENE FOAM
 1.0 PSI STATIC STRESS
 VIRGIN SAMPLES: 8" X 8" X 2"
 # 41 # 42
 (BOTTOM) (TOP)
THICKNESS

BEFORE VIB. 2" 2"
 AFTER VIB. 1 3/4" 1 7/8"

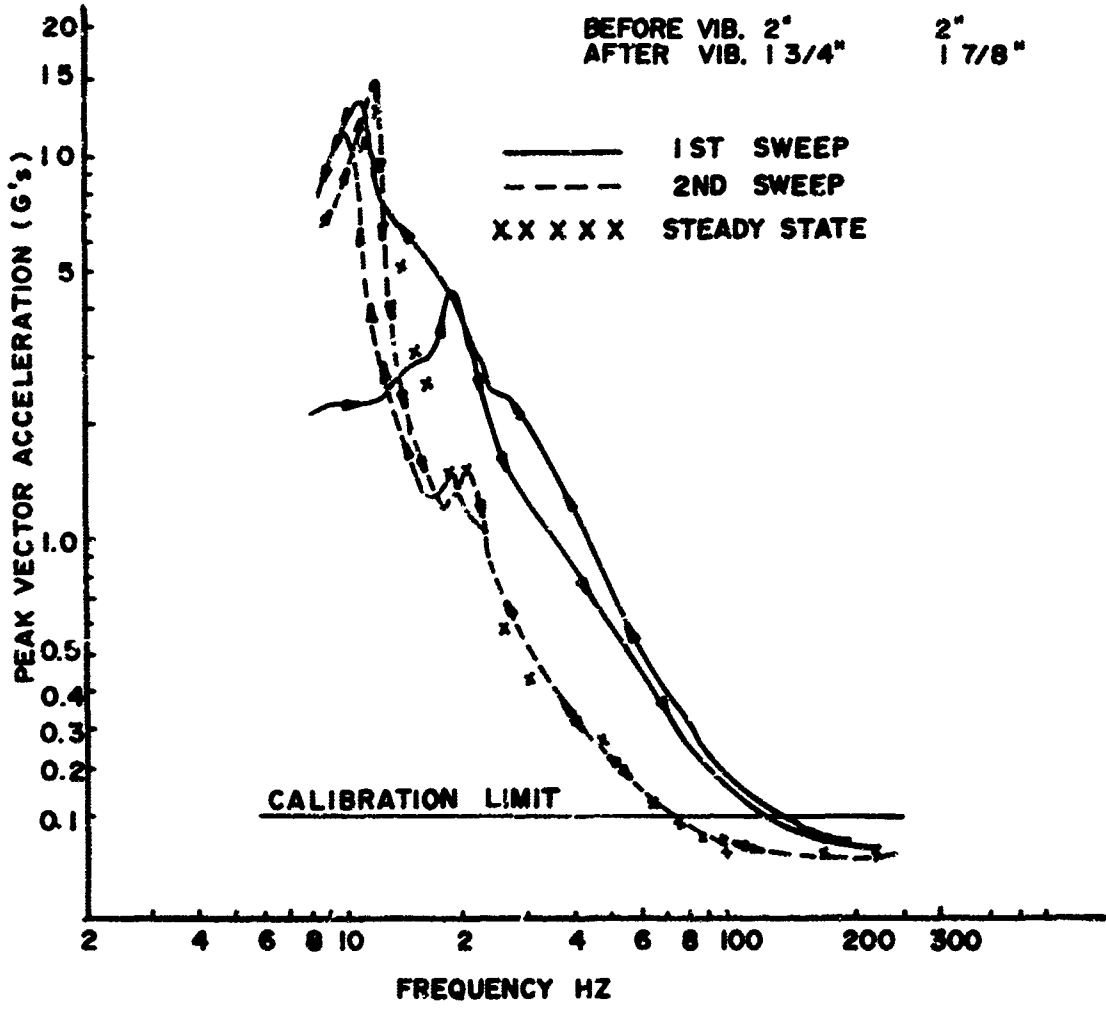


Fig 8 Peak vector acceleration transmitted vs frequency, polyethylene foam, "Virgin" samples, 8" x 8" x 2" thick. 1.0 psi static stress, 2.0 G dynamic input

ASTM RD. ROBIN VIB
 POLYETHYLENE FOAM
 STATIC LOAD: 1.0 PSI
 VIRGIN SAMPLES 4" X 4" X 2"

#31 @ #32
 (BOTTOM) (TOP)

THICKNESS

BEFORE VIB. 2" 2"
 AFTER VIB. 1 3/4" 1 15/16"

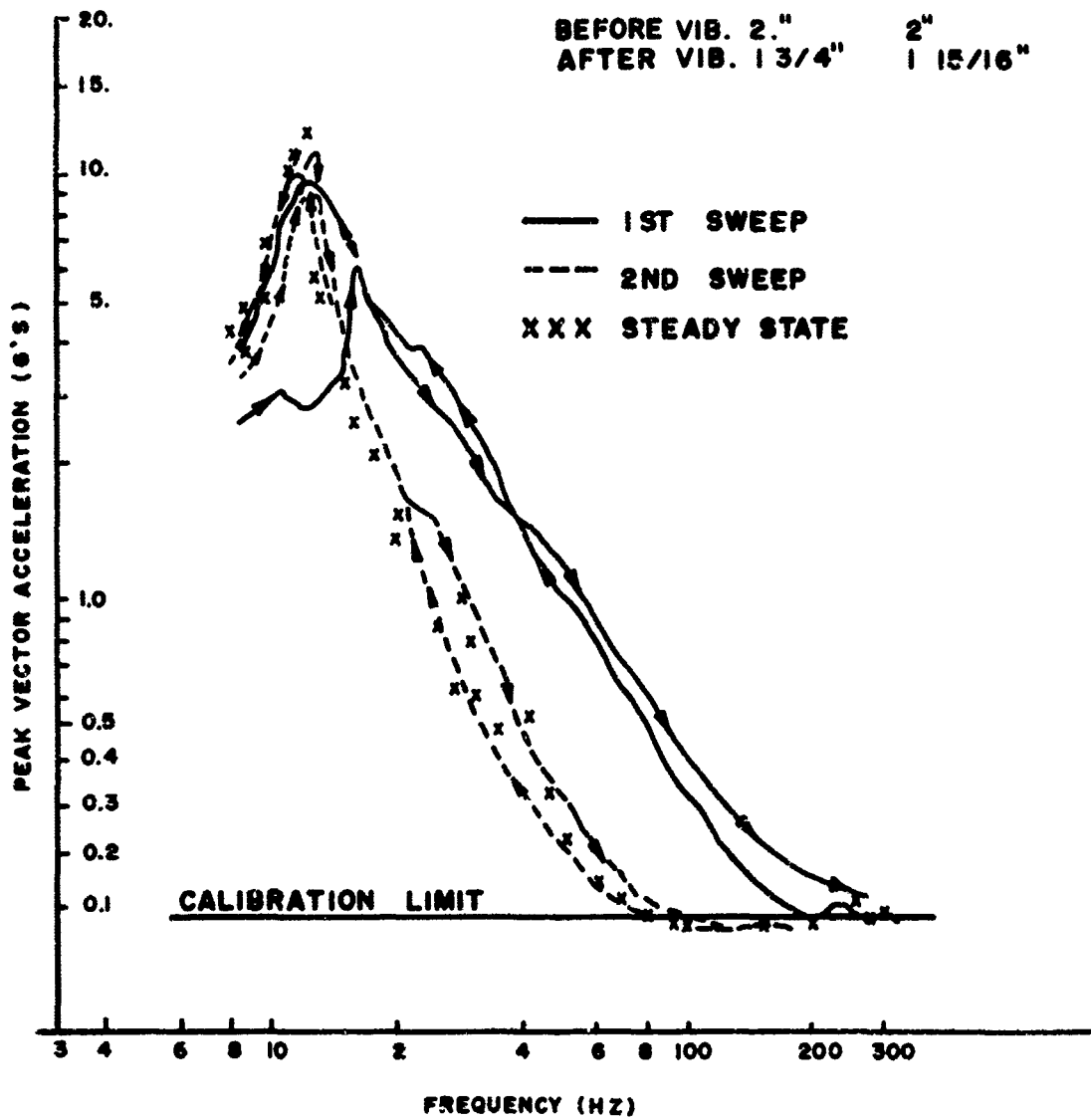


Fig 9 Peak vector acceleration transmitted vs frequency, polyethylene foam, "Virgin" samples, 4" x 4" x 2" thick. 1.0 psi static stress, 2.0 G dynamic output

ASTM RD. ROBIN VIBRATION
 POLYETHYLENE FOAM
 STATIC LOAD: 1.0 PSI
 PREWORKED SAMPLES 8" X 8" X 2"

# 57	#58
(BOTTOM)	(TOP)
<u>THICKNESS</u>	

BEFORE VIB: 2"	2"
AFTER VIB: 1 3/4"	1 7/8"

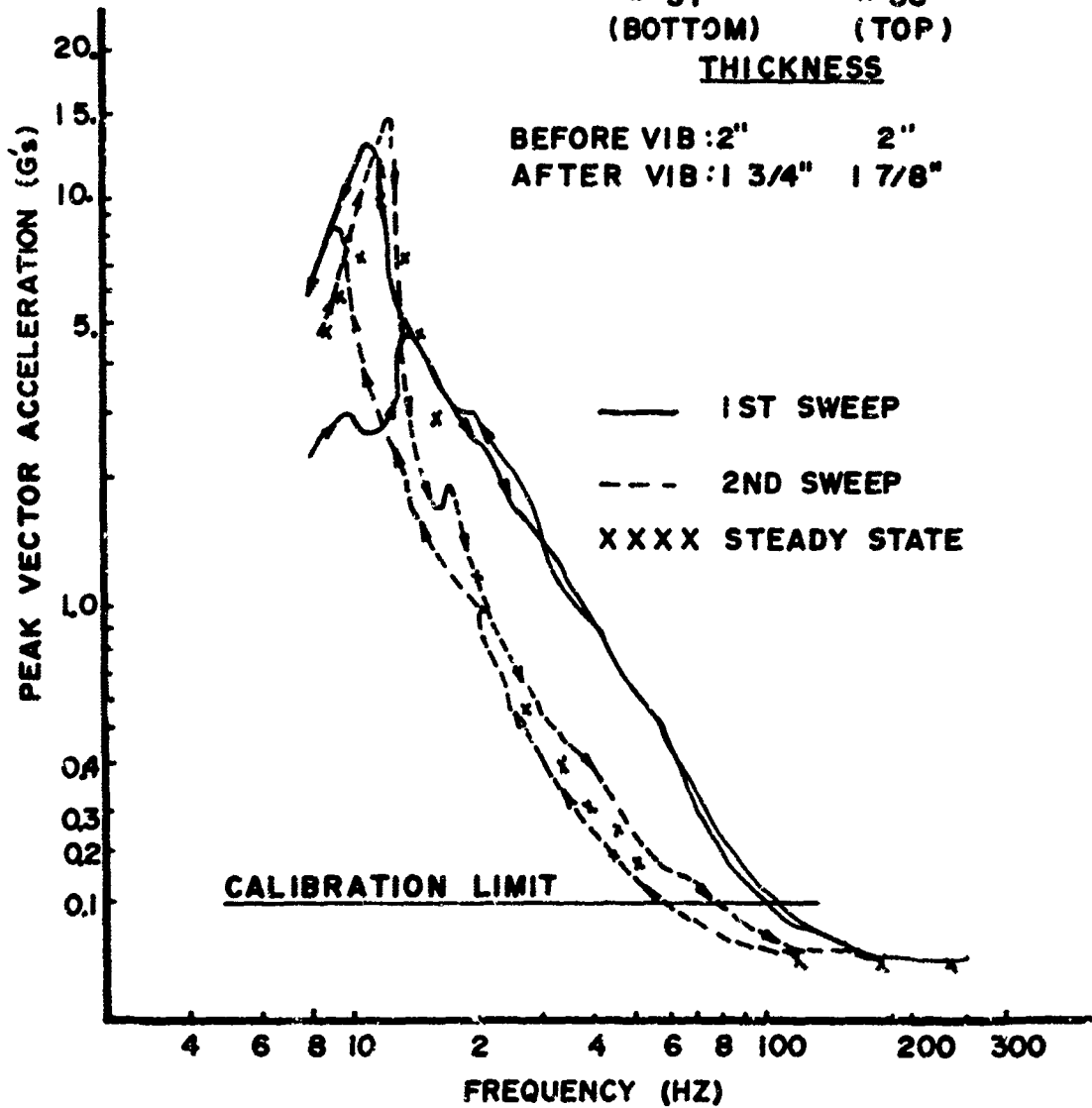


Fig 10 Peak vector acceleration transmitted vs frequency, polyethylene foam, "preworked" samples, 8" x 8" x 2" thick. 1.0 psi static stress, 2.0 G dynamic input

ASTM ROUND ROBIN

VIBRATION TEST

#51 #52
(BOTTOM) (TOP)

THICKNESS

BEFORE VIB. | $\frac{15}{16}$ " | $\frac{15}{16}$ "

AFTER VIB. | $\frac{7}{8}$ " | $\frac{15}{16}$ "

PREWORKED 4"x4"x2" SAMPLES

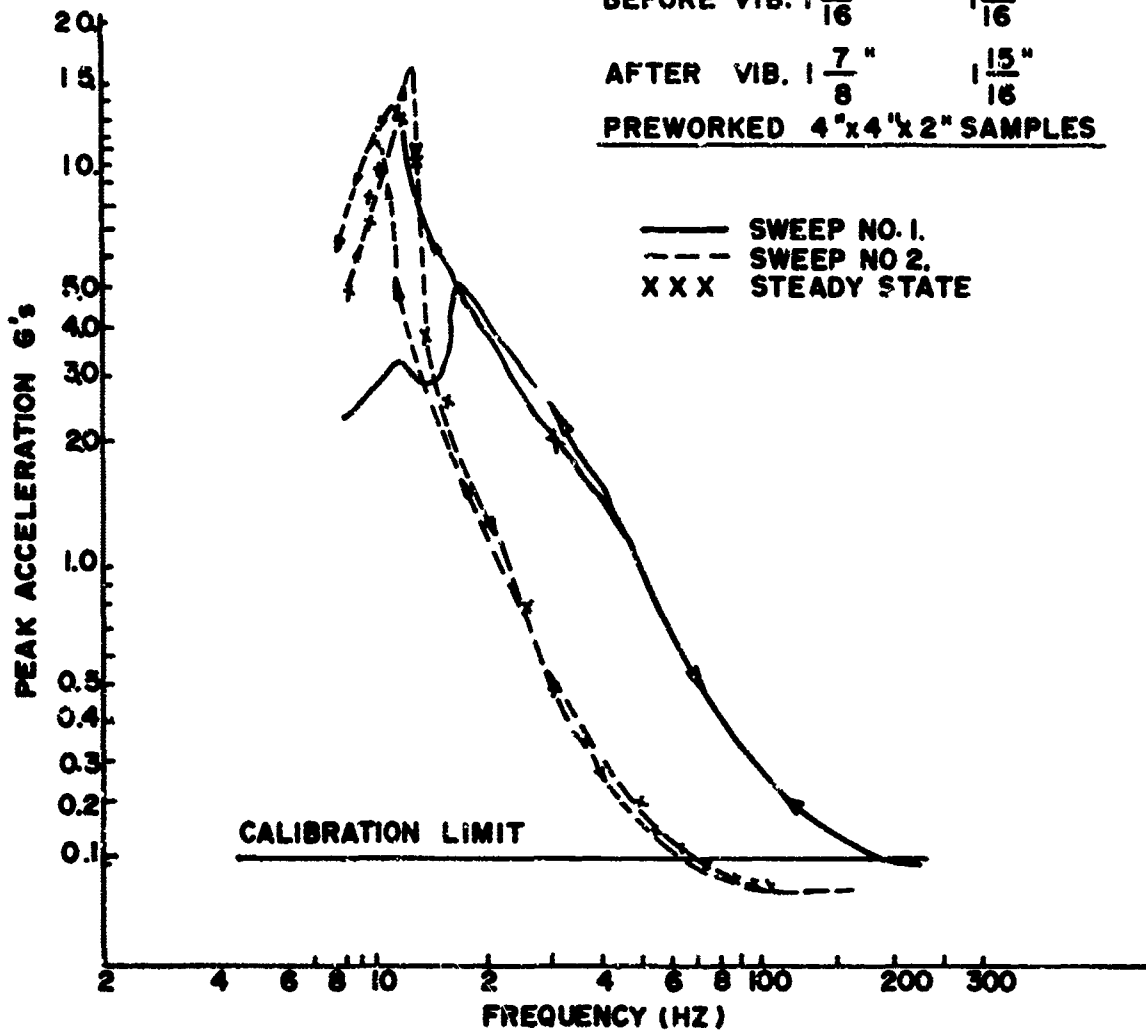


Fig 11 Peak vector acceleration transmitted vs frequency, polyethylene foam, "preworked" samples, 4" x 4" x 2" thick. 1.0 psi static stress, 2.0 G dynamic input

ASTM ROUND ROBIN VIBRATION TEST
POLYETHYLENE FOAM - 2.1 PCF DENSITY
STATIC STRESS: 1.0 P S I 8"X 6"X 2" VIRGIN SAMPLES
INPUT VIBRATION: 2 G

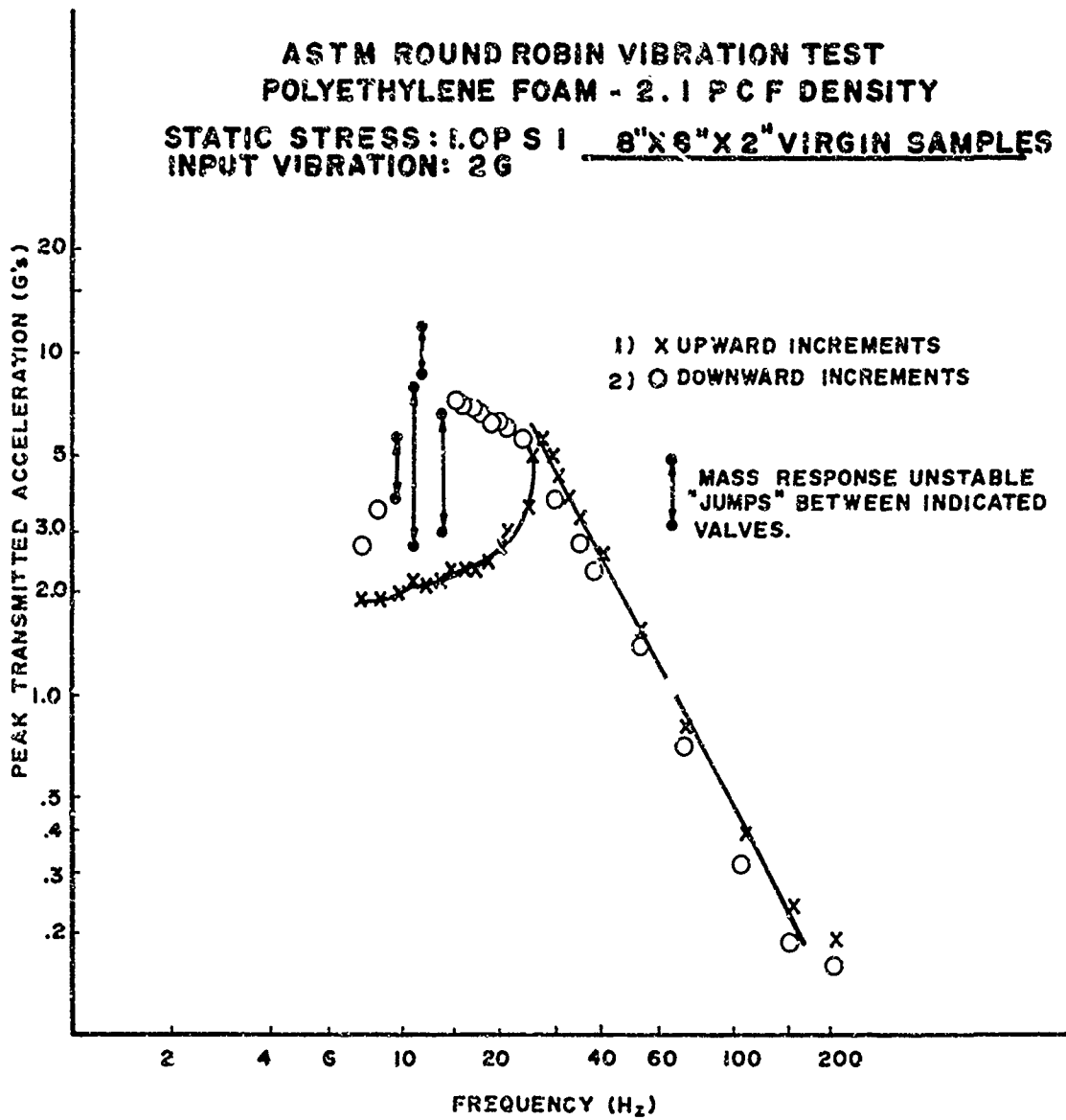


Fig 12 Transmitted peak accelerations vs frequency for steady-state vibrations on virgin cushions. Upward increments first.

**ASTM R.D. ROBIN VIBRATION TEST
 POLYETHYLENE FOAM - 2.1 PCF DENSITY
 8" X 8" X 2" VIRGIN SAMPLES
 10 PSI STATIC LOAD, 2.0G INPUT**

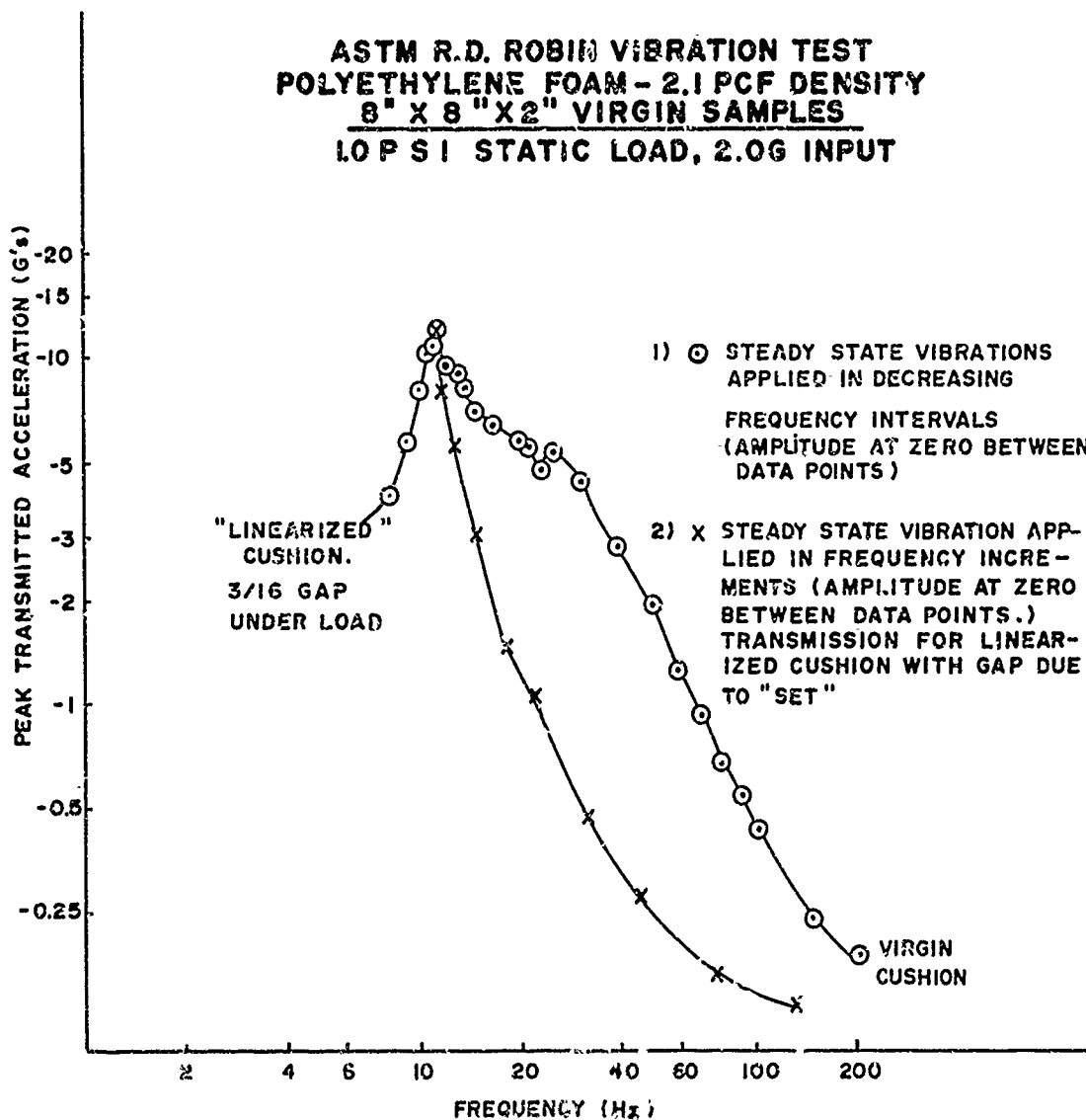


Fig 13 Transmitted peak accelerations vs frequency for steady-state vibrations on virgin cushions. Downward increments first.

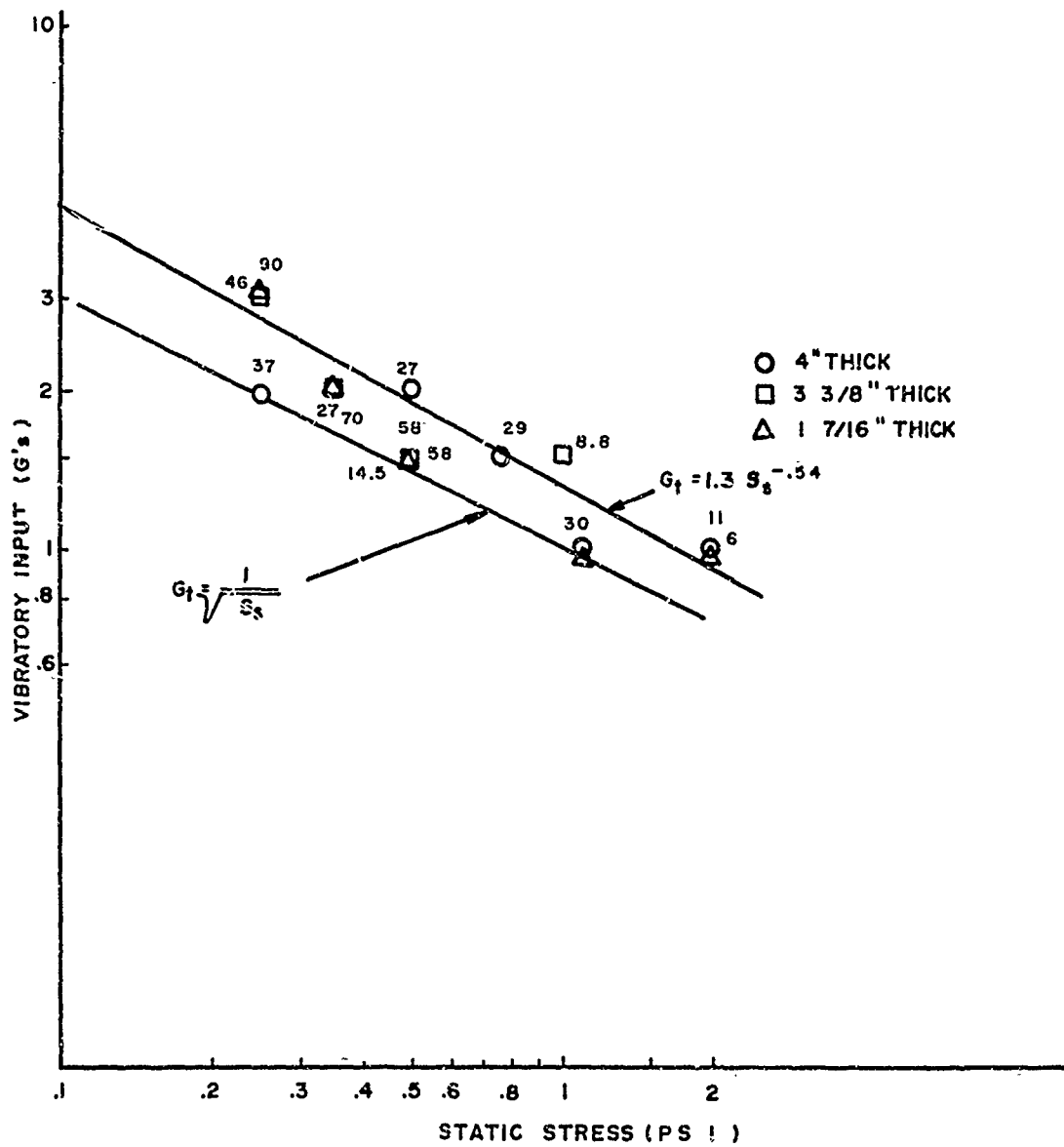


Fig 14 Vibratory input vs static stress for onset of dynamic set and "linearization" of polyethylene foam.

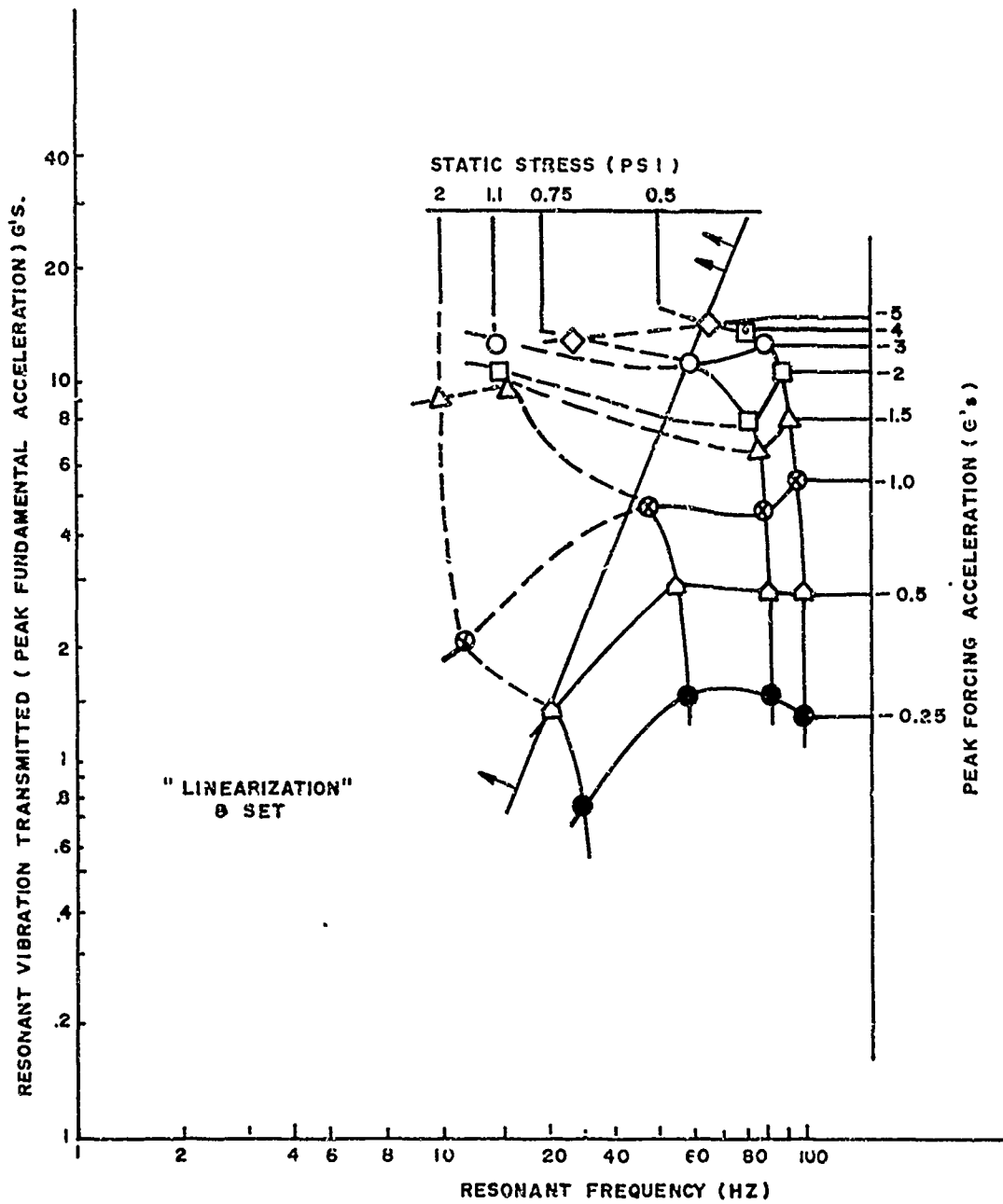


Fig 15 Vibration transmitted at resonance vs resonant frequency. Polyethylene foam, 2 lbs/ft³ (nom.)--1 5/16 in. thick.

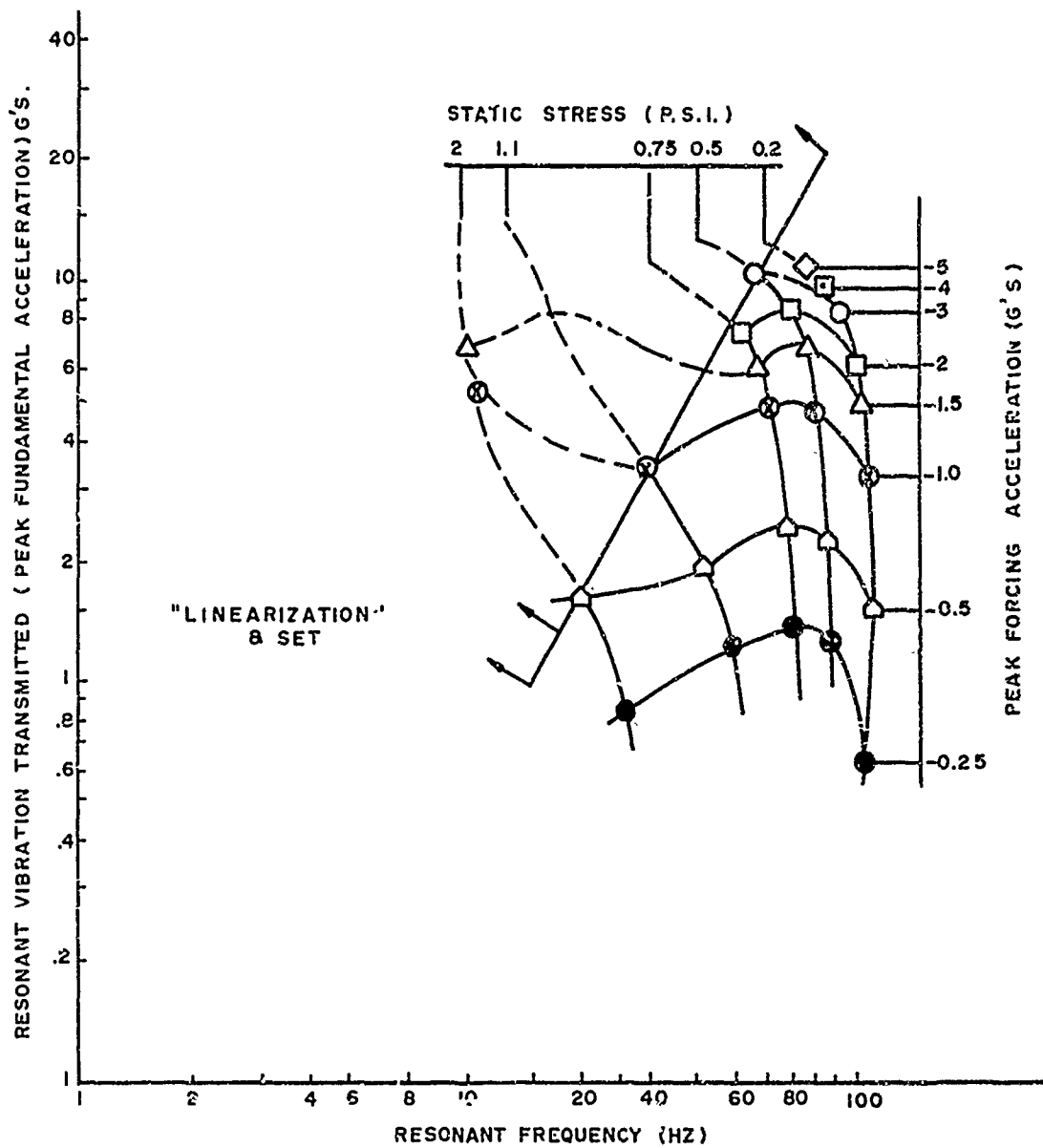


Fig 16 Vibration transmitted at resonance vs resonant frequency. Polyethylene foam, 2.0 lbs/ft³ (nom.)--1 7/16 in. thick.

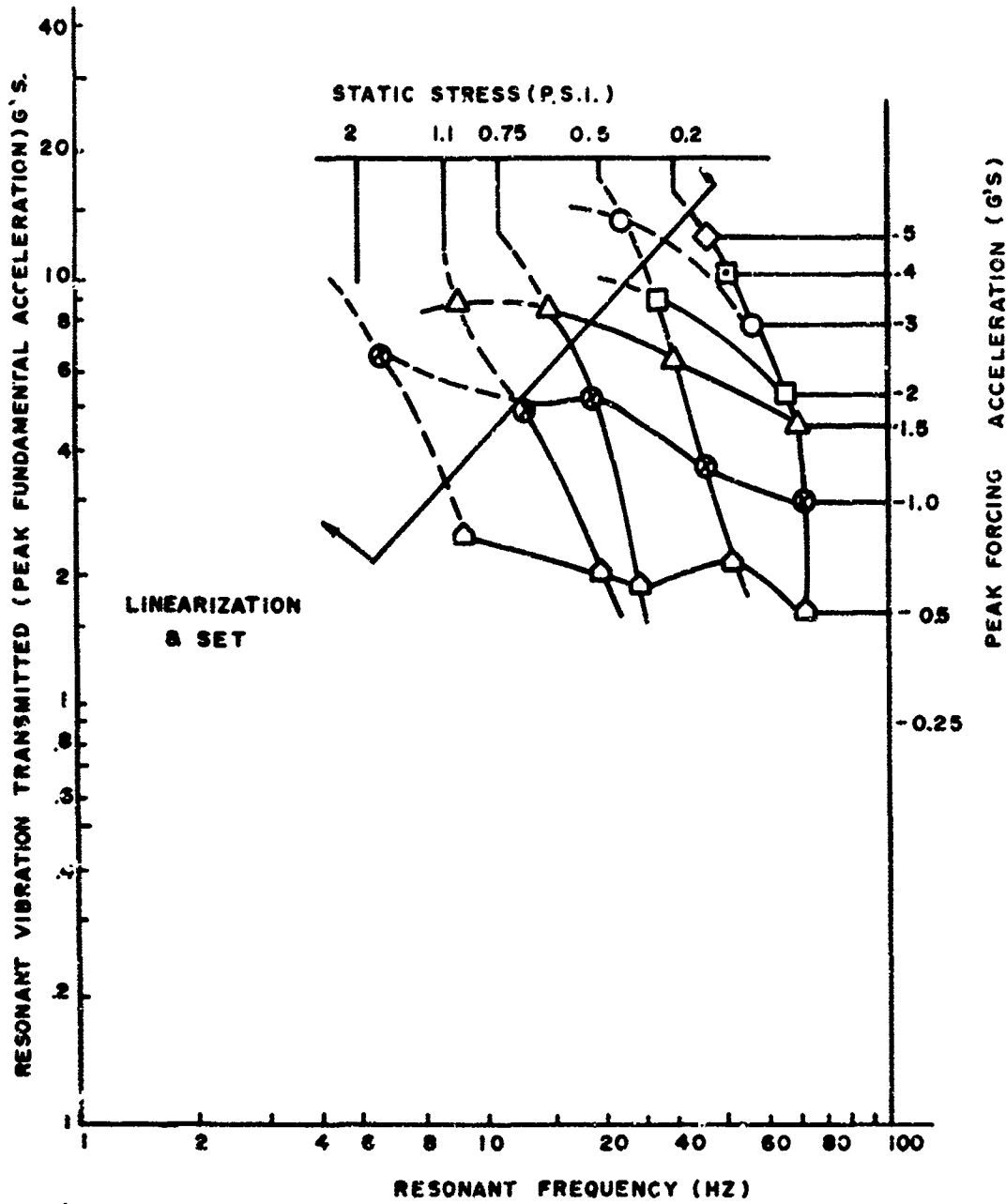


Fig 17 Vibration transmitted at resonance vs resonant frequency. Polyethylene foam, 2 lbs/ft³ (nom.)--3 3/8 in. thick.

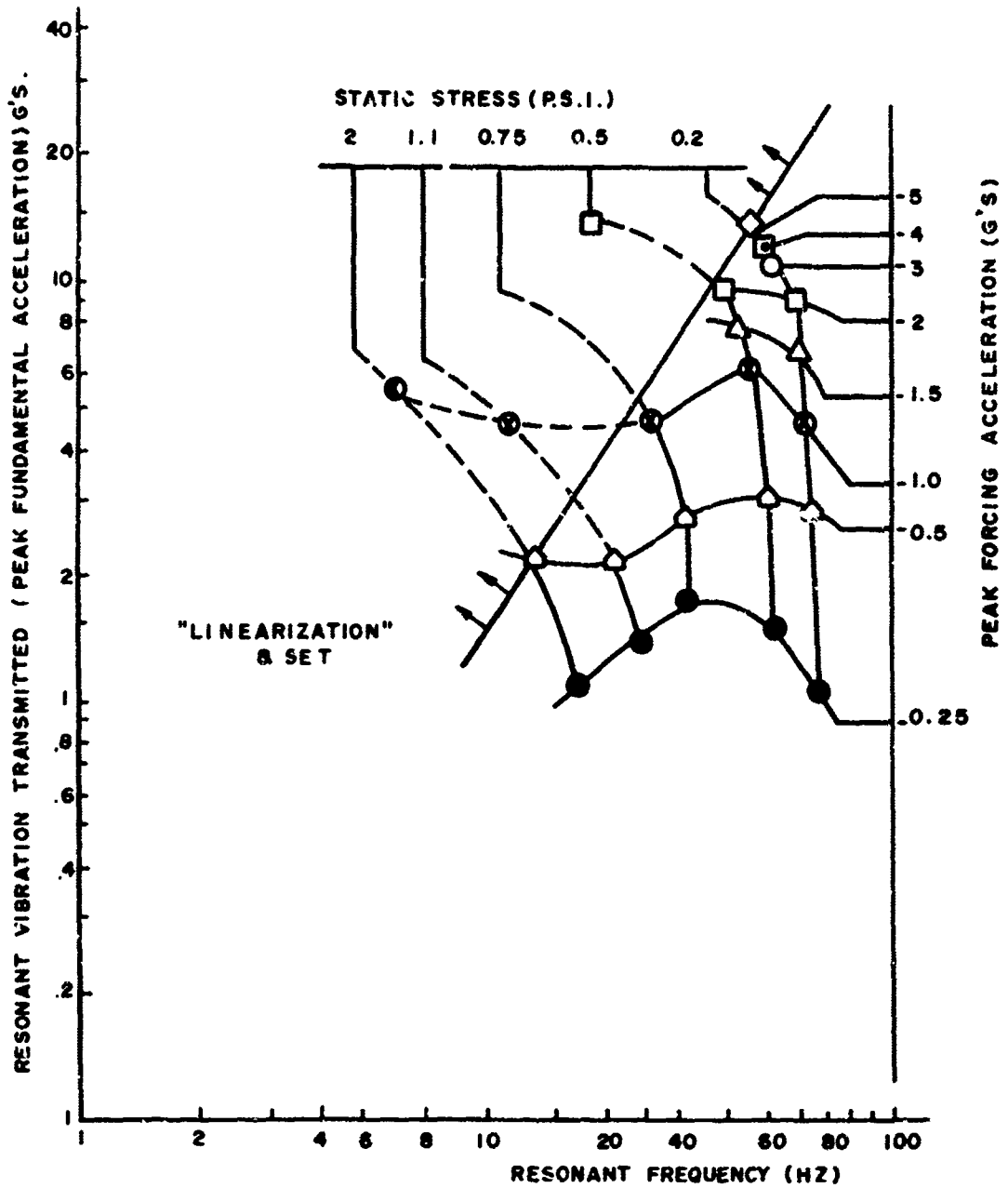


Fig 18 Vibration transmitted at resonance vs resonant frequency. Polyethylene foam, 2 lbs/ft³ (nom.)--4 in. thick (laminated)

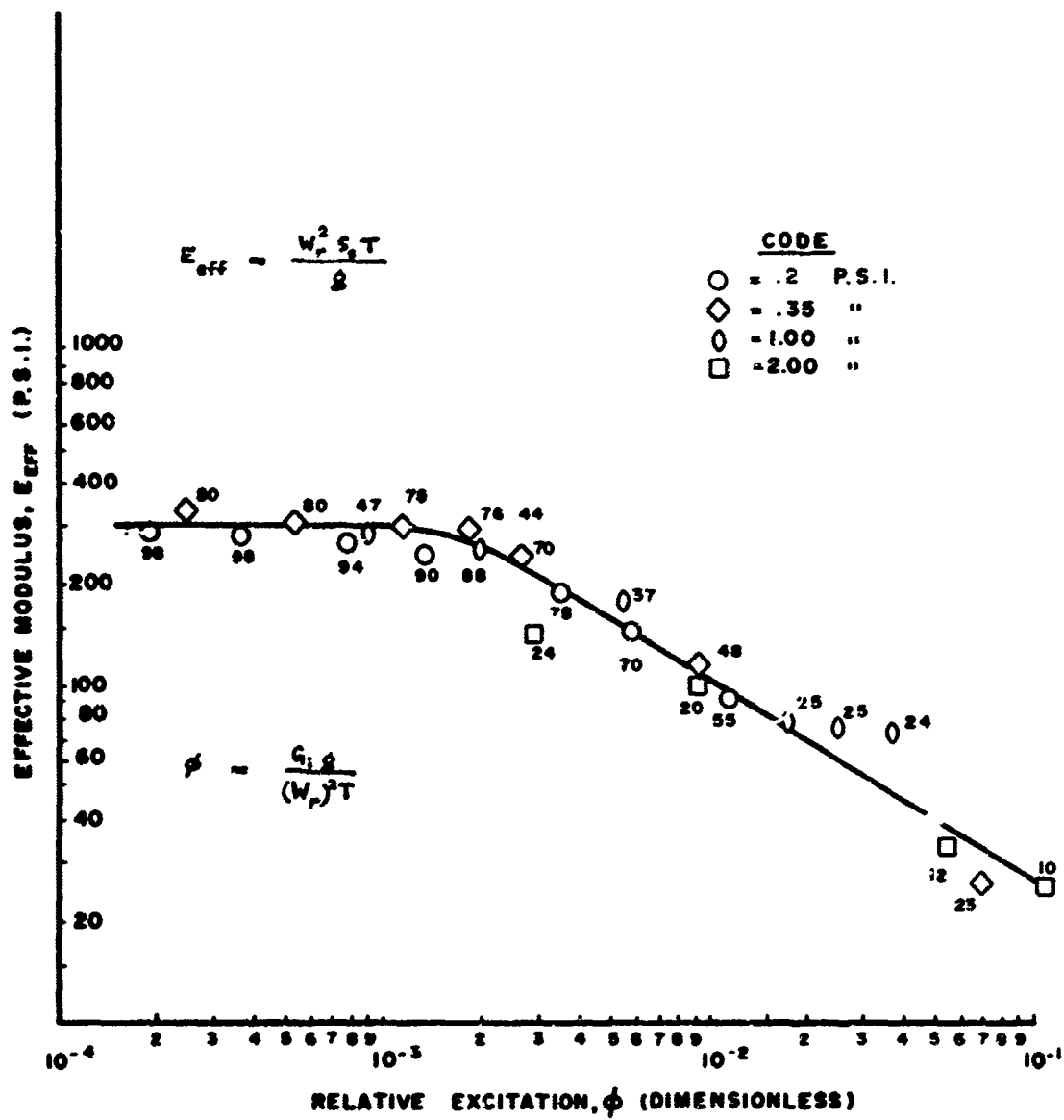


Fig 19 Effective modulus vs relative excitation, polyethylene foam, 1 5/16" thick.

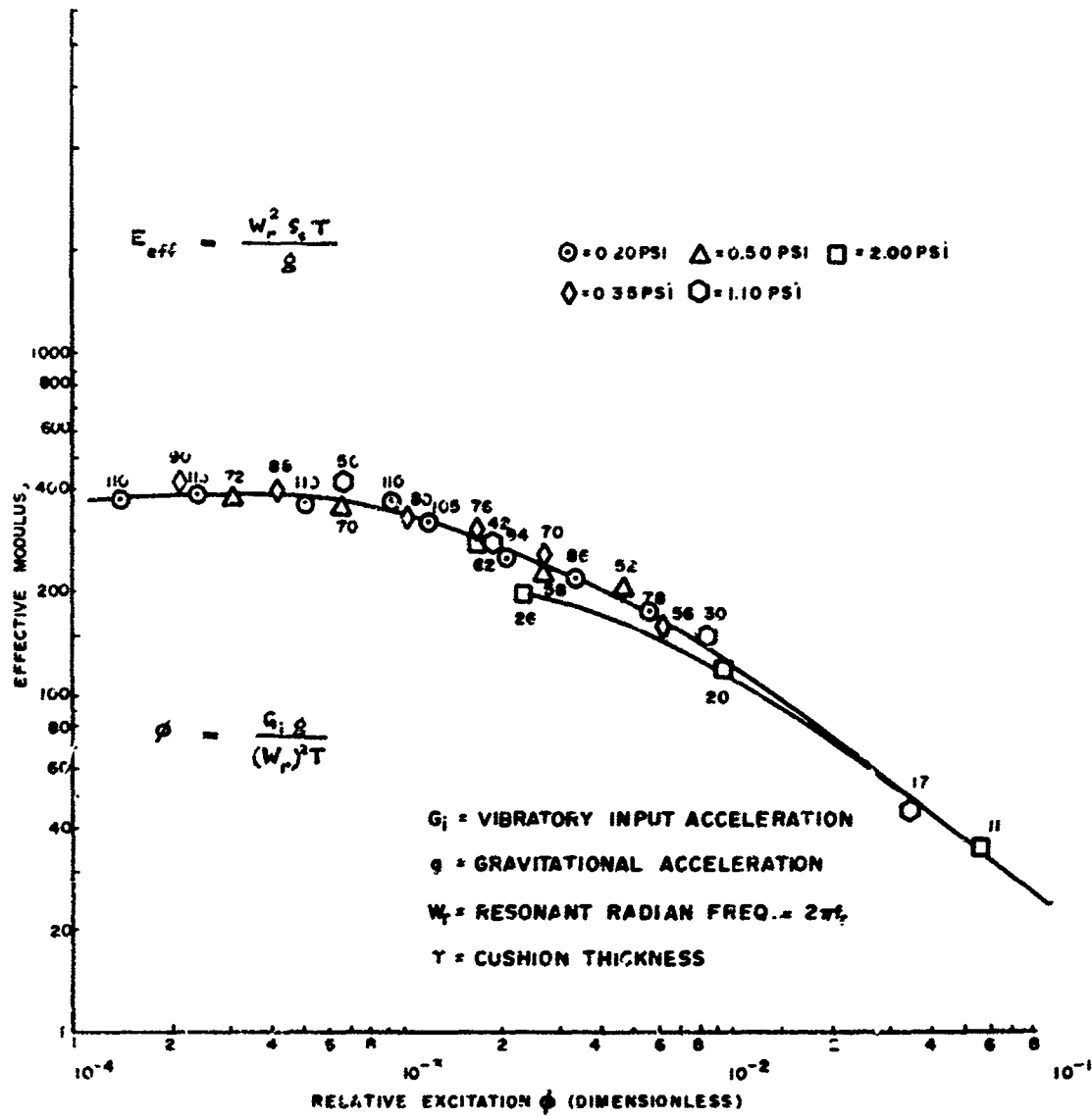


Fig 20 Effective modulus vs relative excitation, polyethylene foam, 1 7/16" thick.

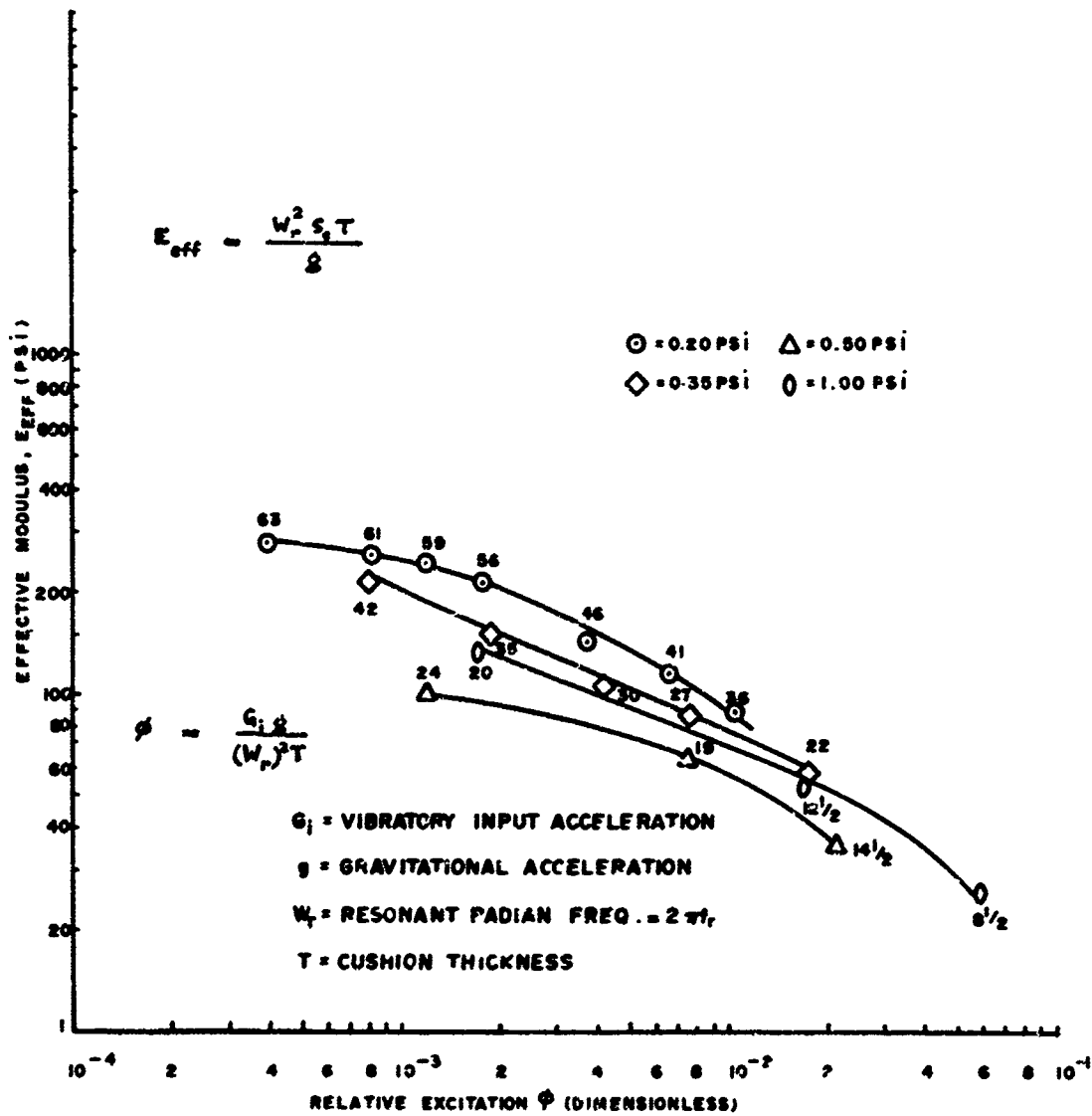


Fig 21 Effective modulus vs relative excitation, polyethylene foam, 3 3/8" thick.

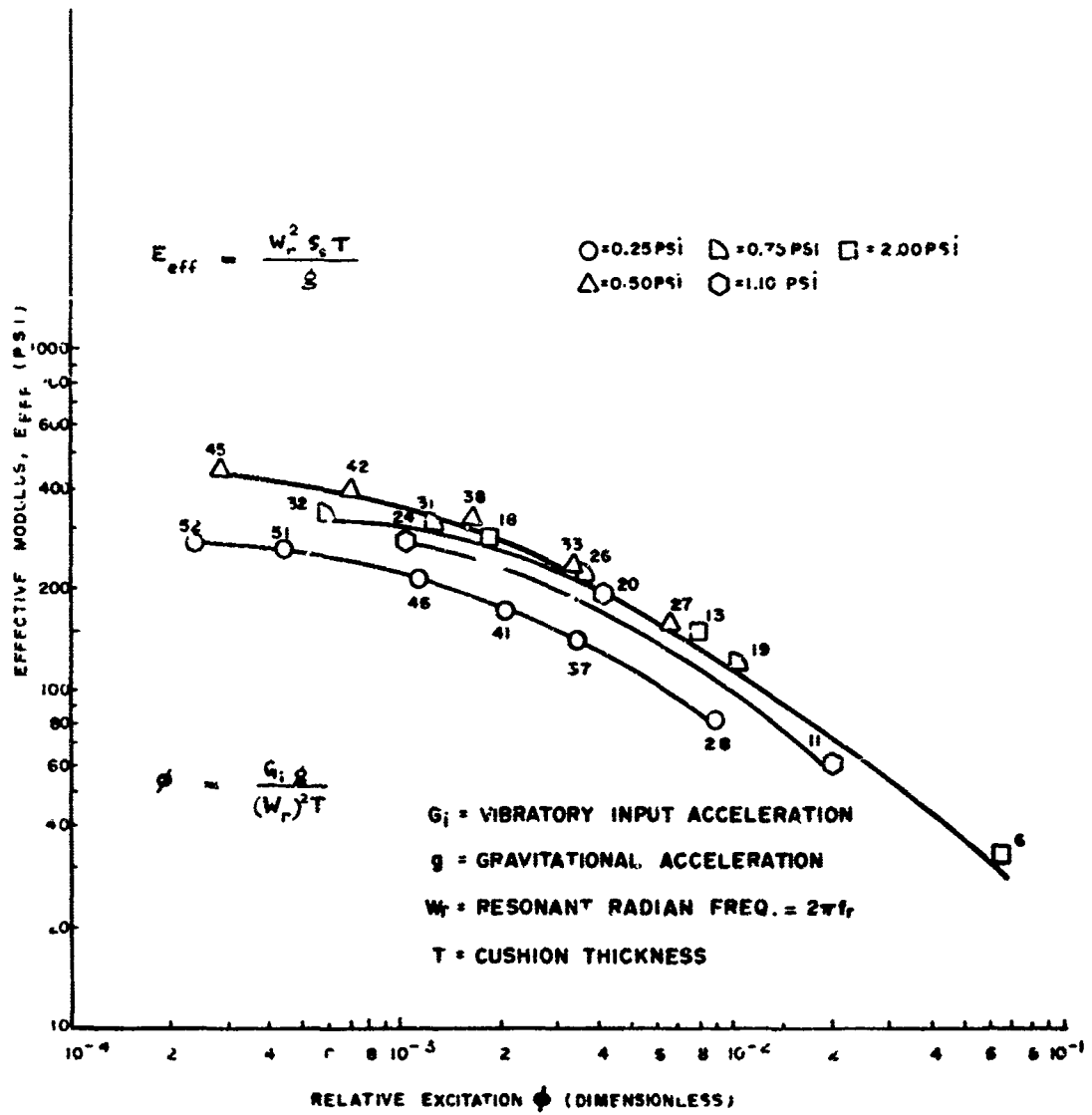


Fig 22 Effective modulus vs relative excitation, polyethylene foam, 4" thick.

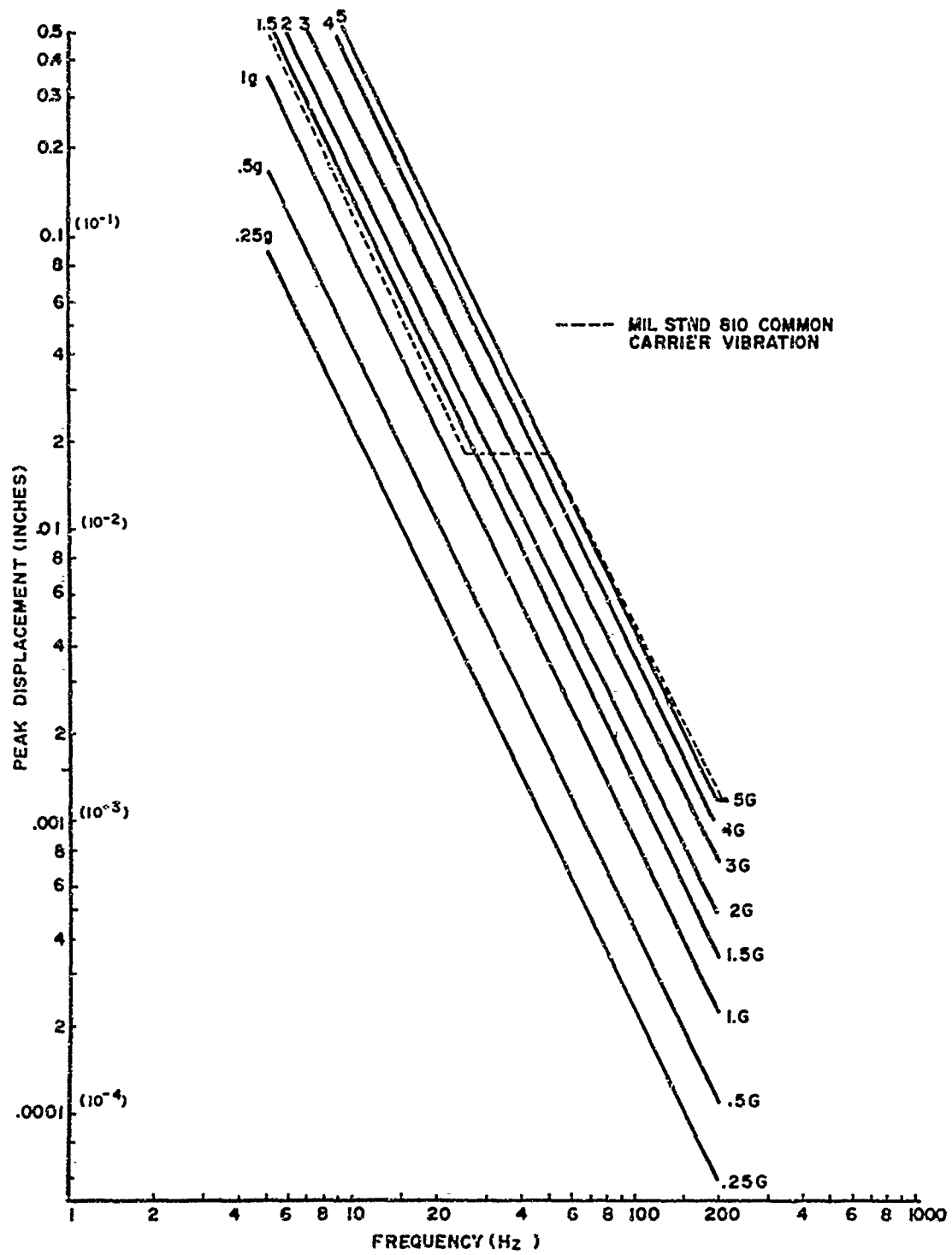


Fig 23 Peak displacement vs frequency for acceleration levels used in transmissibility tests.

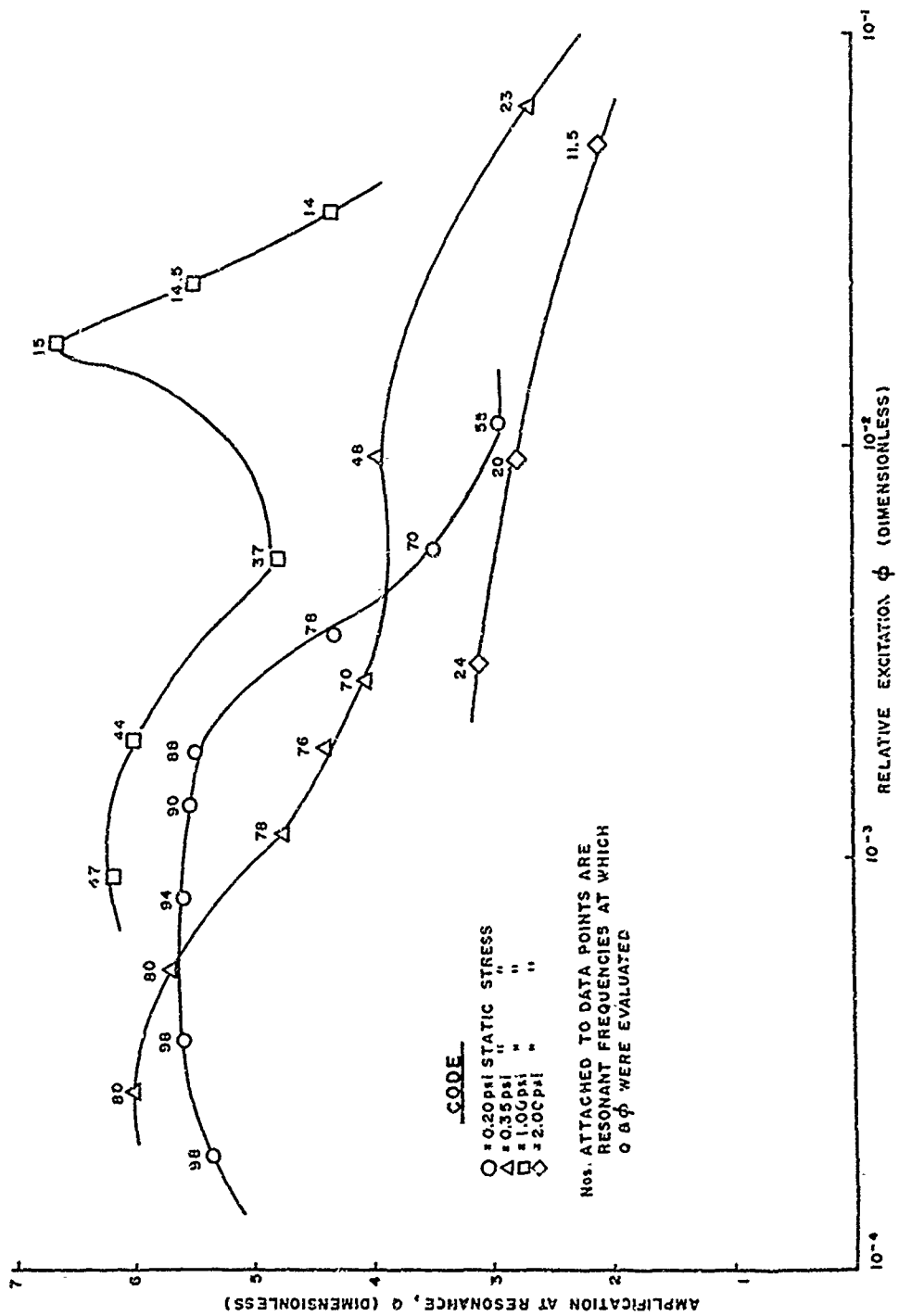
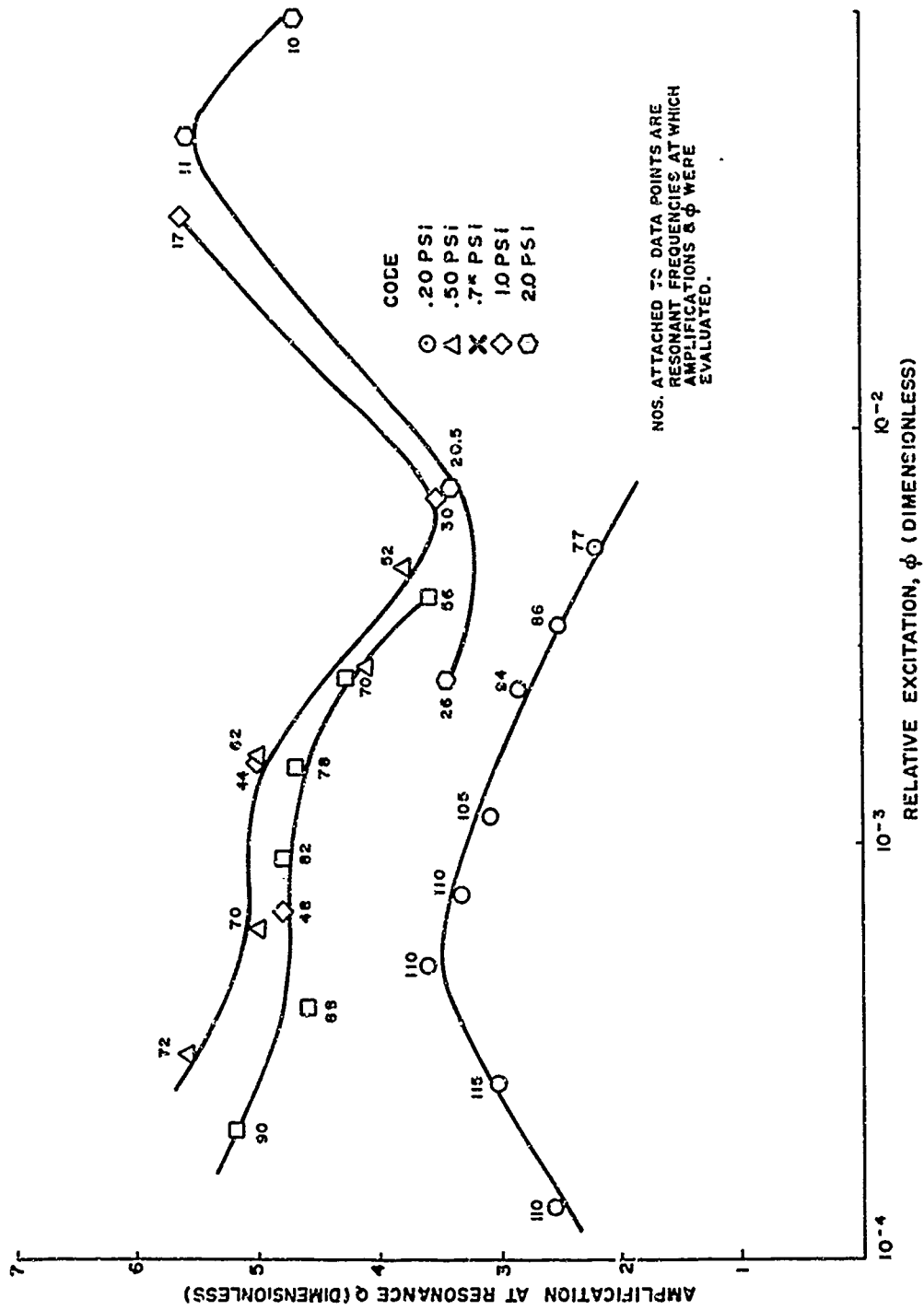


Fig 24 Amplification at resonance vs relative excitation
 (polyethylene foam, 1 5/8 in. thick)



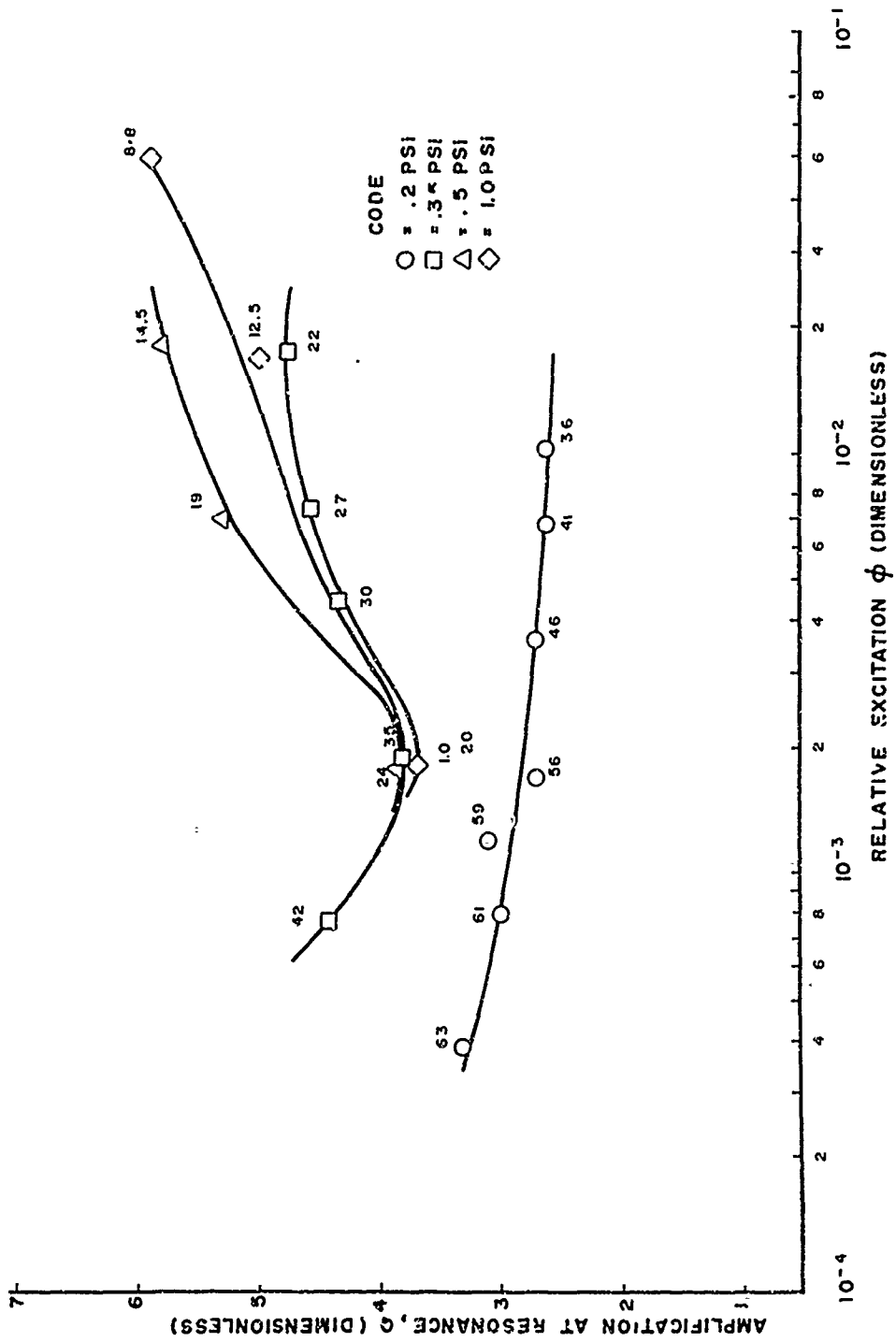


Fig 26 Resonant amplification vs relative excitation, polyethylene foam, 3 3/8" thick.

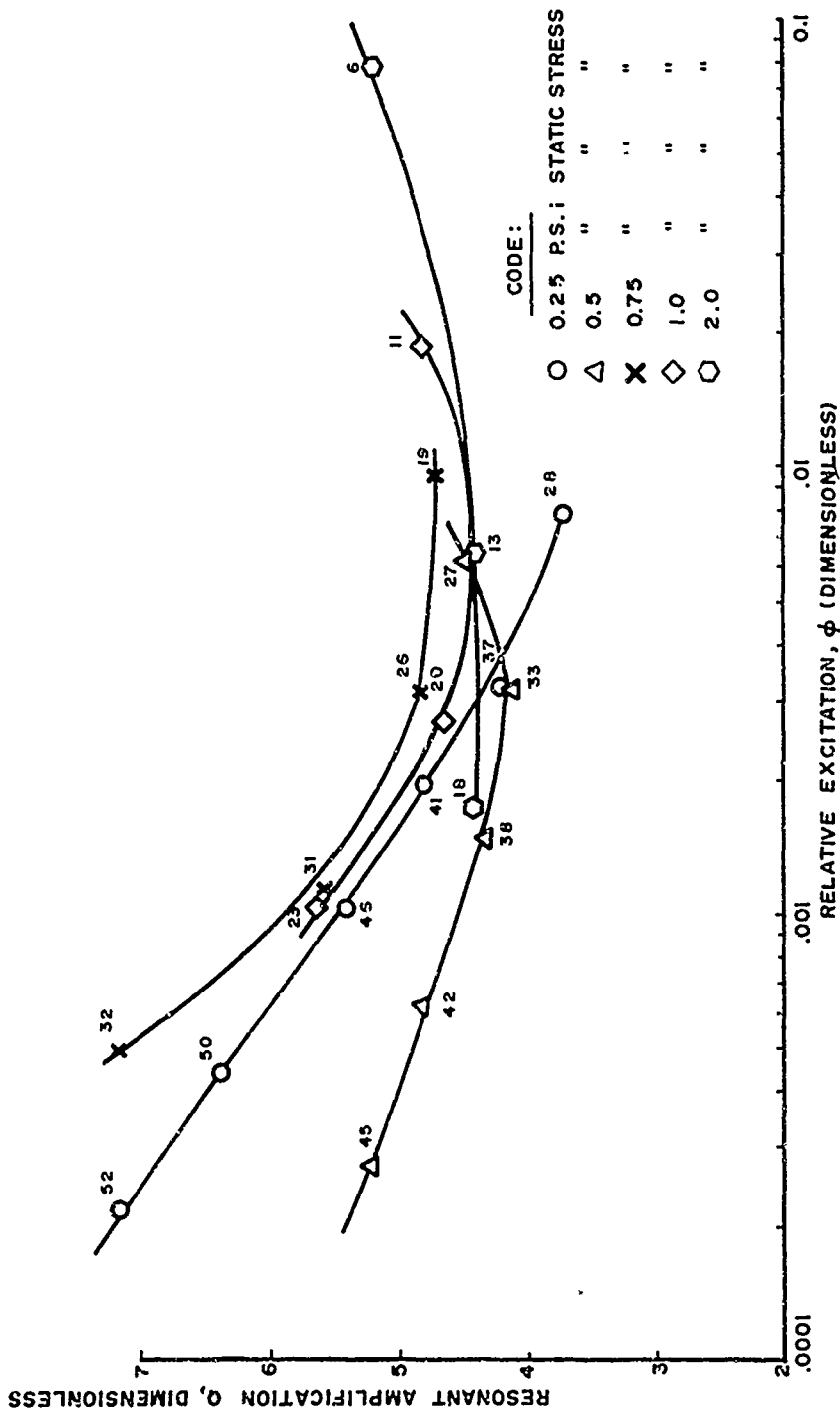


Fig 27 Resonant amplification vs relative excitation, polyethylene foam, 4" thick (laminated.)

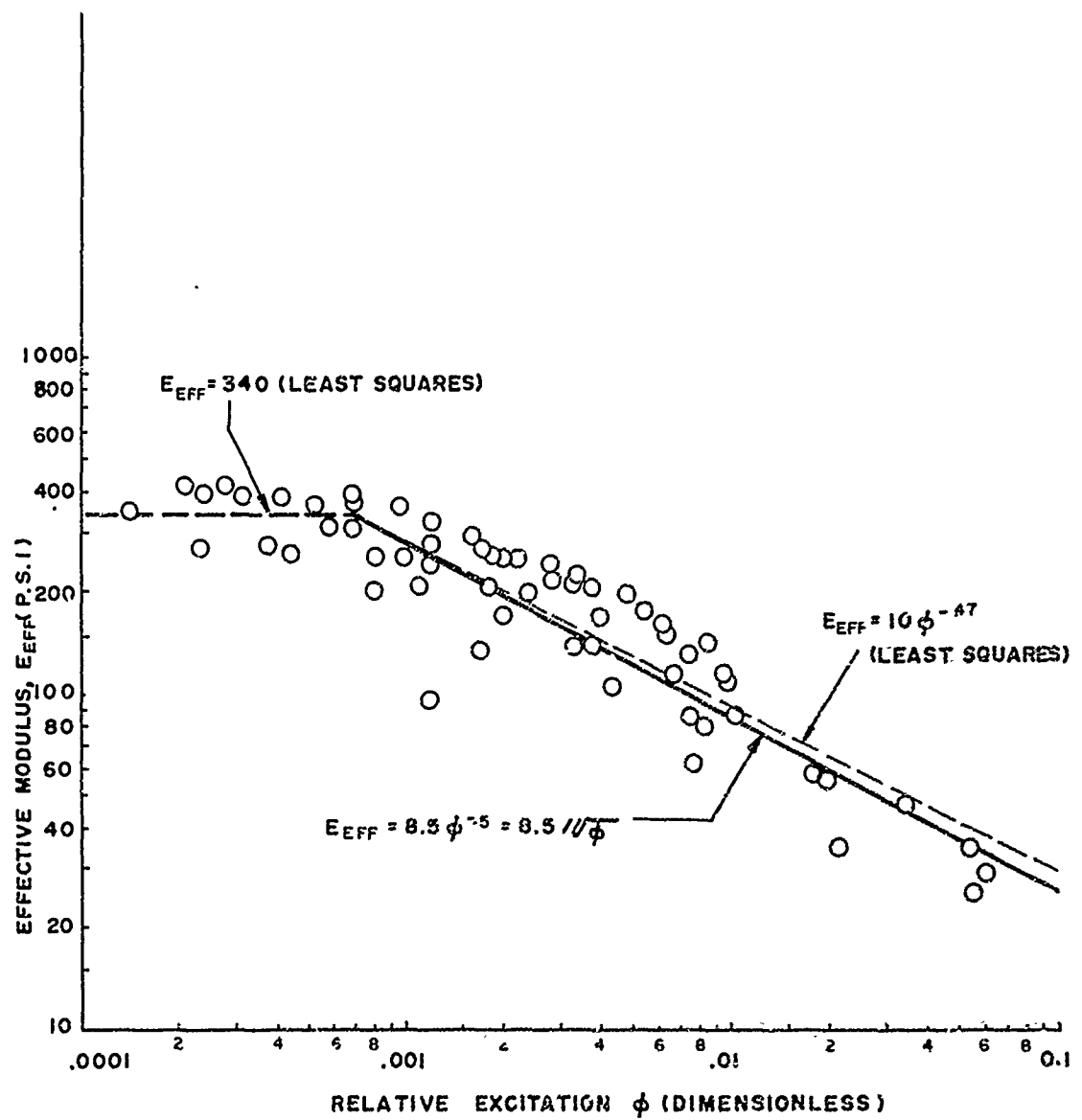


Fig 28 Effective modulus vs relative excitation, polyethylene foam, data from four thicknesses.

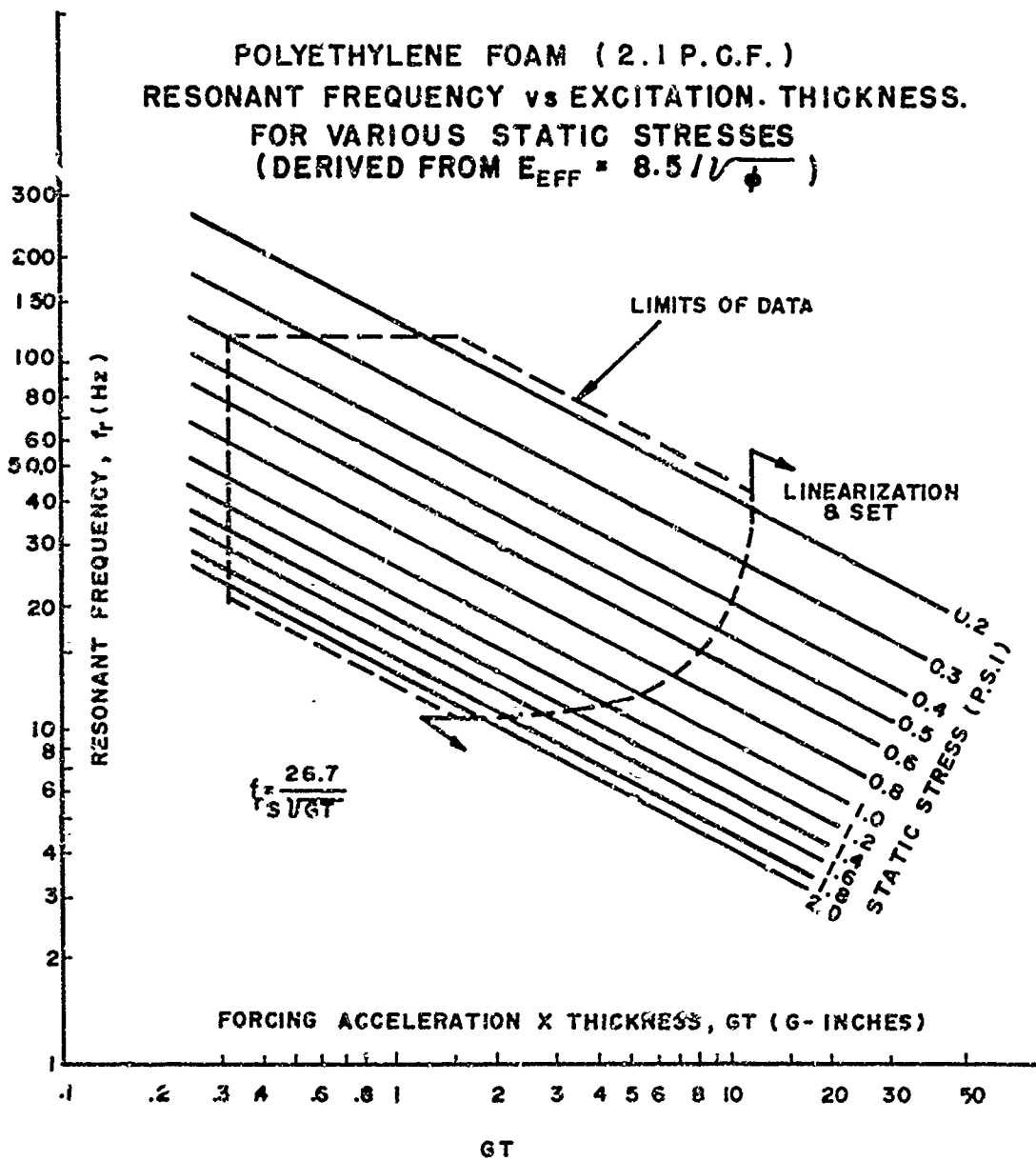


Fig 29 Polyethylene foam, resonant frequency vs acceleration-thickness product.

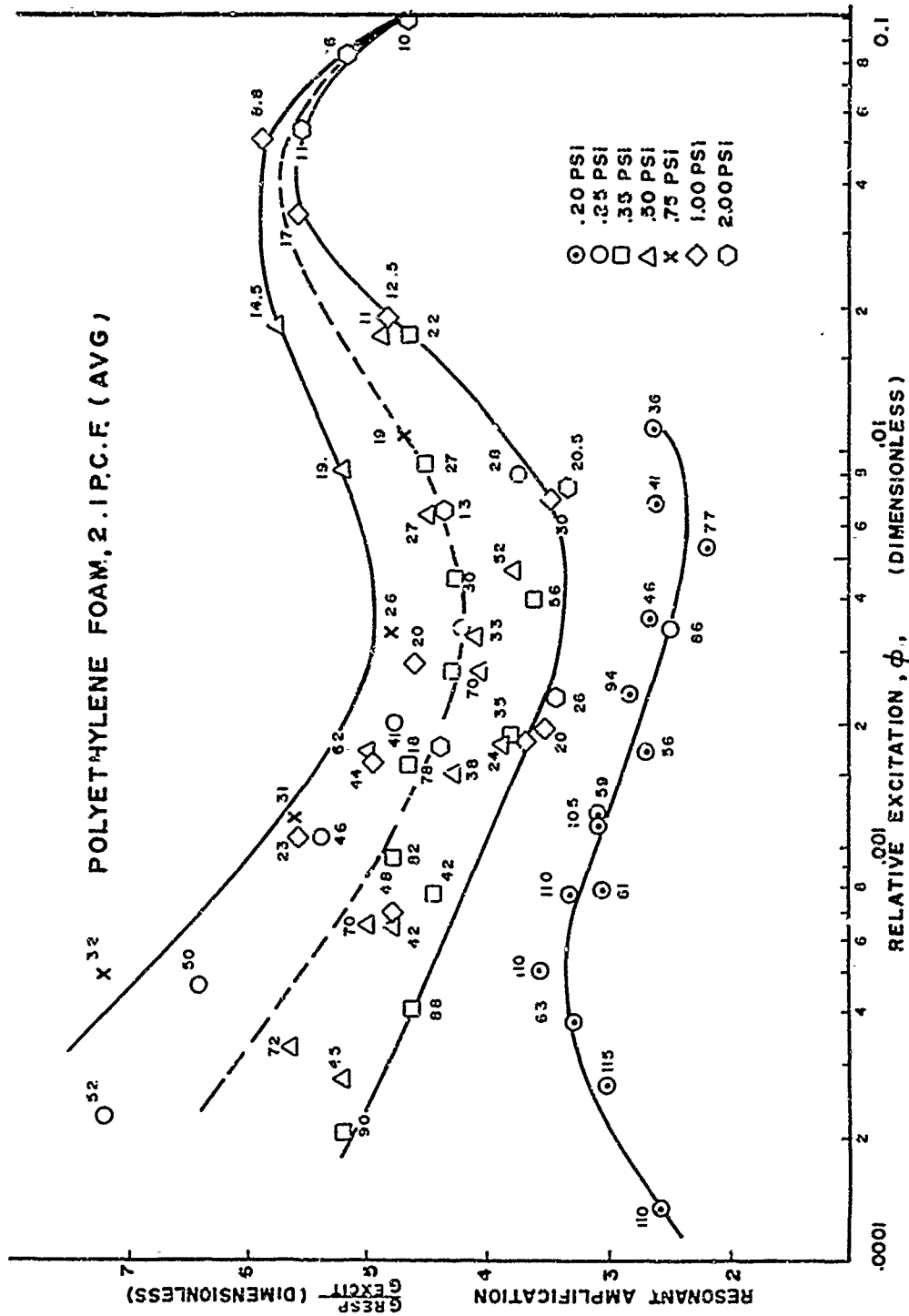


Fig 30 Resonant amplification vs relative excitation, data from four thicknesses.

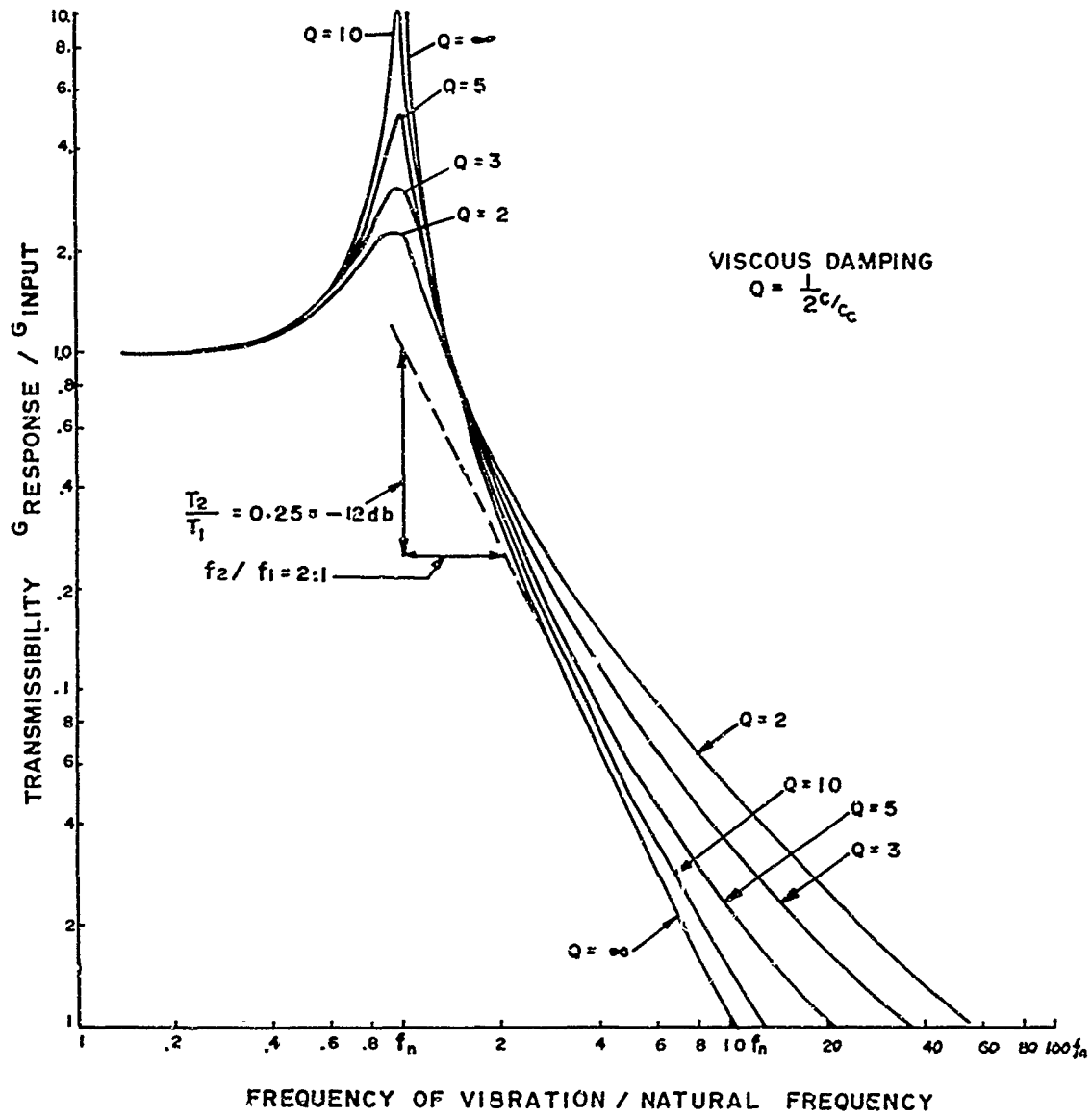


Fig 31 Transmissibility vs frequency ratio for single-degree of freedom system with viscous damping.

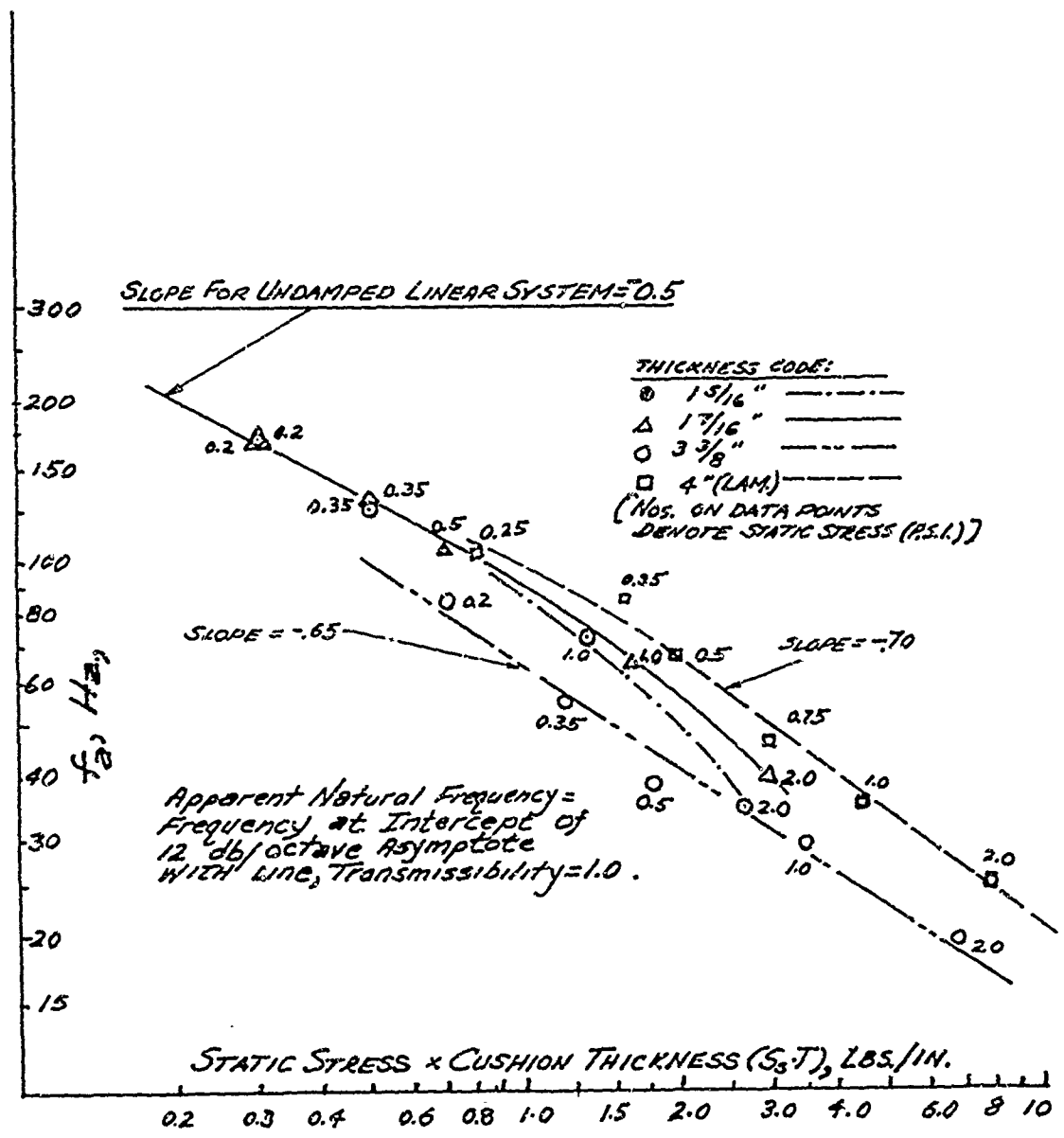


Fig 32 Apparent natural frequency vs static stress-thickness product, four thicknesses. Polyethylene foam (avg density = 2.1 lb/cu. ft)

TRACKING FILTER

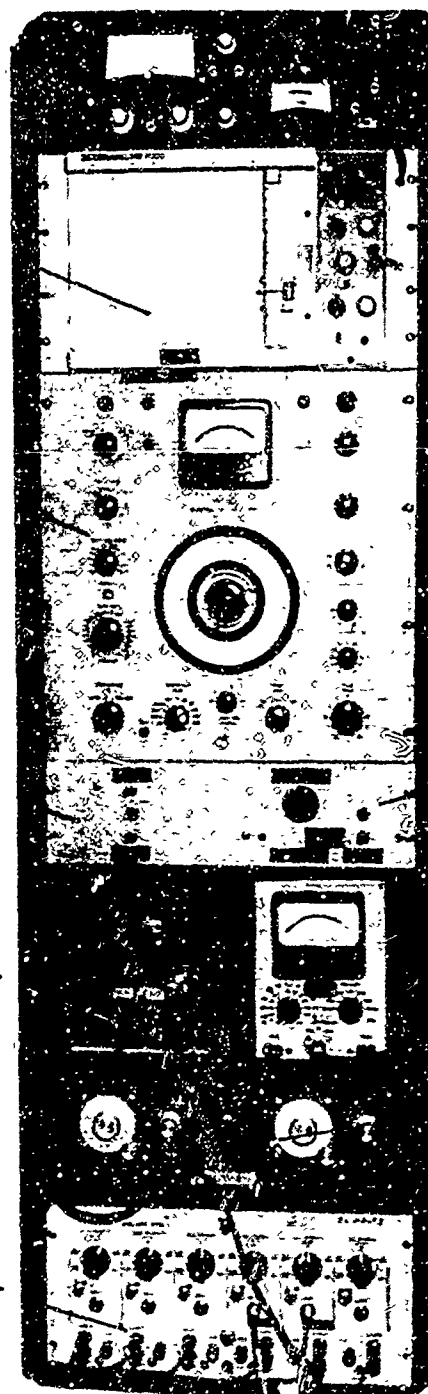
RESPONSE ACCELERATION
VS. FREQUENCY PLOTTER.

SWEEP FREQUENCY
OSCILLATOR.

LOGARITHMIC ATTENUATOR

A.C. AMPLIFIER.
(ATTENUATOR DRIVER)

CATHODE FOLLOWERS



D.C. AMPLIFIER &
RIPPLE FILTER.

A.C. TO D.C. CON-
VERTER. (MODIFIED
A.C. VVVM)

TABLE ACCELERATION
"DITHER" FILTER.

Fig 33 Instrumentation for vibration programming and recording. (Photo)

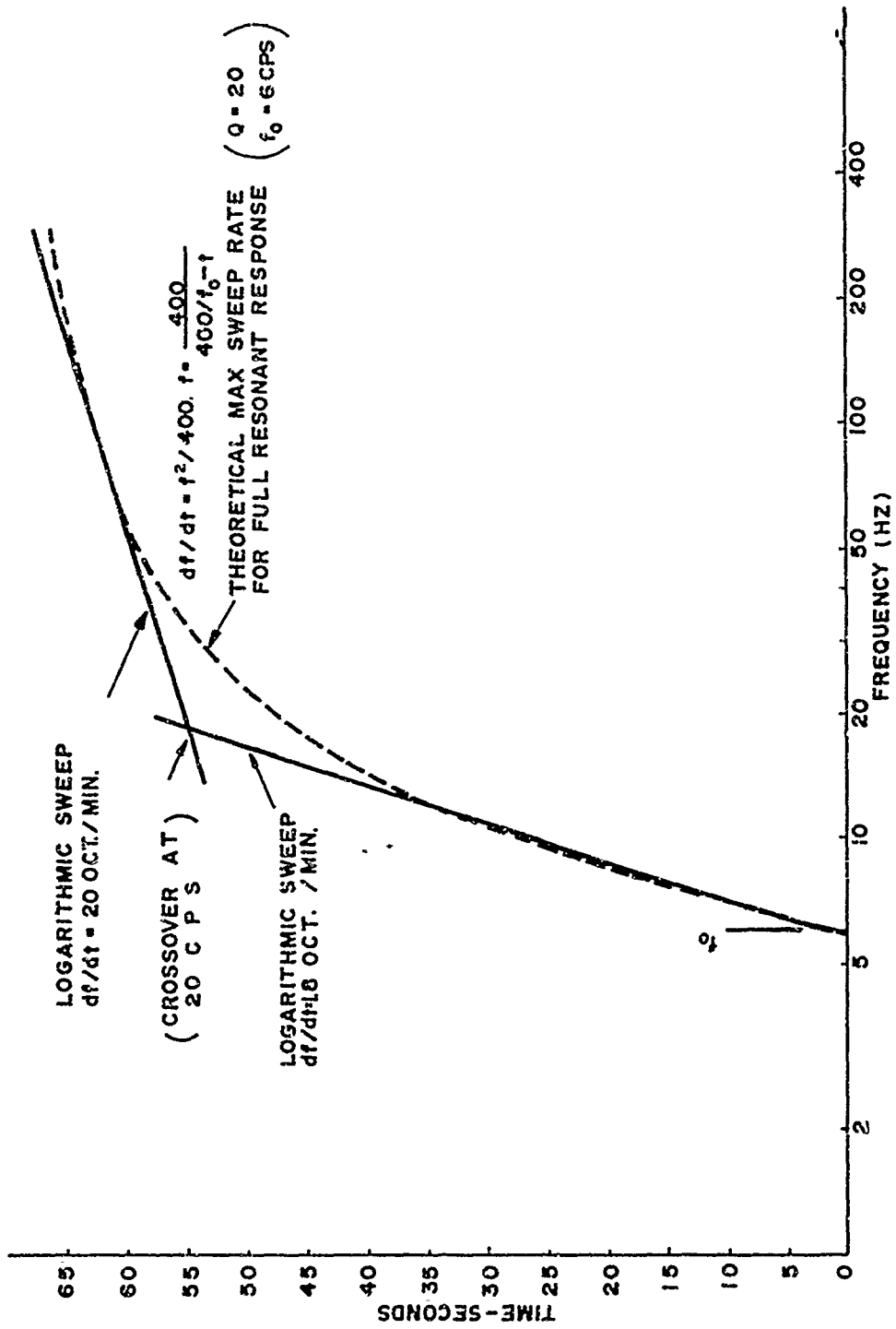


Fig 35 Approximation of idealized maximum sweep rate (for $Q = 20$ systems) with two logarithmic sweeps.

UNCLASSIFIED

Security Classification

DOCUMENT CONTROL DATA - R & D		
<i>(Security classification of title, body of abstract and indexing annotation must be entered when the overall report is classified)</i>		
1. ORIGINATING ACTIVITY (Corporate author)		2a. REPORT SECURITY CLASSIFICATION
Picatinny Arsenal, Dover, N. J.		Unclassified
		2b. GROUP
3. REPORT TITLE		
VIBRATION TESTING OF RESILIENT PACKAGE CUSHIONING MATERIAL: POLYETHYLENE FOAM		
4. DESCRIPTIVE NOTES (Type of report and Inclusive dates)		
5. AUTHOR(S) (First name, middle initial, last name)		
George Zell		
6. REPORT DATE	7a. TOTAL NO. OF PAGES	7b. NO. OF REFS
December 1969	91	
8a. CONTRACT OR GRANT NO.	8a. ORIGINATOR'S REPORT NUMBER(S)	
b. PROJECT NO.	Technical Report 3610	
c.	8b. OTHER REPORT NO(S) (Any other numbers that may be assigned this report)	
d.		
10. DISTRIBUTION STATEMENT		
This document has been approved for public release and sale; its distribution is unlimited.		
11. SUPPLEMENTARY NOTES		12. SPONSORING MILITARY ACTIVITY
13. ABSTRACT		
<p>A 2.3 PCF commercially produced cellular polyethylene cushioning was vibrated under simulated "in package" conditions. Tests were performed on several "as produced" and on a laminated thickness. Vibration was imposed on samples under static loads from 0.20 to 2.0 psi. Transmissibility was recorded in the frequency range 2 to 250 Hz. It was observed that vibration behavior was strongly influenced by material preload state. Effects are discussed and illustrated by dynamic force vs deformation curves measured "in package." One preload state is shown to induce configurational nonlinearity while another is found capable of suppressing a specific type of nonlinear reaction peculiar to compression-loaded cushioning. Pertinence of observations to utilization of cushioning in protective suspensions is considered.</p> <p>A technique for normalizing nonlinear cushion response data is developed. Results of comprehensive tests on polyethylene foam are reduced to this format. Data indicates the dynamic stiffness of the foam at transportation-induced vibration frequencies is increased significantly over values derived from low rate (1.0 in./min) compression tests.</p>		

DD FORM 1473
1 NOV 55

REPLACES DD FORM 1473, 1 JAN 54, WHICH IS
OBSOLETE FOR ARMY USE.

UNCLASSIFIED

Security Classification

UNCLASSIFIED

Security Classification

14. KEY WORDS	LINK A		LINK B		LINK C	
	ROLE	WT	ROLE	WT	ROLE	WT
Vibration testing Package cushioning material Polyethylene foam Transmissibility Dynamic force vs deformation Transportation - induced vibration Compression test Foam cell structure Resonant excitation Static load						

UNCLASSIFIED

Security Classification